Aus dem Institut für Virologie
des Fachbereichs Veterinärmedizin
der Freien Universität Berlin

Tumor promoting functions of cellular telomerase RNA and viral RNAs in herpesvirus-induced cancer formation

Inaugural-Dissertation
zur Erlangung des Grades eines
Doktors der Veterinärmedizin
an der
Freien Universität Berlin

vorgelegt von
Ahmed Mahmoud Osman Kheimar
Tierarzt aus Qena /Ägypten

Berlin 2017
Journal-Nr.: 4010

mbvberlin | mensch und buch verlag

Aus dem Institut für Virologie

des Fachbereichs Veterinärmedizin

der Freien Universität Berlin

Tumor promoting functions of cellular telomerase RNA and viral RNAs in herpesvirus-induced cancer formation

Inaugural-Dissertation

zur Erlangung des Grades eines

Doktors der Veterinärmedizin

an der

Freien Universität Berlin

vorgelegt von

Ahmed Mahmoud Osman Kheimar

Tierarzt

aus Qena /Ägypten

Berlin 2017

Journal-Nr.: 4010

Gedruckt mit Genehmigung des Fachbereichs Veterinärmedizin

der Freien Universität Berlin

Dekan:	Univ.-Prof. Dr. Jürgen Zentek
Erster Gutachter:	Prof. Dr. Benedikt Kaufer
Zweiter Gutachter:	Univ.-Prof. Dr. Alex Greenwood
Dritter Gutachter:	PD Dr. Michael Veit

Deskriptoren (nach CAB-Thesaurus):
Marek's disease; Marek's disease virus; genetics; neoplasms; polymerase chain reaction; T-cell; animal model

Tag der Promotion: 08.11.2017

Bibliografische Information der *Deutschen Nationalbibliothek*
Die Deutsche Nationalbibliothek verzeichnet diese Publikation in der Deutschen Nationalbibliografie; detaillierte bibliografische Daten sind im Internet über <http://dnb.ddb.de> abrufbar.

ISBN: 978-3-86387-857-3
Zugl.: Berlin, Freie Univ., Diss., 2017
Dissertation, Freie Universität Berlin
D 188

Choriner Str. 85 - 10119 Berlin
verlag@menschundbuch.de – www.menschundbuch.de

“As a scientist, you are confronted with something that is beyond what is known”

Dr. Fulvio Reggiori

Table of contents

List of abbreviations

Abbreviation	Refers to
AcHV-	Anatid herpesvirus-
ADOL	The Avian Disease and Oncology Laboratory
ALV	Avian leukosis virus
APC	Antigen-presenting cell
BAC	Bacterial artificial chromosome
bZIP	basic-region leucine zipper
cDNA	Complementary deoxyribonucleic acid
CECs	Chicken embryo fibroblasts
chTR	Chicken telomerase RNA
CMV	Cytomegalovirus
CoHV	Columbid herpesvirus
ConA	Concanavalin A
CR	Conserved Region
ctBP	C-terminal Binding Protein
DC	Dendritic cell
DMEM	Dulbecco's Minimal Essential Medium
DNA	Deoxyribonucleic acid
ds	Double strand
EBV	Epstein-Barr virus
EBER-1	Epstein-Barr virus encoded RNA-1
EBER-2	Epstein-Barr virus encoded RNA-2
EDTA	Ethylendiamin-tetraacetat
EtBr	Ethidium bromide
FBS or FCS	Fetal calf serum or Fetal Bovine Serum (FBS)
FFE	Feather follicle epithelium
GAG	Glycosaminoglycans
GaHV	Gallid herpesvirus
gB	Glycoprotein B
gC	Glycoproteins C
gD	Glycoprotein D

Abbreviation	Refers to
GFP	Green fluorescent protein
HIV	Human Immunodeficiency Virus
HRP	Horse radish peroxidase
HSV	Herpes simplex virus
hTR	Human telomerase RNA
HVEM	herpes virus entry mediator
HVT	Herpesvirus of Turkey
I.E.	Immediate early
ICP0	Infected cell polypeptide number 0
ICTV	International Committee on Taxonomy of Viruses
IFA	Immunofluorescence Assay
IFN	Interferon
IL-	Interleukin-
iNOS	Inducible nitric oxide synthase
IRL	Internal repeat long regions
IRs	Internal repeat short regions
Kbp	Kilo base pair
kDa	Kilodalton
KSHV	Kaposi's Sarcoma Herpesvirus
La antigen	Lupus La protein
LATs	Latency Associated Transcripts
LB	Luria-Bertani
LPS	Lipopolysaccharides
MD	Marek's disease
MDV	Marek's disease virus
MeHV	Meleagrid herpesvirus
MEQ	MDV EcoRI Q
MHC	Major histocompatability complex
miRNA	Micro RNA
mRNA	Messenger ribonucleic acid
MWCO	Molecular weight cut-off

Abbreviation	Refers to
NAE	Non-Essential Amino acids
ng	Nanogram
NGS	Next Generation Sequence
NK	Natural killer
NO	Nitric oxide
NPC	Nuclear pore complex
NTC	No template control
O/N	Overnight
ORF	Open reading frame.
PBS	Phosphate buffered saline
pCMV	Promoter for cytomegalovirus
PCR	Polymerase chain reaction
Pfu	Plaque-forming units
PKR	Protein Kinase R
pp38	Phosphoprotein gene (pp38)
PRRs	Pattern recognition receptors
qRT-PCR	Real Time quantitative reverse transcription PCR
qPCR	Quantitative PCR
RT	Reverse transcriptase
REV	Reticuloendotheliosis virus
RFLP	Restriction Fragment length polymorphism
RNA	Ribonucleic acid
RNP	Ribonucleoprotein
RT	Room temperature
RpL22	Ribosomal Protein Large subunit 22
SDS	Sodium dodecyl sulfate
SOI	Sequence Of Interest
SPF	Specific Pathogen Free
SQRT	Square root
T-ALL	T-cell Acute Lymphocytic Leukemia
TAE	Tris acetic acid EDTA

Abbreviation	Refers to
TCR+	T-cell-receptor-positive
TERT	Telomerase Reverse Transcriptase
TGN	Trans-Golgi network
TK	The Human Thymidine Kinase
TLR	Toll-like receptor
Tm	Melting temperature
TPBS	Tween PBS
TR	Telomerase RNA
TRL	Terminal repeat long
UL	Unique long
US	Unique short region
UV	Ultra Violet
vIL-8	Viral interleukin-8
vv+MDV	Very virulent plus strain
vvMDV	Very virulent MDV strain
vTR	Viral telomerase RNA

List of figures and tables

4. Introduction

Telomeres are repetitive regions $(TTAGGG)_n$ at the ends of the linear chromosomes of vertebrates including mammals and birds [1]. The repetitive sequences are essential for chromosome stability and prevent chromosomal rearrangements [2]. To protect telomeres from deterioration, vertebrates encode the telomerase complex that restores the telomere length by the addition of telomeric repeats. The telomerase complex consists of two components: the catalytic subunit which is the telomerase reverse transcriptase (TERT) and the telomerase RNA (TR), which serves as a template for the addition of the repeats. The telomerase activity is absent in most somatic cells, but is upregulating in cancer cells [3]. Approximately 15% of human cancers are caused by viruses [4]. Some of these viruses are herpesviruses, including Kaposi sarcoma-associated herpesvirus (KSHV) and Epstein-Barr virus (EBV). One animal herpesvirus that infect chickens and is considered the most frequent cancer in the animal kingdom is Marek's disease virus (MDV) [5]. MDV is a member of Alphaherpesvirinae that produces tumors in the infected chickens. Beyond its important role in veterinary medicine, MDV is frequently used as a natural small animal model for herpesvirus-induced lymphomagenesis [6]. Intriguingly, MDV is the only known virus harboring a telomerase RNA subunit, termed (vTR) [7], which is involved in the tumor formation, however, the mechanism is not completely understood [8]. vTR shares 88% sequence identity with the cellular telomerase RNA in chickens (chTR) [7], however, it remains unknown if the overexpression of the cellular TR (chTR) can complement the functions of vTR in MDV-induced tumor formation. Similarly, Epstein Barr-virus, human gammaherpesvirus, encodes two small RNAs, termed EBERs (EBER-1 and EBER-2) which are the most viral transcripts detected in EBV-latently infected and transformed cells. Intriguingly, EBERs and vTR have some interaction partners in common that are highly conserved between human and chickens suggesting a conserved mechanism. The tumor-promoting functions of cellular TRs (chTR) and viral RNAs (EBERs) will be addressed in this doctoral thesis.

4.1 Herpesvirales

Herpesviruses are DNA viruses that can infect an extensive variety of hosts including animals and humans [9]. They can establish a so called latent phase; the ability of the virus to remain dormant within the host cells for long times [10]. In general, herpesviruses are large and enveloped viruses. Their genome consists of large, linear, double-stranded DNA (dsDNA) which is ranging in size from 124 to 235 kbp and is packed in an icosahedral capsid. The capsid is made up of proteins of 162 capsomeres. The outer layer of the virion is envelop, which is pirated from the host nuclear membrane and comprises the viral

glycoproteins which approximately are 8 nm long. Between the capsid and envelop, there is amorphous structure which is called tegument (Figure 1) [10, 11]. Another characteristic for herpesviruses is that they can establish lytic infection and latency with intermittent reactivation and shedding of infectious particles. During lytic infection, the virus is able to replicate and synthesize new viral particles while in latency, the viral replication is suppressed and the virus can persist (long-term infections). The establishment of latency is a specific biological feature of herpesviruses. Following the lytic and latent phases of infection, the virus can reactivate and establish lytic replication and can transmit to infect the adjacent cells (Figure2) [10].

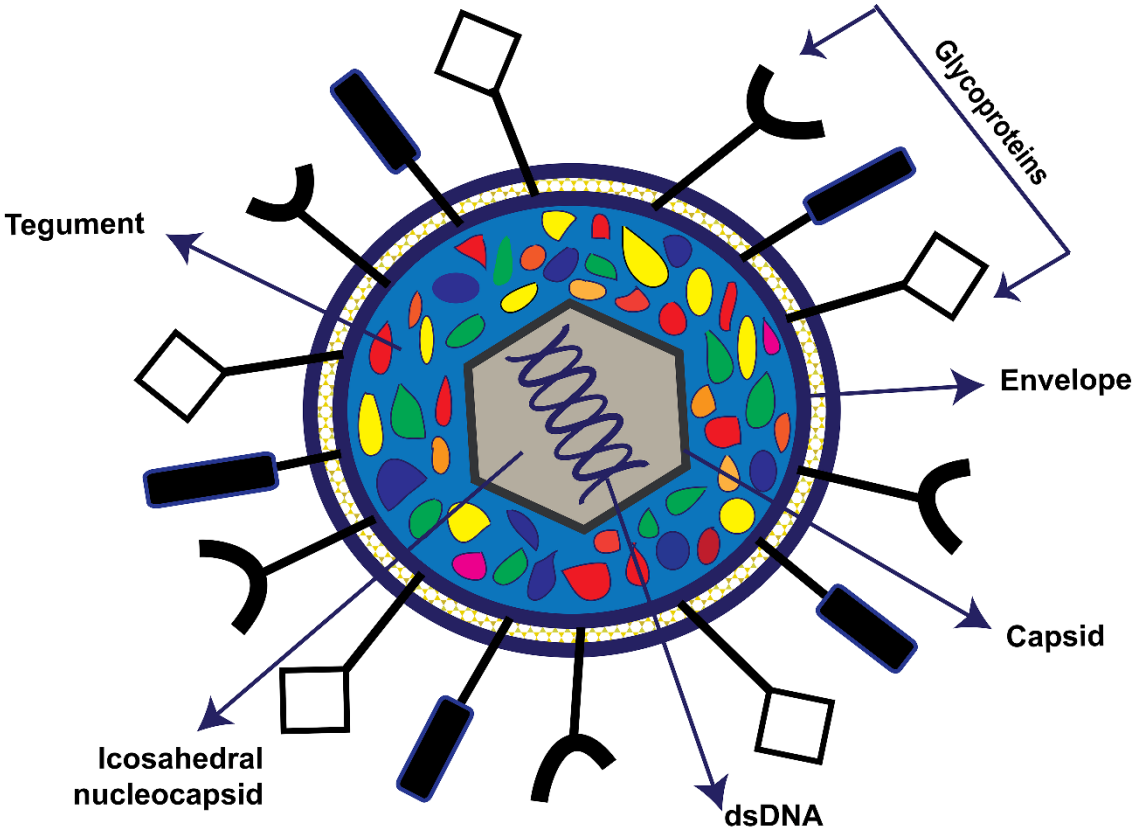

Figure 1. Schematic representation of a herpesvirus virion. All members have a relatively large genome size located in the nucleocapsid which is embedded in the tegument. The outer layer is a lipid envelop which contains the viral glycoproteins.

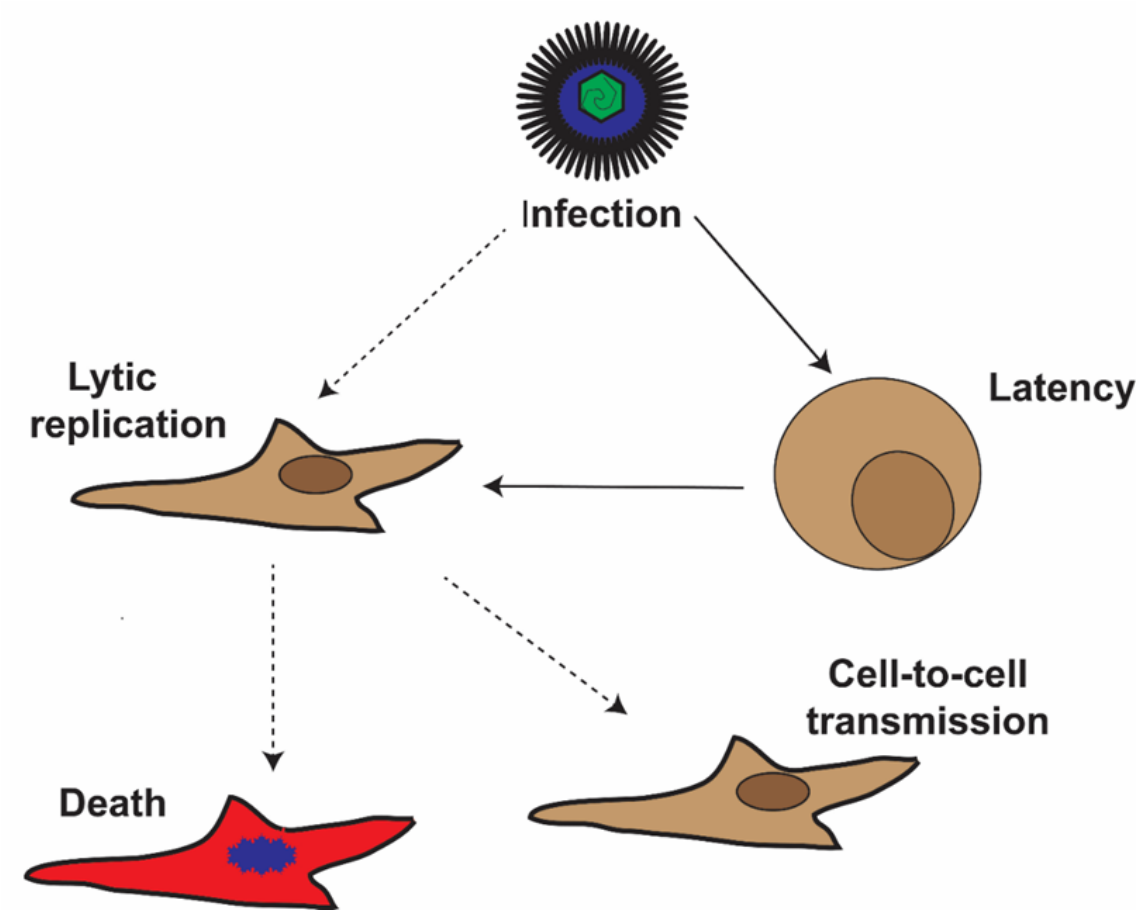

Figure 2. Schematic representation of herpesvirus stages of infection in the host. Possible outcomes of the lytic and latent viral infections. Dotted arrows represent more common events. Modified from Stoopler et al., 2003 [10].

The order *Herpesvirales* contains three families; *Herpesviridae*, which include viruses that infect mammals, birds and reptiles; *Malacoherpesviridae,* which infect the mollusk species; *Alloherpesviridae,* which infect fish and frogs [12]. Based on the biologic and genetic properties, the family *Herpesviridae* can be further divided into three subfamilies; *Alphaherpesvirinae*, *Betaherpesvirinae*, and *Gammaherpesvirinae* [13].

Alphaherpesviruses are characterized by a wide host range, short replication cycles. Members belonging to this subfamily can infect epithelial cells and produce latent infections in sensory ganglia. Common examples of alphaherpesviruses are herpes simplex virus 1 (HSV-1), herpes simplex virus 2 (HSV-2), and varicella-zoster virus (VZV) [13], while Betaherpesviruses are characterized by a narrow host range with a long replication cycle within the host. They can establish latency in lymphocytes. Human herpesvirus cytomegalovirus (CMV), HHV-6, and HHV-7 represent viruses from this subfamily [14].

Gammaherpesviruses such as Epstein-Barr virus (EBV), and newly discovered HHV-8 have a narrow host range with replication and latency restricted to lymphoid tissues (especially B or T cells), [12]. Herpesviruses have been found in all animal species [15] causing a variety of diseases which ranges from asymptomatic infections to deaths. Among these viruses, pseudorabies virus in pigs and Marek's disease virus (MDV) in chickens are of big concern due to the their severe economic losses [16]. Recently, it has been demonstrated that a novel herpesvirus infects elephants. This virus is considered to be a highly fatal disease for both the Asian and African elephant [17]. The infected elephants develop signs as cyanosis of the tongue, internal hemorrhages, with sever decrease of white blood cells. Mortality was shown to be due to heart failure [17].

MDV or *Gallid herpesvirus 2* (GaHV-2) is an alphaherpesvirus and comprises oncogenic strains (RB-1B, MD5, GA, etc.) and non-oncogenic strains as CVI988 / Rispens. The GaHV-2 can be further classified into four pathotypes which are vary from mild (m) to very virulent plus (vv+) pathotypes [18]. Both GaHV-3 and *Melagrid Herpesvirus* 1 (MeHV-1) are mildly pathogenic strains and show an antigenic cross-reactivity to GaHV-2 (Figure 3) [19, 20].

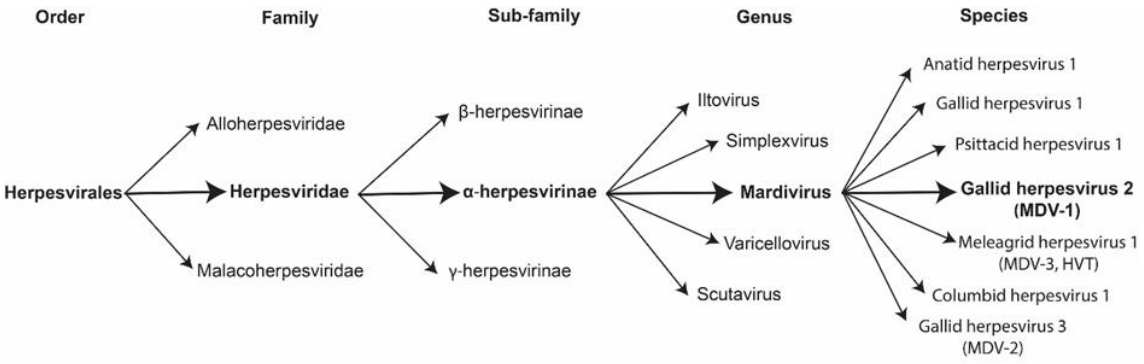

Figure 3. Schematic representation for classification and taxonomy of herpesviruses. Gallid herpesvirus 2 or MDV taxonomy is tracked through bold arrows.

4.1.1 Structure of the herpesvirus genome

Herpesvirus genome is large, linear, double-stranded DNA, and harbors more than 200 proteins [21]. The large genome consists of unique region (U) that is flanked by repeat region (R). *Roizman and Knipe* summarized the classes of the herpesvirus genome structure from A to F (Figure 4). Class A consists of a unique region sequence (U) that is flanked by relatively large repeats. Class A is represented in betaherpesviruses (HHV-6) [22, 23]. In class B, the direct repeats are located at the genome termini and consist of multiple copy numbers of the tandem repeated sequences. The repeated regions might reach to 30% of the DNA molecule. This class is represented in gammaherpesviruses as HVS and HHV-8

[24, 25].Class C is a modified arrangement from class B, where the internal sets of the direct repeats are present but unrelated to the terminal repeats. EBV, gammaherpesvirus, displays this genome class [26]. Class D genomes comprise two unique regions: unique long region (U_L) and unique short region (U_S). These regions are flanked by terminal and internal (inverted) repeats long and short (TR_L/IR_L and TR_S/IR_S). Alphaherpesviruses have this kind of genome are represented by members of varicellovirus genus, such as PRV and VZV [27, 28]. Class E is similar to D except that the TR_L/IR_L is much larger. The larger repeat regions and segment inversions resulted in presence of four gene isomers [29, 30]. Class E is the most complex genome arrangement and was firstly described for HSV-1. MDV has a class E genome [31]. Class F is lacking the repeats and is most common in betaherpesviruses [32, 33].

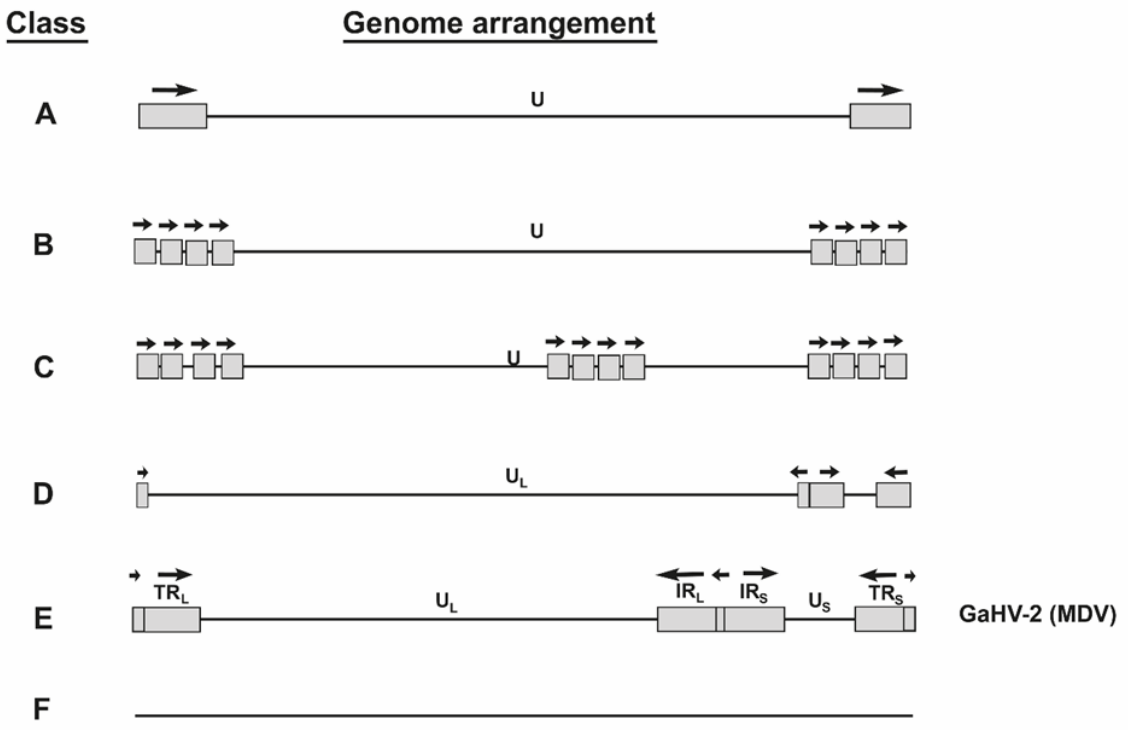

Figure 4. Classes for herpesvirus structure. Unique region sequences are indicated by U, the repeats are indicated by R. The orientation of the repeated sequences is indicated with arrows. L long, S short, I internal, T terminal. Modified from Arvin et al. [34]

4.1.2. Overview of herpesvirus replication cycle

Several studies have been carried out on the HSV-1 replication cycle, which makes HSV-1 a model for herpesvirus replication (Figure 5) [35] while on the other hand, the knowledge about MDV is still quite limited. HSV-1 replication starts with the binding of the virus envelope to the host cell surface, resulting in a fusion. Following the fusion event, the

nucleocapsid enters the cytoplasm and travels to the nuclear membrane [36]. Several viral envelop-glycoproteins such as glycoprotein C, B, D, H, and L, are crucial in the virus entry and fusion through the interaction with several cellular receptors. In HSV-1, the fusion is mediated by the binding of glycoprotein C (gC) and B (gB) with several glycosaminoglycan (GAGs) surface receptors [37]. On the other hand, glycoprotein D (gD) is important for the viral entry in the host specific cell. It has been reported that gB and gD can complement the functions of gC in the initiation of MDV binding [38]. Furthermore, a spliced form of gC that is deficient in its transmembrane domain, make the majority of MDV gC secreted into the cell culture supernatant [39]. In case of HSV-1, the receptors Nectine-1 and herpes virus entry mediator (HVEM) facilitate the binding [40]. Following the attachment of gD to the cellular receptors, conformational changes happen in gD resulting in interaction with other glycoproteins as gH and gL which leads to formation of a complex [40]. This complex facilitates the virus entry by mediating the fusion of the envelop to the cellular membrane and the delivery of the viral capsid into the cell [40]. The virion tegument separates and the capsid goes directly towards the nuclear membrane [35] where the viral genome is delivered into the nucleus where it becomes circularized [41]. Some viral genes have a role in the transportation of the viral DNA into the nucleus such as UL36 gene that encodes for the tegument protein VP1/2. The VP1/2-proteins display nuclear localization signal (NLS) and responsible for the delivery of the viral capsid to the nucleus [42].

Following the circularization, another viral protein VP16 which is encoded by UL48 promotes the viral immediate-early (IE) genes transcription, such as ICP4 and ICP27, which are essential for inhibition the cellular defense against the virus [43]. The UL30 gene which expresses the DNA polymerase is involved in the replication as well [44]. The envelop glycoproteins are harmonized in the cytoplasm and are then transported to the nucleus. The capsid is enclosed with the viral genome resulting in new virions (progeny) which is budding through the nuclear membrane to the cytoplasm. In the current model, the alphaherpesvirus final maturation includes the assembly of the tegument and glycoproteins which occurs in the Golgi-Trans-Golgi-network (TGN), while betaherpesviruses need different vesicular structures for their assembly [35]. At the TGN, the mature capsids then get the final envelop and are subsequently transported to the cell membrane in vesicles. From here, the virus particles are ready to be released [35]. In MDV, for some instances, the replication cycle is not fully understood because MDV is a cell-associated virus and there are huge difficulties to track the virus on avian cells due to the lack of the knowledge required for that purpose. Actually, three steps of the virion morphogenesis are deficient in MDV: the exocytosis process, transportation from the nucleus and the secondary envelopment [45]. The exact mechanism how MDV spreads form infected to uninfected cells *in vivo* is poorly understood.

However, it is assumed that the MDV-encoded glycoproteins gB and gD interact with the host cell receptors and form an intracellular bridge which contributes to the cell associated viral spread [46].

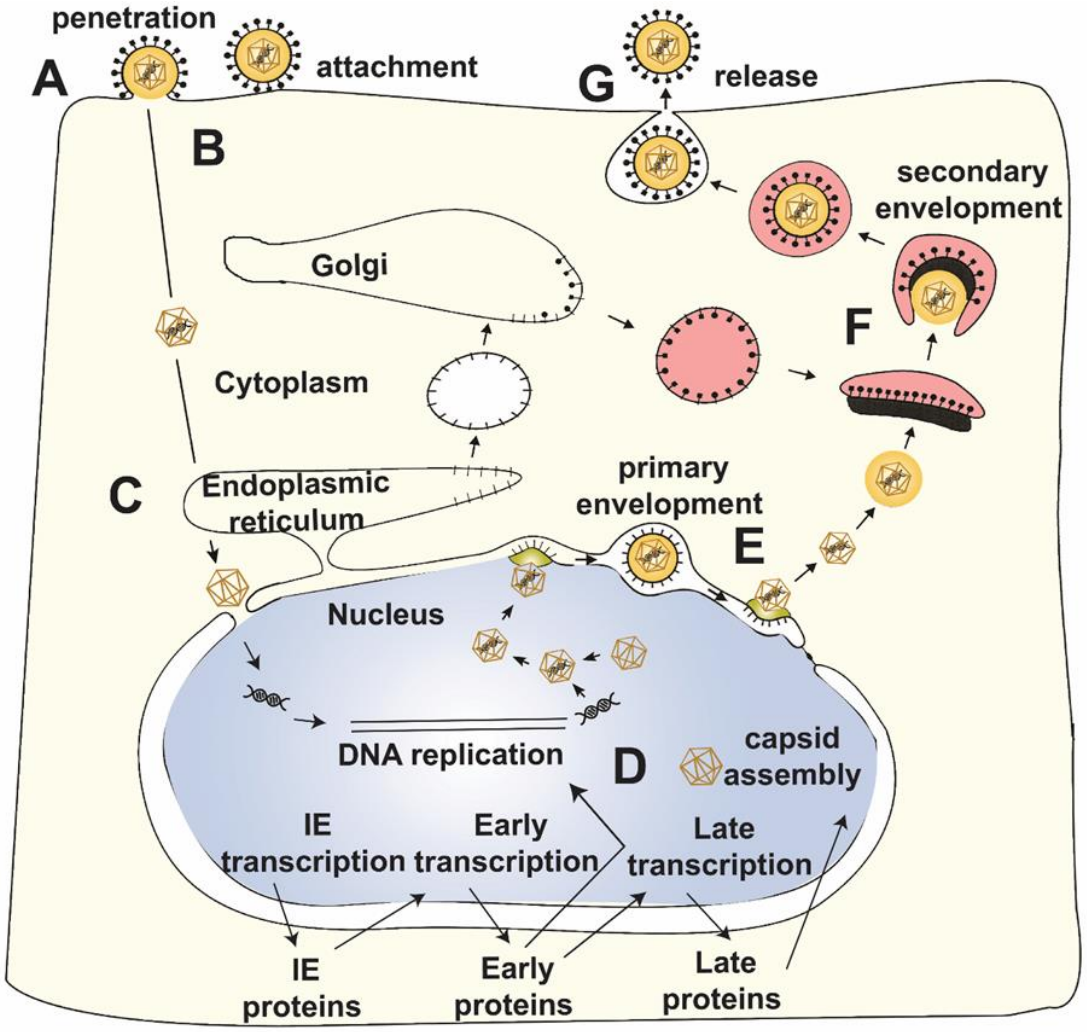

Figure 5. Schematic representation of the herpesvirus lifecycle. A. Virus attachment and penetration: the virus binds to specific receptors on the cell surface. B. Travelling of the nucleocapsid to the nuclear membrane. C. Release of the viral DNA from the nucleocapsid and enters the nucleus. D. DNA synthesis (rolling circle replication) in the nucleus results in concatamers. E. Primary envelopment where the capsid is getting released from the nuclear membrane. F. Final maturation at Golgi-TGN. G. Mature viral particles are released from the cell. Modified from Mettenleiter 2004 [35].

4.1.3. Herpesvirus latency

Latency is a characteristic biological property for herpesviruses which generally means that the virus genome stays dormant within the host cell without replication. The factors responsible for switching between lytic and latency and how can the host cell maintain the

viral genome during latency remain mystery and need further investigations [47]. Later on the virus can reactivate and initiate the replication cycle. The animal model studies demonstrated that the HSV-1 latency occurs in the neuron [48, 49]. Once the virus is in a latent phase, it is assumed that no viral transcripts or protein can be detected. However, it has been shown that some HSV-1 transcripts, called latency-associated transcripts (LATs) were detected during both active and latent infections [50, 51]. Yet, the exact role of those LATs is poorly understood. HSV-1 mutants that lack LATs were able to establish latency [52, 53] , although decreased reactivation frequencies had been reported for these mutants [54, 55]. The reactivated virus produces less clinical symptoms and lesions compared to the primary infection[15]. MDV, as a member of alphaherpesviruses, establishes latency in T-cells. Intriguingly, the MDV latently infected cells are the same that can eventually be transformed but the exact mechanism in not completely known. One of the important factors that facilitates MDV genome maintenance during the latent infection in T-cells, is the genomic integration [56]. On the other hand, the peripheral blood monocytes and bone marrow-derived monocytes represent the target site of latency establishment for betaherpesviruses (like CMV) [57]. In gammaherpesviruses, it has been reported that B-cells represent the site of latent infection. For example, EBV-latency is required for EBV-induced malignancies including; Burkitt's lymphoma (BL), B-cell lymphomatosis and Hodgkin's disease [58].

4.2. Marek's disease

Marek's disease (MD) is a devastating, immunosuppressive disease that is characterized by paralysis of the major nerves, lymphoma formation in the visceral organs and musculature, and blindness in chickens [59]. MD is caused by MDV [60]. The infected chickens develop clinical symptoms between 10-40 days post-infection depending on the virus strain, bird genotype, and the flock immunity [5]. MD mortalities can reach up to 100% in non-immunized chickens, causing severe economic losses [61].

4.2.1. Characteristic and historical prospective

MD was firstly described in four adult cockerels and diagnosed by Dr. Joseph Marek, a renowned veterinary clinician and the head of the department of Veterinary Medicine at the Royal Hungarian Veterinary School in Budapest. The cockerels suffered from paralysis of wings and legs and Dr. Marek decided to perform a detailed examination. He observed that the sacral plexuses were enlarged and infiltrated by mononuclear cells [61]. He termed the disease as a "neuritis interstitialis" or a "polyneuritis". Another case was described by Kaupp in the USA (1921) and Van der Waller and Winkler-Junius (1924) in the Netherlands, where

they reported pathological changes in the central and peripheral nervous system of chickens, a disease they called, “fowl paralysis” [62]. The next study was very important and had been performed by Pappenheimer et.al. in 1926 [63, 64]. They found that apart from the nervous lesions, 10% of the chickens had lymphoid tumors in different organ-systems such as ovaries, liver, kidneys, lungs, and muscles. For that reason they found that the previous terms of the disease were not satisfactory and they suggested ”neuro-lymphomatosis gallinarum” for the disease and “visceral lymphomatosis” for the visceral tumors [63, 64]. At the same time, both Ellerman and Bang were performing studies on neoplastic conditions in chickens called leukosis [62]. Then the poultry industry expanded in the 1950s and the incidence of MD and leukosis increased as well. Clinicians got confused with MD and leukosis at that time because the diagnosis was based only on the pathological examination and it was very difficult to distinguish between the visceral lymphoma of MD and leucosis [62]. By that time both MD and leukosis were described with the general term “lymphomatosis” which was widely used to describe all lymphoproliferative diseases in chickens [65, 66]. In 1960, the World Veterinary Poultry Association organized their first symposium and they selected classification of the avian leukosis complex and fowl paralysis to be the major issue [62]. In this symposium, the two European scientists Campbell and Biggs suggested the separation of the two terms and Biggs suggested MD for the fowl paralysis [67, 68]. The disease after that has been distributed widely among chicken populations and it got markedly more severe than the rather mild form of MD which Biggs described as a classical MD [62]. The disease got somehow controlled in 1970s with the introduction of vaccines albeit the vaccine did not completely protect the chickens against the severe infections [69, 70]. Later on and until now the clinical picture of MD is changing from one time to another and the disease appears in vaccinated flocks. Some outbreaks even displayed with unusual clinical signs as ocular lesions [71], early mortality without development of lymphomas, and encephalitis [72]. The current commercial vaccines protect the chickens from developing tumors but they don’t provide a sterile immunity. This obviously is the reason for recurrent infections occurring in immunized chickens flocks [6, 73].

4.2.2. Clinical manifestations

MD infections display a wide range of symptoms in susceptible chickens but chickens with lymphoma and paralysis present a typical clinical picture of MD [74]. In general, the infected chickens suffer from paresis that can develop into paralysis of one or more of the extremities due to the peripheral nerve malfunctions [75]. The involvement of the vagus nerve results in crop dilatation and respiratory signs. The typical MD picture in chickens is presented by one leg stretched forward and the other stretched back due to unilateral paralysis of the leg

(figure 6A) [75]. Another picture due to the nervous manifestation that can be observed in MD infections is the torticollis that displays 18-26 days after infection [76]. Chickens with MD lymphomas exhibit few clinical signs and often show depression and somnolence prior to death [75]. Some chickens may look normal but still have tumors in different body organs when necropsied. Non-specific signs also recorded in chickens infected with MD such as weight loss, anorexia, indolence, and diarrhea especially in more chronic infections. Additionally, birds also show ocular signs that may develop into blindness [77] which can be uni-or bilateral. The affected eyes may lose the ability to harmonize to the light intensity [75]. The succumbed chickens cannot reach the feed pin or the drinkers due to the paralysis of their legs which can result in death. It has been observed that two common forms for MD appear in the field: an acute form which is characterized by death within 24-72 h following paralysis symptoms [78], and a classical form which causes ataxia and paralysis of the neck or the limbs 8-12 days post infection [78]. Lymphoma can be found in one or more organs and tissues like spleen, kidneys, intestine, lungs, heart, liver, gonads, bursa, thymus, pectoral muscles, and skin (figure 6B) [75]. Tumors can occur without nervous manifestations. Tumors appear as focal, nodular growths which are variable in size or as diffuse enlargements with white or grayish discoloration [75]. Development of large tumors on the ovaries can lead to ovarian dysfunction and the normal foliated appearance of the ovary becomes cauliflower-like [75]. Similarly, other organs such as proventriculus (becomes thick due to the aggregations of the infected lymphocytes), liver (exhibiting granular appearance which is accompanied with the loss of normal lobule architecture), and muscles (primarily regions in the pectoral muscles) can be affected with the disease [79]. Mortalities due to MD can be up to 100% depending on the virus strain, host gender, maternal immunity, host genetic background, age, and environmental factors and stress [75]

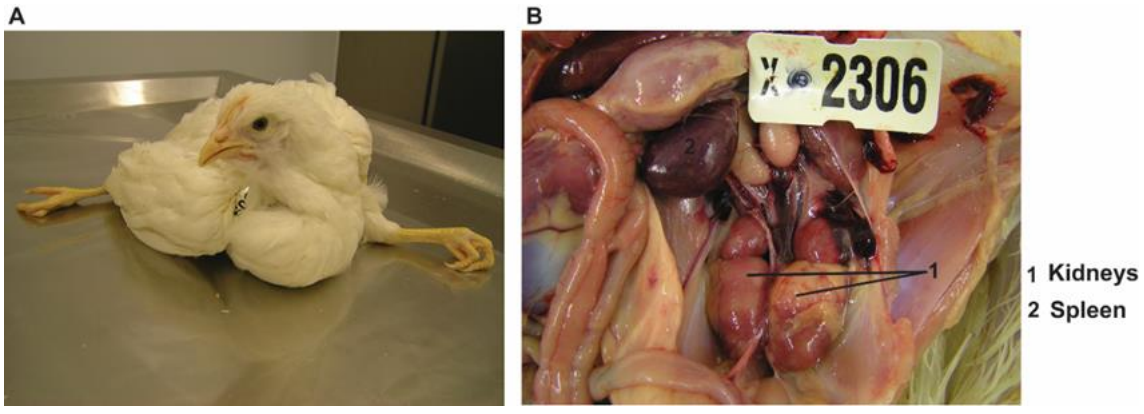

Figure 6. Clinical signs and gross lesions of MD. A. Ataxia which is a characteristic and specific clinical picture of MD due to the enlargement and inflammation of sciatic nerve B. Enlargement of kidneys and spleen due to extensive neoplastic lesions. Organs with gross tumors are indicated in

numbers 1 and 2.

4.3. Marek's disease virus (MDV)

4.3.1. MDV genome structure

MDV, an alphaherpesvirus that classified under the genus *Mardivirus,* has three different serotypes that have been recognized by using monoclonal antibodies that raised by the immune system of the host after infection [80] ; A. The oncogenic serotype 1 strains (RB-1B, GA, CVI988 and Md5) B. Non- oncogenic serotype 2 strains (SB1,HPRS24), and C. serotype 3, (HVT-vaccine strains), known to be non-pathogenic for chickens [7]. Serotype 2 and 3 do not cause MD symptoms or lymphomas but they are antigenetically related to serotype 1 and can be used to protect the chickens against oncogenic serotype 1 infections [81, 82]. MDV serotypes were initially analyzed by gene sequencing which revealed that both MDV serotype 1 and HVT possess similar structures as HSV-1 and VZV which suggested that they should be classified as alphaherpesviruses [83]. The MDV genome is classified as a class E genome and is 175 to 180 kb in size. It consists of unique regions termed unique long (U_L) and unique short (U_S) flanked by repeat regions termed terminal repeat long (TR_L) and terminal repeat short (TR_S) with the corresponding internal repeat long (IR_L) and internal repeat short (IR_S) (figure 7) [84]. The oncogenic MDV serotype 1 encodes the major oncogen *Meq* (MDV-EcoRI-Q), and some genes that are particularly not encoded in serotypes 2 and 3 such as; pp38, vIL8, and vTR [82, 85]. The later genes are important for the malignant activities induced by MDV.

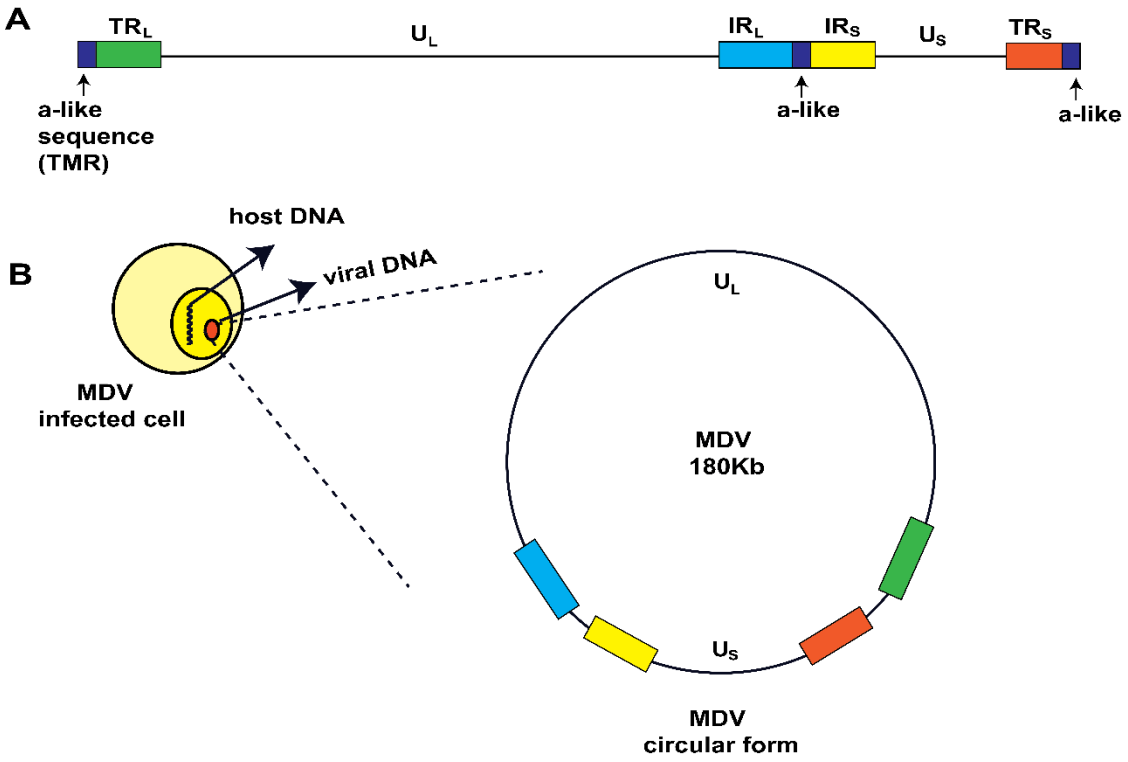

Figure 7. Schematic representation of a linear and a circular MDV dsDNA. A. The linear MDV genome (non-integrated state) consists of unique regions U_L and U_S flanked by terminal repeat regions TR_L, TR_S and internal repeats IR_L and IR_S. Telomeric repeat sequences (TMRs) and alpha-like sequences (a-like) which are located at the genome termini and at the junction between IR_L and IR_S (indicated in dark blue boxes). B. MDV dsDNA during replication (circular form of MDV). (Modified from Osterrieder, et al., 2006) [6].

4.3.2. MDV pathotypes

Only MDV serotype 1 induces a virulence or tumors in the infected chickens, however, the pathogenicity within serotype 1 is ranged from nearly a virulent to very virulent [75]. The evolution of MDV virulence has been identified but the molecular mechanism is not completely understood. There are four groups of viruses according to the current pathotypic pattern; mild (mMDV) such as CVI988 [87] , virulent (vMDV) such as JM, GA, and HPRS-16[88, 89], very virulent (vvMDV) such as RB1B and Md5 [90, 91], and very virulent plus (vv+MDV) such as RK-1 and 648A strains [86]. The MD with classical form which characterized by paralysis in the infected chicken caused by mMDV pathotype and followed by virulent form vMDVs in the late of 1960s, while the vvMDVs was initially identified in the late 1970s and that was in HVT-vaccinated flocks which resulted in vaccination by bivalent vaccine [75]. The vv+ appeared in early 1990s and displays the common MDV pathotype with the vMDV until now. Serotype 2 and 3 remains non-oncogenic and used as a vaccine against serotype 1 (figure 8).

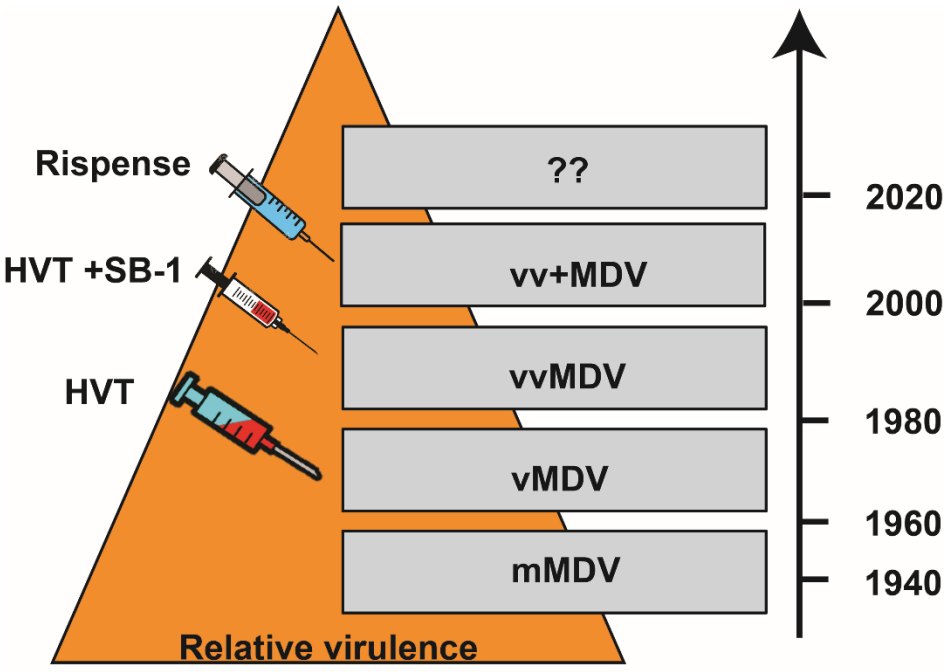

Figure 8. Schematic representation of MDV pathotypes evolution in USA poultry industry from 1940 until now. Different MDV pathotypes are indicated. HVT vaccine was introduced to protect the chickens against mMDV infection and later on bivalent (HVT and serotype 2 SB-1) was used against vvMDV and Rispense (CVI988) used until present time. (Modified from Nazerian et., al., 1996 [92]

4.3.3. MDV pathogenesis

As MDV is a cell-associated virus, in order to spread from cell to cell *in vivo*, the contact between infected and non-infected cell must occur. The nature of the interaction between these cells is not completely understood [75]. Four general types of virus-cell interactions are known for MDV pathogenesis: i) early cytolytic infection (2-7 dpi), ii) latency (7-10 dpi), iii) late cytolytic infection (18 dpi), and iv) transformation (28 dpi) (figure 9) [93]. Chickens are infected via inhalation of virus contaminated dust particles from the environment, and then the virus is transmitted to primary lymphoid organs through macrophages or dendritic cells recruited in the lung epithelium [94]. Viral replication happens initially in bursa of Fabricius and thymus resulting in atrophy in these organs due to apoptosis of the infected cells [95]. Moreover, MDV also replicates in spleen which displays a major site of replication, leading to hyperplasia or enlargement which is followed by necrosis of the organ. The host induces immune response to contain and diminish virus replication. Upon this immune response, the virus establishes latency mainly in CD4+T cells [96]. In the latent state, the viral lytic genes are not expressed and latently infected cells proliferate and could be transported to the peripheral sites where the virus reactivates (feather follicle epithelium FFE, Schwan cells, etc). The transformed T-cells proliferate in the host body causing tumors that could disseminate to most of the internal organs [97]. It has been shown that MDV genome

integrated into the host chromosomes for all lymphoma established-cell lines. Furthermore, the meq gene plays a crucial role in MDV-induced transformation of latently infected cells [5]. Meq is the major oncogene that is encoded by MDV and it can modulate the host genomic activity. Additionally, previous studies performed on Md5 pathotype revealed that Md5-lacking meq mutants replicated efficiently *in vivo* and *in vitro*, however, tumor formation was extremely abrogated in the chickens infected with the meq-deleted virus compared to the wild-type underlining that meq is an essential gene for MDV-induced tumorigenesis [98].

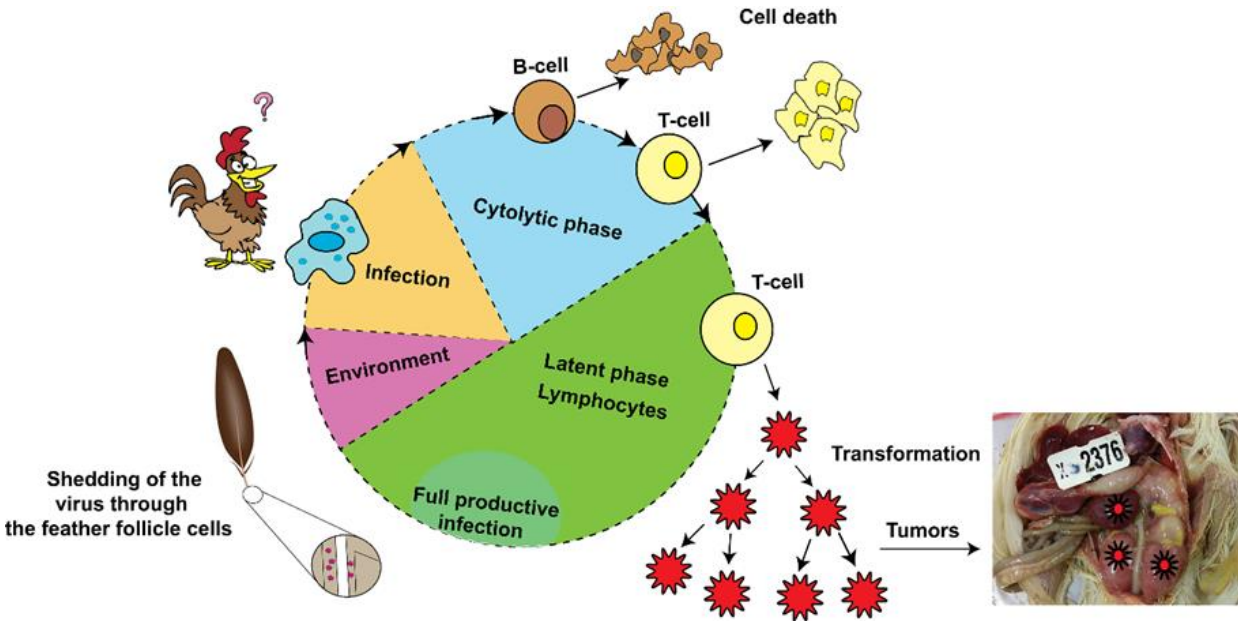

Figure 9. Cornell model of MDV infection *in vivo*. Initially chickens get infected via inhalation of infected dust particles. In the lungs, the virus infects macrophage or dendritic cells which migrates to spleen and lymphoid organs. Eventually infected B-cells will die due to lytic replication, while others will transmit the virus to T-cells. In those cells, the virus undergoes cytolytic replication followed by the establishment of latency in T-cells. T-cell will be transformed resulting in lymphomas formation, which spreads to other organs, leading to metastasis. MDV also could reactivate and this happen in FFE producing the infectious viral particles. Modified from Baigent et al [99].

4.3.4. MDV-induced lymphomagenesis

The MDV-mediated cellular transformation process is not fully understood. The current model for transformation, as well as the virus-cellular interaction, is based on the relative understanding of MDV-biology [100]. In general, following viral lytic replication, T-cells become activated and switch into latently infected cells at 10-14 days post infection. The factors involved in the transition of the latently infected cells to transformed cells remain unknown due to the lack of appropriate markers that can distinguish the MDV-transformed cells. However, in the current model, the exact state of T-cells is correlated to expression of

different oncogenes encoded by the virus [100]. The transformed cells harbor different set of viral gene products such as Meq splice variants, viral miRNAs, UL36, as well as the constitutive expression of vTR (figure 10). These genes are found to be abundantly expressed in the MDV- tumor cells [100]. Additionally, the continued expression of Meq-splice variants lead to effect on T-cell phenotype via CtBP-1-mediated repression of specific loci resulting in transforming T_{reg} cell, from which the virus can reactivate [100] (figure 10). Factors that are expressed for the cells provide the tumor microenvironment and suppress the antitumor responses. MDV has been thought to induce multiple-monoclonal tumors [56, 101].

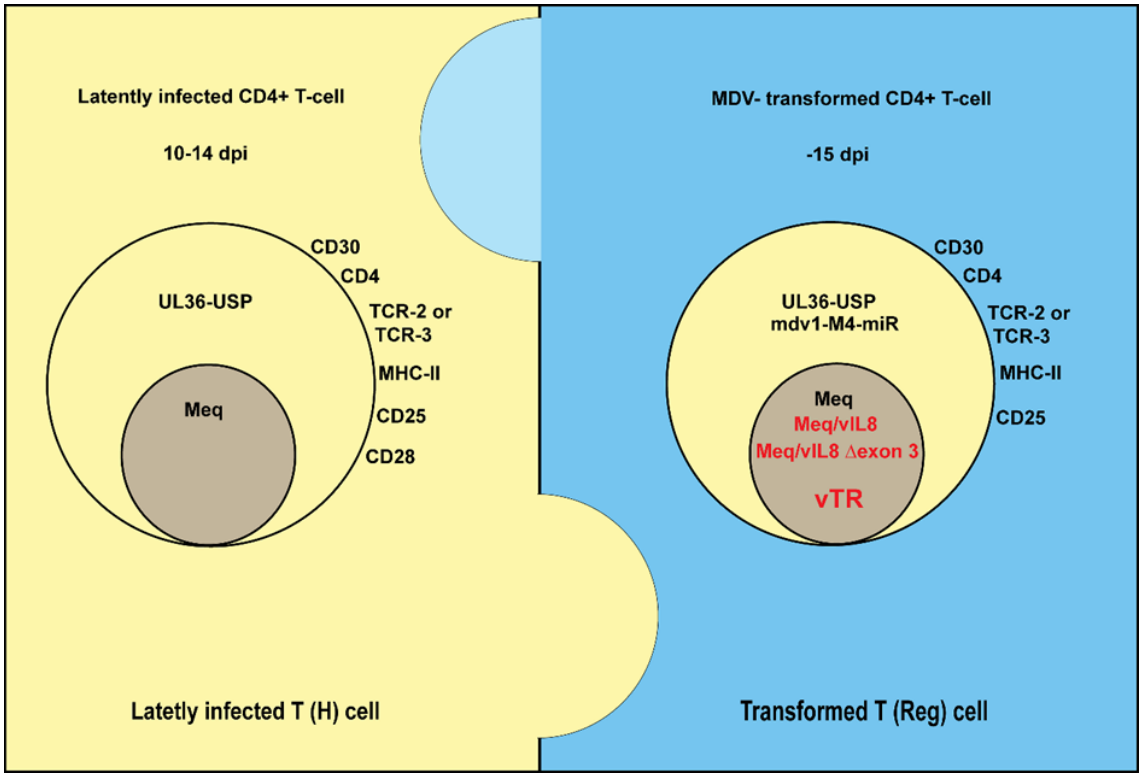

Figure 10. Schematic representation illustrating model for MDV-induced lymphomagenesis. The latently infected cell becomes transformed approximately 15 dpi, the factors responsible for inducing transformation in latent cells are not clear. The viral genes products determined the state of the cells according to the present model. Meq splice variants, miRNA, and vTR are found to be highly expressed in the transformed cells so far. There are no available cell markers to provide a precise tool to differentiate between the latently infected and transformed T-cells by MDV. Modified from Parcells, et, al., 2012 [100].

4.4. Telomeres and Telomerase

Telomeres are tandem nucleotide repeats of $(TTAGGG)_n$ at the ends of the linear chromosomes of vertebrates including mammals and birds [1]. The repeat sequences are

associated with a number of proteins that together form a shelterin complex. Telomeres are essential for chromosome stability and prevent chromosomal rearrangements [102]. The telomerase complex is maintaining the telomere length through the addition of the repeats to the end of the chromosomes [3]. Both of the stem cells and the progenitor cells, type of origin of cancer formation, are expressing telomerase [103]. Telomerase activity is essential in tumor development as rapidly dividing cells as cancer cells are dependent on efficient telomere maintenance [104]. Telomerase is a ribonucleoprotein complex that contains two main components; TERT and the telomerase RNA (TR). In the majority of human cancers, the telomerase is up-regulated in order to maintain the telomeres and this mainly depends on TERT expression suggesting that TERT is the limiting component of the telomerase activity [105]. However, the role of the constitutively expressed TRs in cancer development remains elusive. TRs consist of eight highly conserved regions (CR1-CR8) which have 90% or greater identity and have conserved binding-motifs in vertebrates, from humans and chickens [106]. Several oncogenic viruses such as human T-cell lymphotropic virus (HTLV), human papillomavirus (HPV), hepatitis C virus (HCV) as well as herpesviruses; Epstein-Barr virus (EBV) and Kaposi sarcoma-associated herpesvirus (KSHV) have an effect on the telomerase activity during the infection; however, they are lacking telomerase components [7]. MDV is the only known virus that harbors a telomerase RNA subunit gene, termed (vTR) [7].

4.4.1. MDV telomerase RNA (vTR)

vTR genes are represented by two copies in the TR_L and IR_L region of the MDV genome (Figure 11A) and located between the telomere sequences (TMR) and the vIL-8 gene [107]. vTR is incorporated into the chicken telomerase complex and enhances its activity [108]. vTR shares 88% sequence identity with the chicken telomerase RNA (chTR) [107]. Compared to chTR, vTR enhances a higher telomerase activity when combined with the chicken TERT [107]. In general, vTR secondary structure consists of four main structural domains that are conserved in all TRs sequences (figure 11B) [8]. The pseudoknot (core) domain that contains the template sequence (CR-1) for extension of the telomeric repeats [109]. The CR4-CR5 domains that are essential for interaction with TERT [109]. The H/ACA box and CR-7 domain are responsible for TR stability and localization. Studies showed that mutation of the H/ACA box results in decreased telomerase activity [107, 108, 110]. Furthermore, it has been demonstrated that the overexpression of vTR can transform the chicken fibroblast cell line DF-1 inducing a phenotype similar to that induced by MDV major oncogene Meq [111] underlying that vTR plays an important role in MDV-induced cellular transformation.

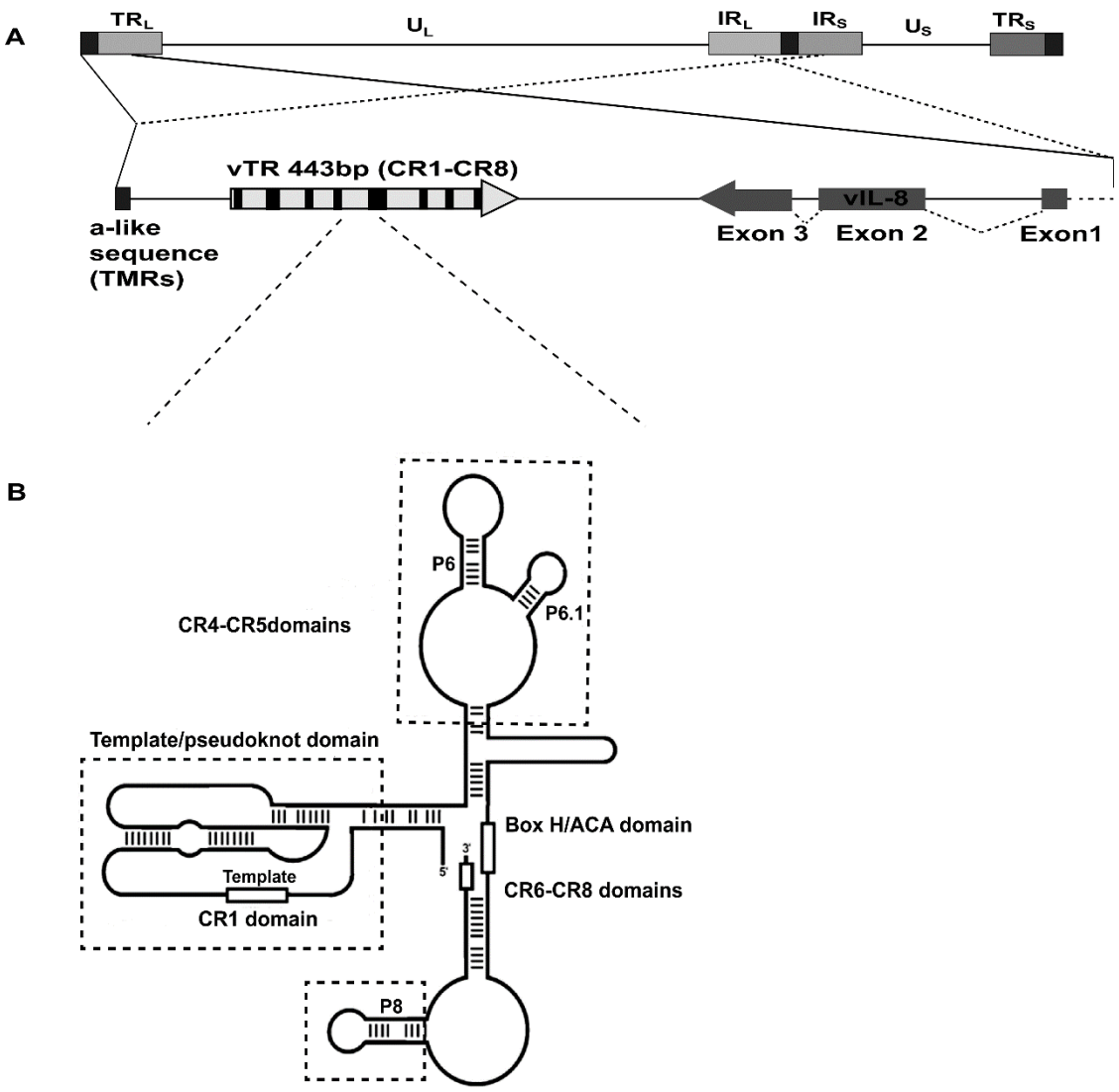

Figure 11. MDV genome overview illustrating vTR region. A. Schematic representation showing vTR region with the entire conserved regions (CR1-CR8) and the three exons of the neighboring vIL-8 gene. B. Secondary structures of MDV vTR. The conserved domains are shown that present also in cellular TRs (chTR).

4.4.1.1 Role of vTR in tumorigenesis

It has been shown that vTR plays a crucial role in MDV-induced tumorigenesis [8]. Recombinant MDVs lacking the major part of vTR (ΔCR1-CR4) were generated and characterized *in vitro* and *in vivo* [8]. Recombinant viruses lacking vTR were replicating efficiently comparable to parental virus *in vitro* and *in vivo*, implying that vTR is dispensable for lytic replication [8]. Tumor formation in the infected chickens was extremely reduced in the absence of vTR [8]. Furthermore, the deletion of vTR resulted in a decreased tumor size and less dissemination into other organs. In addition, the over-expression of vTR increased the cellular proliferation and induced up-regulation of the cell-surface adhesion molecule integrin

α-V, suggesting functions beyond its role in telomerase activity [8]. It is not known also if vTR can support the MDV-integration into the host chromosomes. However, the mechanism of vTR in MDV-induced tumor formation is not completely understood.

4.4.1.2 vTR expression levels

vTR is highly expressed during all stages of the virus lifecycle including the virus replication, persistent infection and in MDV-tumor cells [8]. Compared to the chTR promoter, the promoter of vTR in MDV genome has a much higher activity [112]. vTR promoter is crucial for its function [112], as the replacement of the vTR promoter with the chTR promoter in the MDV-genome resulted in reduction of the tumor development compared to the wild-type [112]. Furthermore, the exchange of the vTR promoter resulted in smaller tumors and less disseminated compared to the wild-type. [112].

4.4.1.3 Telomerase independent functions of vTR

A previous study was performed in order to determine whether the vTR function(s) in MDV-induced tumor formation is dependent on its role in the telomerase complex [113]. Recombinant MDVs-carrying mutations in vTR-P6.1-stem-loop were generated. These mutations resulted in abrogation of the vTR-incorporated telomerase activity hence the stem-loop contributes to the formation of proper telomerase complex via vTR-TERT interaction [7]. The generated mutants replicated efficiently *in vitro* and *in vivo* [113]. Tumor development in the animals infected with the vTR P6.1 mutants had no significant difference when compared to those infected with the wild-type, nevertheless, the onset of the tumor development was significantly delayed [113]. Furthermore, the mutation of P6.1 stem-loop of vTR did not alter the tumor dissemination compared to the wild-type virus. This study provided the first description of the telomerase independent functions of vTR in MDV-induced transformation suggesting new function(s). Additionally, vTR has been shown to interact with and affect the localization of the cellular protein RpL22 (Ribosomal Protein Large subunit 22) [114] which plays an important role in T-cell development and lymphoma formation [115, 116].

4.5. RpL22 and its interaction partners

RpL22 is a component of the 60S ribosomal subunit and estimated to be present at roughly 10^7 copies per cell [117]. Ribosomes lacking detectable levels of RpL22 are translationally active *in vitro*, indicating that RpL22 is not essential for ribosome activity, but rather plays a regulatory role [118]. RpL22 has been reported to act as a tumor suppressor in T-cell acute lymphoblastic leukemia/lymphoma (T-ALL), as the mono-allelic loss of RpL22 accelerates T-cell lymphomagenesis [116]. Furthermore, it has been recently shown that RpL22 controls the

dissemination pattern of T-cell lymphoma [115]. RpL22 not only interacts with vTR but also with the Epstein-Barr virus-encoded RNA 1 (EBER-1) (figure 12) [114] and this EBER-1-RpL22 interaction plays a role in EBV-induced transformation [119].

4.6. Epstein-Barr virus-encoded RNAs (EBERs)

EBERs (EBER-1 and EBER-2) are two small non-coding RNAs encoded by EBV and they are 166 and 172 nucleotide long respectively with primary sequence identity of 54% and a high similarity in their secondary structures. EBERs are highly expressed in EBV-latently infected cells but their functions are not fully understood [120]. EBERs contribute to malignant phenotypes and resistance to apoptosis in BL cell line [121] and [122]. The sequence conservation of EBERs is interpreted to be important for EBV persistence [123]. EBER-1 is highly conservative among different EBV strains while EBER-2 has two base substitutions within its sequence and eight are outside the coding regions [124]. Although EBERs are transcribed at comparable levels (10^7 copies) per EBV-infected cell [125], EBER-1 has been detected to be transcribed higher than EBER-2 [126]. The functions of EBERs are thought to be dependent on the interaction with some cellular proteins and assemble stable ribonucleoprotein particles such as; (La) which is necessary to facilitate the correct folding and maturation of RNA polymerase III [127], double-stranded-RNA-activated protein kinase PKR [128]. EBERs-induced PKR inhibition is important for EBV persistence [129], and RpL22 [130]. Approximately 30-50 % of RpL22 is found to be associated with EBER1 (figure 12) [131], resulting in the re-localization from the nucleolus to the nucleoplasm. EBER1-RpL22 interaction plays an important role in EBV-induced transformation [132]. Several studies showed another role of EBERs in oncogenesis through different processes as increase of cell-proliferation [133] and [134], inhibition of apoptosis [121], [135] and [129], and induction of tumor formation [121], [136], [129] and [137]. However, the exact mechanisms for these processes are still unclear. Until now it is not known whether these functions are representing the exact role of EBERs in the viral persistence or they have another contributions in the viral induced transformation.

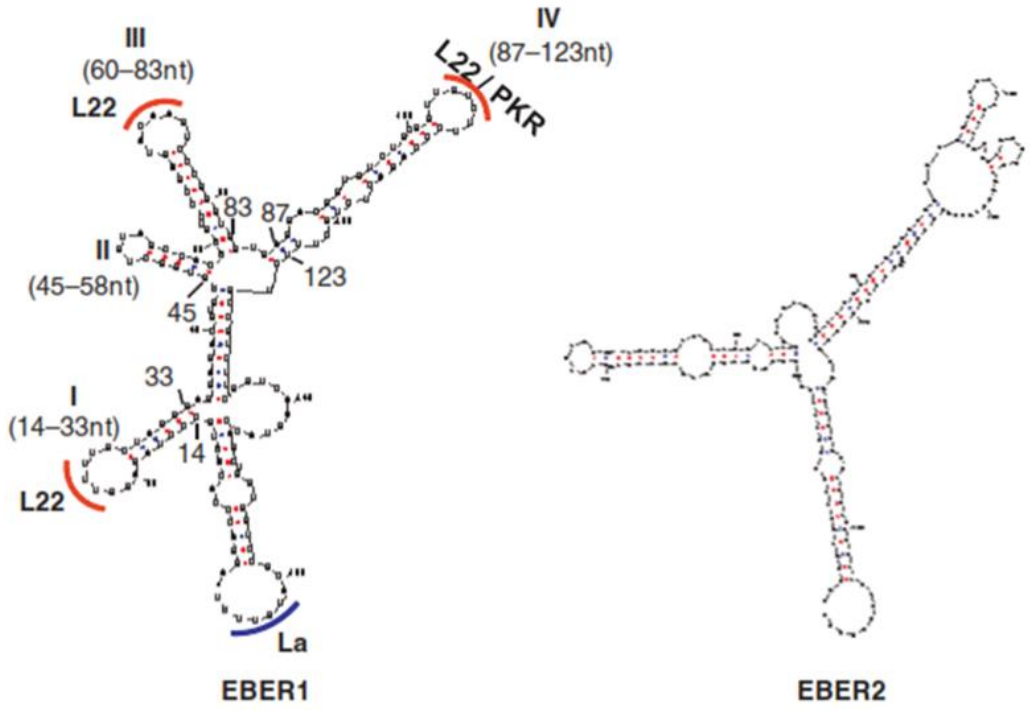

Figure 12. Secondary structures of EBV-EBERs (EBER-1 and EBER-2). This figure illustrate the high similarity between EBERs secondary structures underlying that their secondary structures are important for their functions. EBER-1 has affinity to bind multiple cellular proteins. Three binding sites are recognized for RpL22 for EBER-1 (I, III, and IV). From Rosa, et al., 1981 [138].

4.7. Project outline

Until now, the role of TRs in tumorigenesis is not completely understood. The high sequence identity between vTR and chTR, leads to speculations that vTR was pirated initially form the chicken genome. Furthermore, recent work has been demonstrated that the overexpression of human telomerase RNA (hTR) has anti-apoptotic role in human immune cells independently of its role in telomerase enzymatic activity [139]. In this prospective, our aims would be to evaluate the tumor promoting-functions of the overexpression of cellular TRs (chTR). Similarity, the interaction partners between vTR and EBER-1 are highly conserved (97.7% consensus position), suggesting a conserved mechanism for both viral RNAs. We hypothesized that over-expression of chTR and /or EBERs has tumor-promoting functions and can complement the loss of vTR in MDV-induced tumor formation using a small animal model for herpesvirus tumorigenesis. This hypotheses were addressed in two main aims as follow (figure 13A):

1. To investigate if the over-expression of chTR promotes tumor development in MDV-induced tumorigenesis.
2. To evaluate the tumor-promoting properties of EBERs using a natural host-virus infection model for herpesviruses tumorigenesis, which helps to determine more contributions of EBERs into cellular transformation.

The novelty of this work that it provides the first description for the tumor-promoting properties of the overexpression of cellular TRs *in vivo*, and offers animal model to study the EBV-carcinogenic components and the underlying mechanisms.

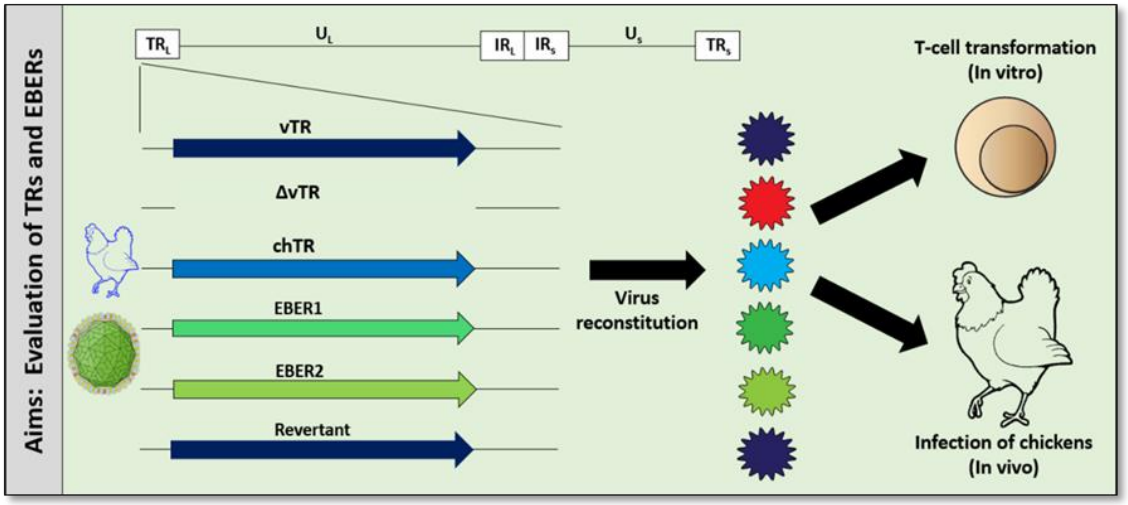

Figure 13A. The role of cellular telomerase RNAs (chTR) and viral RNAs (EBERs) in herpesvirus induced cancer formation. *In vitro* and *in vivo* evaluation the tumor-promoting functions of the host TRs (chTR) and viral RNAs (EBERs) using our small animal model for cancer formation.

vTR is overlapped with another MDV ORF which is ICP0-homologue, the reason that's why the previous study only deleted four CRs from vTR (CR1-CR4) [8]. On the other hand to test whether chTR or EBERs can complement the loss of vTR in MDV-tumorigenesis, this requires the deletion of the entire vTR sequences (CR1-CR8) which means deletion of major part of ICP0. Since no evidences are available about ICP0 whether it plays a role in MDV-pathogenesis, we decided to start first with ICP0 characterization by inserting stop codons and determine if there is any phenotype changes (Figure 13B).

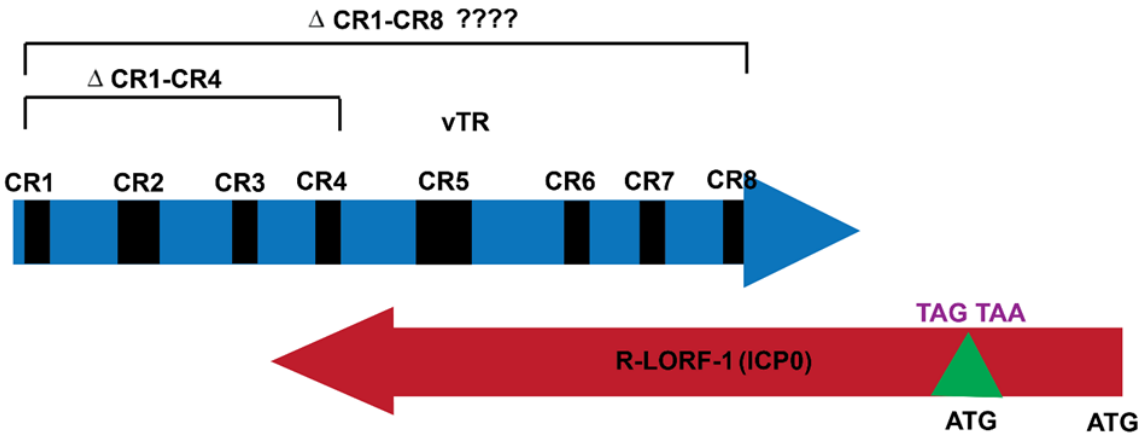

Figure 13B. Schematic representation to determine the role of ICP0 in MDV replication. Insertion of double stop-codon mutations instead of the second start codon and then insertion of HA-tag in the C-terminus of the ICP0-ORF.

5. Materials and Methods

5.1. Materials

The chemicals, enzymes, antibodies, media, and instruments used in this study were used according to the manufacturer's recommendations.

5.1.1. Chemicals, consumables and equipment

5.1.1.1. Chemicals

Chemicals are listed in table 1:

Chemical	Catalog Number	Supplier
Acetone ((CH3)2CO)	Cat. No. A160, 2500	AppliChem, Darmstadt
Agar (agar bacteriological)	Cat. No. 2266.2	Carl-Roth, Karlsruhe
Agarose-Standard Roti® grade	Cat. No.3810.4	Carl-Roth, Karlsruhe
Ampicillin Na-salt	Cat. No.K029.2	Carl-Roth, Karlsruhe
Ammonium chloride (NH_4Cl)	Cat. No. A9493	Sigma-Aldrich, St Louis
Ammoniumpersulfate (APS)	Cat. No. K38297601	Merck, Darmstadt
L-(+)-Arabinose	Cat. No. A11921	Alfa Aesar, Karlsruhe
Biotin RNA labelling mix (10X)	Ref. No. 11685597910	Roche diagnostic, Mannheim
Bromophenol blue	Cat. No. B1793	Alfa Aesar, Karlsruhe
BSA (Albumin Bovine Fraction V)	Cat. No. A6588.0100	AppliChem, Darmstadt
Calcium chloride dihydrate	Cat. No. T885, 2	Carl-Roth, Karlsruhe
Acetic acid (CH_3COOH)	Cat. No. A3686, 2500	AppliChem, Darmstadt
Chloramphenicol	Cat. No. 3886.1	Roth, Karlsruhe
Chloroform	Cat. No. 411K3944831	Merck, Darmstadt
Coomassie Brilliant Blue	Product No. B8522	Sigma-Aldrich, St. Louis
Diethylpyrocarbonate (DEPC)	Product No. A0881	AppliChem, Darmstadt
Dimethyl sulfoxide (DMSO)	Cat. No. 1.02952.2500	Merck, Darmstadt
Dithiotheritol (DTT)	Cat. No. 3483-12-3	Sigma-Aldrich, St. Louis
Dulbecco's MEM (DMEM)	Cat. No. MP0239-TS	Biochrom AG, Berlin
dNTP Mix (10mM)	Cat. No. BIO-39053	Bioline, Luckenwalde
EDTA	Cat. No. A2937, 1000	AppliChem, Darmstadt
Ethidium bromide (1%)	Cat. No. 2218.2	Carl-Roth, Karlsruhe

Chemical	Catalog Number	Supplier
Ethanol	Cat. No. A1613	AppliChem, Darmstadt
Fetal Bovine Serum (FBS)	Cat. No. 10270106	Biochrom AG, Berlin
Formamide (deionized)	Product No. A2156	AppliChem, Darmstadt
Glycerol	Cat. No. A2926, 2500	AppliChem, Darmstadt
HCl 37% (hydrochloric acid)	Cat. No. 4625.2	Roth, Karlsruhe
Isopropyl alcohol (2-propanol)	Cat. No. A0892	AppliChem, Darmstadt
ß-mercaptoethanol	Cat. No.28625	Serva, Heidelberg
$MgCl_2$	Cat. No.5883.025	Merck, Darmstadt
MOPS	Cas.No.1132-61-2	Sigma-Aldrich, St Louis
NaCl (sodium chloride)	Cat. No. A3597, 5000	AppliChem, Darmstadt
NaOH (sodium hydroxide)	Cat. No. 1.06462	Merck, Darmstadt
Opti-mem I	Cat. No. 31985062	Life Tech., Carlsbad
Paraformaldehyde	Cat. No. P6148	Sigma-Aldrich, St Louis
Pepsin	Cat.No. P7012	Sigma-Aldrich, St Louis
PIPES	Cas.No. 5625-37-6	Sigma-Aldrich, St Louis
PMSF	Cas.No. 329-98-6	Sigma-Aldrich, St Louis
(PEI) MW 25,000	Cat. No. 26008	Polysciences, USA
Phenol/Chloroform	Cat. No. A0889, 0500	AppliChem, Darmstadt
SDS (sodium dodecyl sulfate)	Cat. No. 75746	Sigma-Aldrich, St Louis
Sodium Phosphate	Cat. No. S9638	Sigma-Aldrich, St Louis
EZview™ Red Streptavidin Affinity Gel	Product. No. E5529-1ML	Sigma-Aldrich, St Louis
Monobasic, monohydrate di-Sodium Hydrogenophsohate	Cat. No. A3906	AppliChem, Darmstadt
Temed	Cat. No. 2367.3	Roth, Karlsruhe
Tetracyclin	Product No. A2228	AppliChem, Darmstadt
Tergitol type NP40	Cas No. 127087-87-0	Sigma-Aldrich, St Louis
Tris	Cat. No. A1086, 5000	AppliChem, Darmstadt
Triton X-100	Cat. No. 8603	Merck, Darmstadt
Trypsin/EDTA 0, 05%	Cat. No. 25300054	Life Technologies, Grand Island
Tween-20	Cat. No. 9127.2	Roth, Karlsruhe
Water Molecular biology grade	Cat. No. A7398	AppliChem, Darmstadt

Chemical	Catalog Number	Supplier
Yeast extract granulated	Cat. No. 212750	Carl-Roth, Karlsruhe
Yeast tRNA (10mg /ml)	Cat. No. AM7119	Thermofisher scientific

5.1.1.2. Consumables

Consumables are listed in table 2:

Name	Feature	Manufacturer
Cell culture dishes	6-well, 24-well, 96 well	Sarstedt, Nümbrecht
Cell culture flasks	25 ml, 75 ml	Sarstedt, Nümbrecht
Conical test tubes	17x120 15 ml	Sarstedt, Nümbrecht
Conical test tubes 30x115	50 ml, with and without feet	Sarstedt, Nümbrecht
Cryotubes	1.8 ml	Nunc, Roskilde
Eppendorf tubes 1.5 ml	1.5	Sarstedt, Nümbrecht
Electroporation cuvettes	1mm	Biodeal, Markkleeberg
Falcon bacteria	13ml	Sartsedt, Nümbrecht
Falcon tubes	15 ml, 50 ml	BD Falcon, Heidelberg,GER
Latex gloves Size	L	Unigloves, Troisdorf
PCR tube	0.2 ml	Applied Biosystems, UK
Parafilm® M		Bems, Neenah
PVDF membrane		Carl-Roth, Karlsruhe
Whatman blotting paper		GE Healthcare, Freiburg
Petri dish for cell culture	60mm, 100mm, 150mm	Sartsedt, Nümbrecht
Petri dish for bacteria		Sartsedt, Nümbrecht
Pipette tips	(1000, 200, 100 and 10)	VWR International, West
PVDF membrane	Cat. No. T830	Roth, Karlsruhe
Sterile Pipettes for culture	5, 10, 25 ml)	Sartsedt, Nümbrecht
Transfection polypropylene tubes	round, short 17.1 x 105	TPP, Trasadingen

5.1.1.3. Equipment

Equipment are listed in table 3:

Name	Feature / Catalog Number	Company
1. General Equipment:		
Fast Real-time PCR system	ABI Prism 7500	Invitrogen Life technologies Grand Island
Bacterial incubator	07-26860	Binder, Turtlingen
Bacterial incubator shaker	Innova 44	New Brunswick Scientific, New Jersey
Cell incubator	Excella ECO-1	New Brunswick Scientific,New Jersey
Centrifuge 5424	Rotor FA-45-24-11	Eppendorf, Hamburg
Centrifuge 5804R	Rotors A-4-44	Eppendorf, Hamburg
Centrifuge Sorvall RC 6+	F45-30-11	Thermo Scientific, Dreieich
Cytospin3	Shandon	Thermo Scientific, Dreieich
DNA / RNA shearing for NGS- Covaris		Covaris, Inc, USA
Illumina MiSeq		San Diego, California, USA
Imaging system	Chemismart 5100	Peqlab, Erlangen
Electroporator	Genepulser Xcell	Bio-Rad, München
Electrophoresis power supply		VWR International, West Chester
Freezer	-20°C	Liebherr, Bulle
Freezer	-80°C	GFL,Burgwedel
Mini centrifuge	Galaxy	VWR International, West Chester
Gel electrophoresis chamber	SUB-Cell GT	Bio-Rad, München
Heating, mixing, and cooling thermomixer C		Eppendorf, Hamburg
Ice machine	AF100 AF100	Scotsman, Vernon Hills
Pipetboy	INTEGRA	Integrated Biosciences

Name	Feature / Catalog Number	Company
Magnetic stirrer	RH basic KT/C	IKA, Staufen
Gel chambers Mini Protean	2D	Bio-Rad, München
Nanodrop 1000		Peqlab, Erlangen
Newbauer counting chamber		Assistant Sondheim/Rhön
Nitrogen tank	ARPEGE70	Air liquide, Düsseldorf
Orbital shaker	0S-10	Peqlab, Erlangen
Pipets	P1000, P200, P100, P10	Eppendorf, Hamburg
pH-meter	RHBKT/C WTW pH level 1	Inolab, Weilheim
Sterile laminar flow	ScanLaf, Mars, Safety Class 2	Bleymehl, Inden
Thermocyclar Flexcyclar		Analytik Jena, Jena
Thermocycler T-Gradient		Biometra, Göttingen
UV Transiluminator	Bio-Vision-3026	Peqlab, Erlangen
Vortex Genie 2™		Bender&Hobein AG, Zurich
Water baths	TW2 and TW12	Julabo, Seelbach
Water bath shaker	C76	Brunswick Scientific, New Jersey
2. Microscopes		
Fluorescence microscope	Axiovert S 100	Carl Zeiss MicroImagiJena
Fluorescence microscope	Axio Imager M1	Carl Zeiss MicroImagiJena
Inverted microscope	AE20	Motic, Wetzlar

5.1.2. Software

Software listed in table 4:

Software	Version	Supplier or Reference
Burrows-Wheeler transform BWA		[140]
AxioVision Microscopy	4.8	Carl Zeiss MicroImaging, Jena
Chemi-Capt		Vilber-Lourmat, Eberhardzell
Graphpad Prism 7	7	Graphpad Software Inc.
Image J 1.41	1.41	NIH, Bethesda
ND-1000	3.0.7	PeqLab, Erlangen
Vector NTI 9	9	Invitrogen Life Technologies, Grand Island

Software	Version	Supplier or Reference
Vision-Capt		Vilber-Lourmat, Eberhardzel
Endnote	X5	THMSON REUTERS
Applied Biosystems 7500/7500 Fast Real-Time PCR System Software	v2.0.6	Invitrogen.
Finch TV	1.4.0	Geospiza, Inc
NA Copy Number and Dilution Calculator		Thermo Fisher Scientific, UK.
Primer Express Software	2.0	Applied Biosystem, USA
iThenticate (Professional Plagiarism Prevention)		http://www.ithenticate.com

5.1.3. Enzymes and markers

Enzymes and markers are listed in table 5:

Enzyme	Catalog Number	Supplier
CIP	M0290S	New England Biolabs, Ipswich
Antarctic phosphatase	M0289L	New England Biolabs, Ipswich
BamHI	R0136	New England Biolabs, Ipswich
DpnI	ER1701	New England Biolabs, Ipswich
EcoRI	R0101S	New England Biolabs, Ipswich
HindIII	R0104	New England Biolabs, Ipswich
KpnI	R0142S	New England Biolabs, Ipswich
PpuMI	R0506S	New England Biolabs, Ipswich
SmaI	R0141S	New England Biolabs, Ipswich
Phusion-High Fidelity DNA Polymerase	M0530S	Thermo Scientific, Rochester
Proteinase K	7528.2	Roth, Karlsruhe
RNase A	2326466	AppliChem, Darmstadt
RQ1-RNas-free DNase	M6101	Promega, USA
T4 DNA Ligase	01-1020	Peqlab, Erlangen
Taq DNA-Polymerase	01-1020	Peqlab, Erlangen
SensiFast probe lo-ROX mix 2x	BIO-84020	Bioline, Luckenwalde
Protein Prestained plus marker	26619	Thermo Scientific
Generuler TM 1kb Plus DNA Ladder	SM0311	Darmstadt Fermentas, Mannheim

Enzyme	Catalog Number	Supplier
0.5-10 kb RNA Ladder	15623-200	Invitrogen Life Technologies, Grand Island

5.1.4. Antibodies

Antibodies are listed in table 6:

Antibody	Catalog Number or Conc.	Company or Reference
Chicken anti MDV US2, polyclonal	1:1,000	[141]
Alexa goat anti-chicken IgG (H+L) 488	1:1,000	Invitrogen Life Technologies Grand Island
Anti-ß-Actin	49705	Cell Signaling, Cambridge
Anti-6x-His Tag	200-301-382	Rockland, Limerik
HA-Tag (6E2) mouse mAB	23675	Cell Signaling, Cambridge
RpL22 Antibody Rabbit Polyclonal	25002-1-AP	Protein tech Europe, UK
Anti-RPL22 antibody	AB77720	Abcam, Cambridge, UK
Goat-anti-mouse IgG HRP	Sc-2031	Santa Cruz, Santa Cruz
Goat-anti-rabbit HRP	7074S	Cell Signaling, Cambridge

5.1.5. Kits

Kits are listed in table 7:

Name	Catalog Number	Company
ECL Prime Western Blotting Detection Reagent	RPN2236	Amersham Biosciences
E-Z96 96-well blood DNA isolation	D1192-01	Omega Biotek, USA
GF-1 AmbiClean PCR/Gel Purification kit	GF-GC-200	Vivantis, Malaysia
Hi Yield Gel/PCR DNA kit	30 HYDF100-1	SLG, Gauting
High-capacity cDNA Reverse Transcription Kit	4368814	Thermo Scientific, Darmstadt
MAXIscript® T7 in vitro transcription Kit	AM1312	Ambion, USA
Miseq Reagent Kit v3	MS-102-2003	Illumina, San Diego, California, USA
Monarch DNA Gel Extraction Kit	T1020S	New England Biolabs, Ipswich
PeqGold Plasmid Mini Kit	12-6942-02	Peqlab, Erlangen

Name	Catalog Number	Company
Qiagen Plasmid Midi Kit	12145	Qiagen, Hilden
RNeasy Plus Mini Kit	74134	Qigane, Hilden
RTP® DNA/RNA Virus Mini Kit	1040100300	STRATEC Molecular GmbH, Berlin
TNT® Couples Reticulocyte Lysate Systems	L4610	Promega, Germany

5.1.6. Antibiotics

Antibiotics are listed in table 8:

Name and Cat. No.	Working Sol. Conc.	Manufacturer
Ampicillin Cat. No. K0292	100 µg/ml in ddH2O	Roth, Karlsruhe
Kanamycin sulphate Cat. No. T832.3	50 µg/ml in ddH2O	Roth, Karlsruhe
Chloramphenicol Cat. No. 3886.3	30 µg/ml in 96 % EtOH	Roth, Karlsruhe
Streptomycin Cat. No. A1852	100 U/ml in MEM	AppliChem, Darmstadt

5.1.7. Bacteria, cells, viruses, plasmids and animals

Bacteria, cells, viruses, plasmids and animals are listed in table 9:

Name	Genotype	Reference
5.1.7.1. Bacteria		
Top10	F-mcrA Δ (mrr-hsdRMS-mcrBC) φ80lacZΔM15 ΔlacX74 nupG recA1 araD139 Δ (ara-leu) 7697 galE15 galK16 rpsL(Str R) endA1	Invitrogen, Carlsbad
GS1783	EL250 λcI857 Δ (cro-bioA)<>araC-PBAD, I-SceI	[142]
5.1.7.2. Cells		
CEC	Chicken Embryo fibroblasts Cells, VALO SPF strain	Primary cells
HEK293	Human embryonic kidney cell line	ATCC® CRL 1573™
DF-1	Chicken fibroblasts	Cell line
5.1.7.3. Viruses		
rRB-1B	Bacterial artificial chromosome (BAC) of vvMDV strain RB-1	[143]

Name	Genotype	Reference
5.1.7.4. Plasmids		
pEP Kan-S	Mammalian expression vector; T7prom, f1 ori, SV40 ori, SV40 pr, KanR, I-Sce-I restriction site, AmpR, ColE1 ori, NeoR	[144]
PVitro-2-Hygro-MCS	Mammalian dual expression vector; Catalog # pvitro2-mcs	InvivoGen
pcDNA3.1	Mammalian expression vector; ; Catalog #V790-20	Invitrogen
pSG5	Eukaryotic expression vector constructed by combining pKCR2 and the startagene pBS vector, used for both in vivo and in vitro expression; Catalog No. 216201	Startagene
5.1.7.5. Animals		
Specific Pathogen Free chicks (SPF)	SPF eggs and kept for hatching then infection	ValoBioMedia, Germany

5.1.8. Buffers, Gels and Media

5.1.8.1. Buffers and Gels:

Buffers and Gels are listed in table 10:

Buffer or gel	Composition
1x PBS	2 Mm KH2PO4 10 Mm Na2HPO4 137 Mm NaCl 2.7 mM KCl pH 7.3
1x TAE	40 mM Tris 1mM Na2EDTAx2H2O 20 mM Acetic acid 99%, PH 8.0
10x SDS-page running buffer	250mM Tris 1.9M Glycine 1% SDS
Western Blot transfer buffer	25 mM Tris 192 mM Gycine 20 % (v/v) MeOH

Buffer or gel	Composition
10x Lämmli buffer	1.25 M Tris-HCl pH 6.8 10% SDS 0.2% Bromophenol blue
RIPA buffer	20 mM Tris-HCl 150 mM NaCl 1 % (v/v) Nonidet P-40 0.5 % (w/v) Sodium deoxycholate 0.1 % (w/v) SDS Complete® Mini protease/phosphatase inhibitor cocktail
Basic Net-2 buffer	150 mM NaCl 50 mM Tris pH 7.5 0.05% NP40
RNA CoIP washing buffer	250 mM NaCl 50 mM Tris pH 7.5 0.1% Tween 20 0.5 mM DTT 0.5 mM PMSF 1ug/ml yeast Trna
RNA CoIP washing buffer	250 mM NaCl 50 mM Tris pH 7.5 0.1% Tween 20 0.5 mM DTT 0.5 mM PMSF 1ug/ml yeast Trna
5x RNA loading buffer	16 µl saturated bromophenol blue solution 80 µl 500 mM EDTA, pH 8.0 720 µl 37% (12.3 M) formaldehyde
10x FA gel buffer	200 mM MOPS 50 mM sodium acetate 10mM EDTA pH 7.0 with NaOH

Buffer or gel	Composition
1x FA gel running buffer	100 ml 10x FA gel buffer 80 ml RNase-free water 3.084 ml formamide 20 ml 37% (12.3 M) formaldehyde 2 ml 100% glycerol 4 ml 10 x FA gel buffer
Inoue transformation buffer (1L)	dissolve the following solutes in 800 ml Milli-Q H_2O: 10.88 gm $MnCl_2$-$4H_2O$ with final conc. 55mM 2.20 gm $CaCL_2$-2 H_2O with final conc. 15mM 18.65 gm KCL with final conc. 250Mm. 20 mL PIPES (0.5M, pH 6.7), adjust the volume to 1 L with Milli-Q H_2O Sterilize by filtration through pre-rinsed 0.45 um Nalgene filter
0.8 % Agarose Gel	80 mM Agarose 1x TAE buffer 4 uL Ethidium bromide 10 mg/ml
F.A gel preparation (1.2 %)	1.2 g agarose 10 ml 10x FA gel buffer RNase-free water to 100 ml

5.1.8.2. Media and supplements for propagation of bacteria (E.coli)

Media and supplements are listed in table 11:

Media	Composition
LB medium (for 1L)	10 g Bacto™ Tryptone 5 g Bacto™ Yeast Extract 10 g NaCl 15 g Bacto™ Agar
SOB medium (1L pH to 7.0)	20 g Bacto™ Tryptone 5 g Bacto™ Yeast Extract 0.584 g NaCl 0.186 g KCl

Media	Composition
SOC medium	SOB medium
	20 mM Glucose

5.1.9. Plasmid and BAC DNA preparation buffers

Plasmid-preparation buffers are listed in table 12:

Buffer	Composition
Buffer (P1)	50 mM Tris HCL pH 8.0
	10 mM EDTA
	100 µg/ml RNase
Lysis buffer (P2)	200 mM NaOH
	1 % SDS
Genomic DNA Lysis buffer	10 mM Tris-Cl pH 8.0
	0.1 M EDTA pH 8.0
	0.5% (w/v) SDS
	20 ug/ml RNase A
Neutralization buffer (P3)	3M K-acetate pH 5.5
Buffer TE	10 mM Tris HCl pH 7.4
	1 mM Na_2EDTA

5.1.10. Media and supplements for cultivation of mammalian cells

Media and supplements are listed in table 13:

Name	Catalog No.	Company
Chicken Serum	Cat.No. C5405	Sigma-Aldrich, St Louis
Fetal bovine serum (FBS)	Cat. No. S 0415	Biochrom AG, Berlin
L-alanyl-L-Glutamine	Cat.No. K 0302	Biochrom AG, Berlin
Minimum essential Medium Eagle (MEM)	Cat.No. F 0315	Biochrom AG, Berlin
Trypsin	Cat.No. L 2103-20G	Biochrom AG, Berlin

5.1.11. Cell culture media and buffers.

Media and buffers are listed in table 14:

Name	Composition
Chicken Embryonic Cells Medium	MEM 10% FBS 1x Penicillin/Streptomycin
2x HBS buffer (pH 7.05)	140 mM NaCl 1.5 mM $Na_2HPO4 \times 2H_2O$ 50 mM HEPES
HEK 293T Cell medium	DMEM 10% FBS 1x Penicillin/Streptomycin
Trypsin	1.5 M NaCl 0.054 M KCl 0.055 M C6H12O6 0.042 M NaHCO3 106 U Penicillin (P) 1457.4 Streptomycin (S) 0.0084 M Versene (EDTA) Ethhylene diaminetetracetate Trypsin 1:250

5.1.12. Primers and probes

5.1.12.1. Primers used to characterize MDV ICP0-Project (table 15)

Primers	Sequence (5'→3')
Cloning of MDV-ICP0-HA tag into PVitro-2-Hygro-MCS plasmid:	
ICP0- into PVitro-For	ATATCGGATCCATGACCCGGGGGCATCG
ICP0- into PVitro-Rev	CGACAATCGATTCAGGTGGTAGTCGCATAATCCGG
Sequencing Primers for cloning screening:	
Seq- PVitro-For	GGGATGTAATGGCGTTGGAG
Seq- PVitro-Rev	GCTAGTTATTGCTCAGCGG
Generation of MDV-ICP0-HA tag-GS linker:	
MDV-ICP0-HA tag-GS linker-Kana-in-For	ACCGAAAGGGGCTCCACGGCAAACAAAAAAAAAAAACGTCAGGT**GGTAGTCGC**ATAATCC GGCACATCATACGGATATAGGGATAACAGGGTAATCGATTT
MDV-ICP0-HA tag-GS linker-Kana-in-Rev	CGAGGACCCCAGGGCGGATGGGGGCGAGAGGACCCCTCGCTATCCGTATGATGTGCCGG ATTATGCG**ACTACCACC**GCCAGTGTTACAACCAATTAACC
MDV-ICP0-Stop2x -Kana-in-For	CTCCGCAATAAGCGTGGGCACACGTGTGGGCCGTGCAGGGCTATTAGAGCGTGCACTAGG GATAACAGGGTAATCGATTT
MDV-ICP0-Stop2x -Kana-in-Rev	CAGCCCAAGCCCCAGGGCCACGTCTTTGTGCACGCTCTAATAGCCCTGCACGGCCCACAC GTGGCCAGTGTTACAACCAATTAACC
Generation of MDV-ICP0- Revertant virus:	
MDV-ICP0-Revertant -Kana-in-For	CTCCGCAATAAGCGTGGGCACACGTGTGGGCCGTGCAGGGCATGAGCGTGCACAAATAG GGATAACAGGGTAATCGATTT
MDV-ICP0-Revertant -Kana-in-Rev	GCTCAGCCCAAGCCCCAGGGCCACGTCTTTGTGCACGCTCATGCCCTGCACGGCCCACA CGTGGCCAGTGTTACAACCAATTAACC

Sequences underlines represent restriction enzymes, **G-S Linker sequence**, stop codons, and start codon for revertant viruses.

Primers	Sequence (5'⟶3')
Sequencing Primers for final mutants:	
MDV-ICP0-Stop2x -For	CTGTTTACTCGCTGACTTTCAGC
MDV-ICP0-Stop2x -Rev	ATTAAAGCACGATTAAGTACCCCA

5.1.12.2. Primers used in the vTR-deletion, chTR and EBERs insertion project (table 16)

Primers	Sequence (5'⟶3')
vΔvTR-Kana-in-For	CGGAGGAAGCTACAAGAGCCCCACGCGGGGTTCCCCCGGCGCGGCCCCGCGCGCACGACCT AGGGATAACAGGGTAATCGATTT
vΔvTR-Kana-in-Rev	TCTACTCACAGAGCCCCGCGCGCGGCTCAACGGCTCCAACGGTCGTGCGCGCGGGGCCGCG CCAGTGTTACAACCAATTAACC
vchTR-Kana-in-For	CGGAGGAAGCTACAAGAGCCCCACGCGGGGTTCCCCCGGCACGCGTGGCGGGTGGAAGGC
vchTR-Kana-in-Rev	ACGGCGTCGCTCCCACACGCGCGGCCCCGCGCGCACGACCGTTGGAGCCGTTGAGCCGCGC
vEBER-1-Kana-in-For	CGGAGGAAGCTACAAGAGCCCCACGCGGGGTTCCCCCGGCAGGACCTACGCTGCCCTAGA
vEBER-1-Kana-in-Rev	CGCGGCTCAACGGCTCCAACGGTCGTGCGCGCGGGGCCGCAAAACATGCGGACCACCAGC
vEBER-2-Kana-in-For	CGGAGGAAGCTACAAGAGCCCCACGCGGGGTTCCCCCGGCAGGACAGCCGTTGCCCTAGT
vEBER-2-Kana-in-Rev	GCGCGGCTCAACGGCTCCAACGGTCGTGCGCGCGGGGCCGCAAAAATAGCGGACAAGCCGA
vRevertant-Kana-in-For	CGGAGGAAGCTACAAGAGCCCCACGCGGGGTTCCCCCGGCACACGTGGCGGGTGGAAGGC
vRevertant-Kana-in-Rev	ACGGCGTCGCTCCCACACGCGCGGCCCCGCGCGCACGACCGTTGGAGCCGTTGAGCCGCG
Primers for sequencing over vTR-region:	
MDV-vTR-For	GCCCCTCTCTGCTCGCTCT
MDV-vTR-Rev	TCCTGGCCTGGACGTGTG

5.1.12.3. Primers used in cDNA synthesis and qRT-PCR for RNAs expression (table 17)

Primers	Sequence (5'⟶3')
Definite oligos used for cDNA synthesis:	
vTR, vchTR, and vEBERs cDNA synthesis	CCCCTTTCGGTCCTTTCTC
MDV-ICP4	CGTGTTTTCCGGCATGTG
Ch-GAPDH	GAAGCTTACTGGAATGGCTTTCC
Primers set designed to confirm the RNAs expression by qRT-PCR:	
qRT-PCR- vTR-For	CCTAATCGGAGGTATT GATGGTACTG
qRT-PCR- vTR-Rev	CCCTAGCCCGCTGAAAGTC
qRT-PCR- chTR-For	TGGAAGGCTCCGCTGTGC
qRT-PCR- chTR-Rev	GGAGCGCGGCGACAGC
qRT-PCR- EBER-1-For	GTGAGGACGGTGTCTGTGGTT
qRT-PCR- EBER-1-Rev	TTGACCGAAGACGGCAGAA
qRT-PCR- EBER-2-For	GCTACCGACCCGAGGTCAA
qRT-PCR- EBER-2-Rev	GAGAATCCTGACTTGCAAATGCT
Primers used to amplify the genes for normalization:	
MDV-ICP4-For	CGTGTTTTCCGGCATGTG
MDV-ICP4-Rev	TCCCATACCAATCCTCATCCA
Ch-GAPDH-For	GAAGCTTACTGGAATGGCTTTCC
Ch-GAPDH-Rev	GGCAGGTCAGGTGAACAACA
Ch-iNOS-For	GAGTGGTTTAAGGAGTTGGATCTGA

Primers	Sequence (5'⟶3')
Ch-iNOS-Rev	TTCCAGACCTCCCACCTCAA

5.1.12.4. qPCR probes used in the study (table 18)

Target gene	Probe Sequence (FAM ⟶TAMRA)
vTR	CCCTCCGCCCGCTGTTTACTCG
chTR	CTAATCGGGGGAATTGATGG
EBER-1	TCTTCCCAGACTCTGC
EBER-2	AAGAGAGGCTTCCCGCC
MDV-ICP4	CCCCCACCAGGTGCAGGCA
Ch-GAPDH	TGTGCCAACCCCCAAT
Ch-iNOS	CTCTGCCTGCTGTTGCCAACATGC

5.2. Methods

5.2.1. Molecular biology methods

5.2.1.1. Two-step Red-mediated mutagenesis system [145]

All recombinant viruses in this study were generated by using an efficient mutagenesis system that allows introduction of the desired mutations including, insertions, deletions, point mutations or tags into herpesvirus DNA called Two-step Red-mediated mutagenesis technique. The system is originated form the phage λ (lambda phage) and comprises three major proteins called; *Exo*, *Beta*, and *Gam* that mediate the homologues recombination of double-stranded DNA [146, 147]. GS1783, the *E.coli* strain which is derived from DH10B strain, expresses the Red-recombination system under a temperature-inducible promoter which is activated at 42°C [144]. Gam can protect the double strand breaks from the degradation induced by the *E.coli* RecB/C/D system [148]. The 5'-3' exonuclease *Exo* generates free 3' single strand overhangs in the DNA template and Beta protein protects and stabilizes those free strands [149]. Additionally, *Beta* protein has another role during the amplification of the target BAC DNA is that it helps in the annealing of single-stranded substrate to complementary sequences to achieve homologues recombination with the target sequence [150].

This system is an efficient tool which can be used to introduce the desired modifications into the BACs together with a resistant marker (*PSM*) or Kanamycin cassette. In addition to Red recombination system, GS1783 expresses *I-SceI* which is regulated under an arabinose-inducible promoter [144]. *I-SceI* is an endonuclease that its origin is *Saccaromyces cerevisiae*. The enzyme has an 18 bp restriction site, which are specifically found for this enzyme and rarely to find in genome sequences (figure 14) [151]. In this study, I used the Red-recombination system to generate recombinant MDV mutants that carry stop-codon mutations for ICP0, other mutants with vTR-deletion and replacements with chTR or EBERs. Briefly, the sequence of interest was flanked by homologous arms and amplified using a kanamycin-resistance cassette (PSM) from plasmid pEP-Kan-S using primers listed in (Table 1and 2).

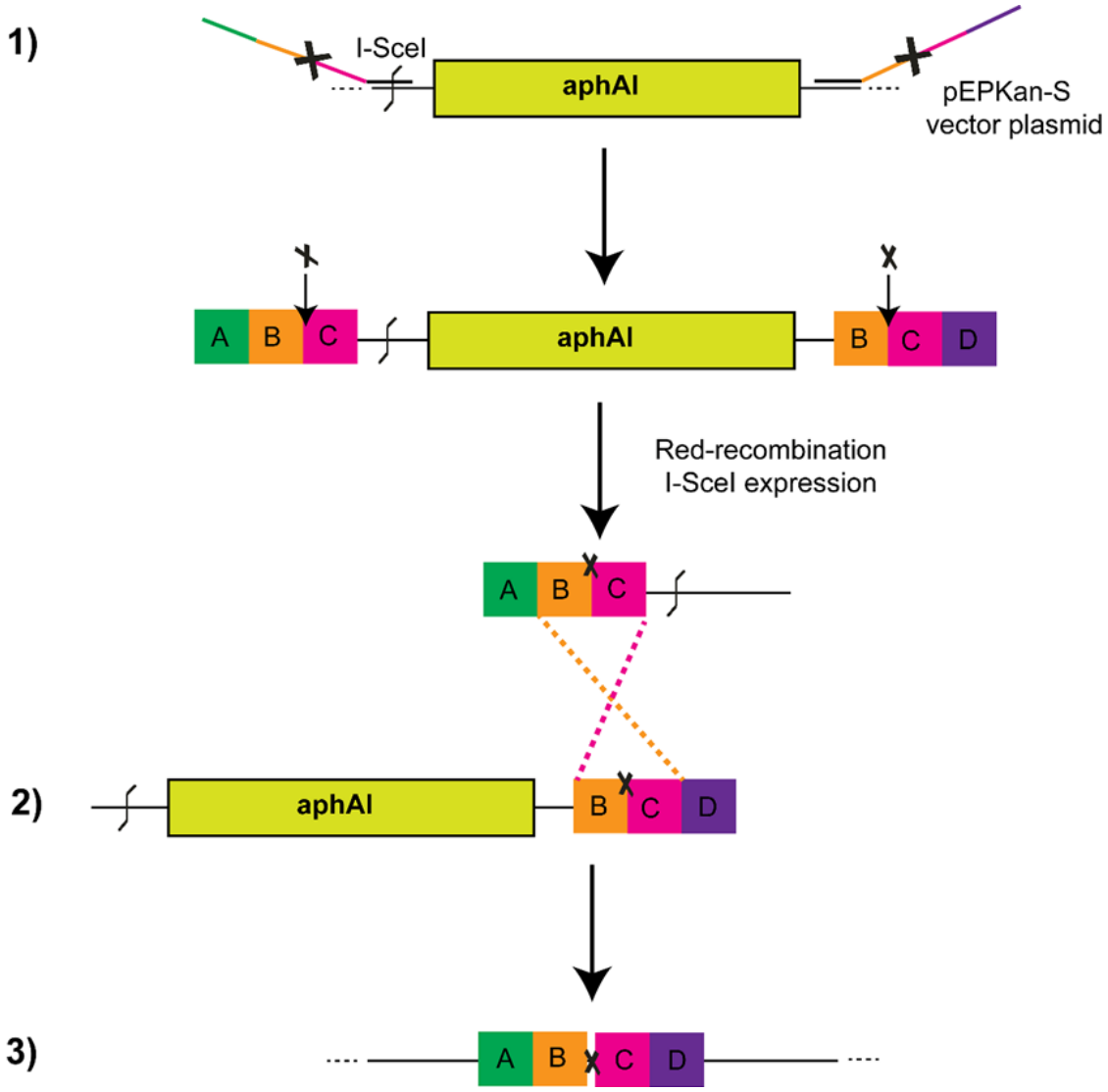

Figure 14. Schematic overview of Two-step Red-mediated recombination (insertion of point mutations). 1) Mutagenesis PCR, amplification of the aphAI- *PSM* cassette containing the target sequences (green, orange, pink, and violet) with the introduced mutation. 2) First recombination step, the dotted lines show the homologous recombination resulting in intermediate clones which should have the desired mutation and the *PSM*. 3) Second recombination step which is initiated due to I-SceI induction which cut the PSM cassette resulting final clones.

In this study, the point mutations have been introduced to ICP0 as described in (figure 14), while chTR, and EBERs have been inserted to the MDV-BAC as described in (figure 15) using the same mutagenesis technique but primers designed to achieve the target were different.

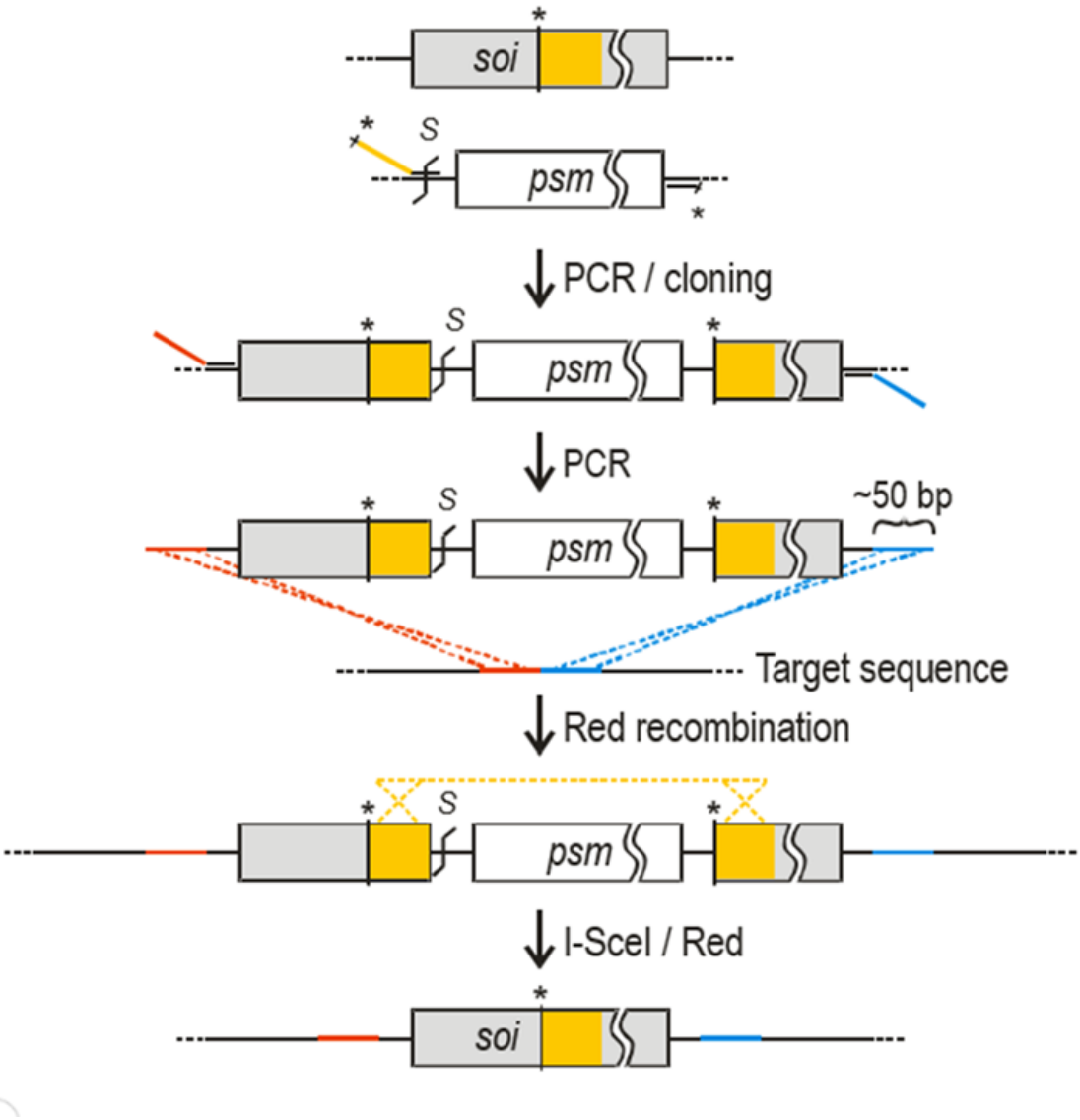

Figure 15. Schematic overview of Two-step Red-mediated recombination (insertion of the sequence of interest (SOi). This technique has been used to insert chTR, and EBERs into MDV-BAC-lacking vTR. The PSM is cloned onto the vector containing the Soi, resulting in shuttle plasmid, mutagenesis PCR to amplify the Soi with PSM and HRs. This PCR product is electroporated into E.coli GS1783 to get the intermediated clones. The correct clones undergoing second round of mutagenesis to get rid of the PSM resulting the final clones. Adapted from Tischer et al. [144]

For ICP0 project, the recombinant MDV carry substitution mutation in ICP0 where ATG > TAG TTA, was termed (vICP0-Stop), while the MDV-lacking vTR, termed (vΔvTR), the recombinant MDV expressing chTR instead of vTR, termed (vchTR), and that expresses EBERs, termed (vEBER-1), (v-EBER-2). The revertant virus termed (vchTR-rev) or (vEBER-2-rev). The recombinant viruses were generated in a sequential approach, in the form of chain of clones, one mutant after the other and ended by the revertant virus which was confirmed by NGS before performing the downstream steps.

5.2.1.2. Engineering of the MDV recombinant viruses

All recombinant viruses used in this work have been engineered by Two-Red recombination system using primers designed to achieve the desired modification (Table 1, 2), which was either introduce mutations in ICP0 (figure 14) or deletion of vTR and insertion of cellular and viral RNAs instead (figure 15). In general, mutagenesis PCR has been performed on two annealing steps (Table 5). The PCR products were cleaned up and digested with DpnI to get rid of the residual plasmid. The GS1783 competent cells were electroporated (1.25 kV, 25 µF and 200 Ω) with 100 ng of purified-PCR products followed by addition of 900 uL and incubated at 32ºC for 48 h. The kanamycin-resistant colonies were isolated and confirmed by restriction fragment length polymorphism (RFLP) analysis compared to a predicted pattern. The correct clones were used for a second round of Red-mediated recombination in the presence of 1% L-(+)-Arabinose that induces the removal of the PSM form the intermediate clones. After 48 hrs. at 32ºC in the incubator, the final clones were tested for the absence of kanamycin resistance on replica plates with LB+ kanamycin, LB+ Kanamycin+ chloramphenicol followed by RFLP screening analysis using multiple restriction enzymes compared to a predicted banding pattern and the introduced mutations were confirmed via sequencing as well.

Table 19. Two-step mutagenesis PCR protocol using Long Amp DNA polymerase for generation of MDV-lCP0 (vlCP0-Stop, vlCP0-Rev), and vTR mutants (vΔvTR, vchTR, vEBER-1, vEBER-2, or v-revertant)

PCR step	Temperature (°C)	Time	Cycles
Initial denaturation	94°C	5 min	
Denaturation	94°C	30 s	
Annealing	Various	30 s	10 cycles
Elongation	72°C	Various	
Denaturation	94°C	30 s	
Annealing	68°C	30 s	30 cycles
Elongation	72°C	Various	
Extension	72°C	8 min	

5.2.1.3. Sequencing PCR

To assure the desired modification, the area of mutagenesis for each generated mutant has been analyzed via Sanger Sequencing using sequencing primer listed in (table1 and 2), several DNA polymerase have been used for that purpose as Taq-polymerase, Phusion-High fidelity DNA polymerase and Long Amp Polymerase, the general cycling profile condition are listed in table 20.

Table 20: Sequencing PCR protocol:

PCR step	Temperature (°C)	Time	Cycles
Initial denaturation	94°C	5 min	
Denaturation	94°C	30 s	
Annealing	52-56°C	30-45 s	30 x
Extension	68-72°C	Various	
Final extension (Elongation)	72°C	8 min	

5.2.1.4. MDV-MiSeq: Sequencing of the wild-type and revertant BAC DNAs

The mutant viruses for vTR project were generated in a sequential approach and to ensure the genome integrity after several mutagenesis steps, The wild-type and revertant BAC DNAs were analyzed using high throughput illumine Miseq sequencing system (sequencing lab., institute of microbiology and epizootics, FU.). The Library preparation was performed by using NEB Ultra II DNA Library Prep Kit for Illumina according to the manufacturer protocol as follow:

Starting material:

MDV-BAC DNAs were prepared from the wild-type and the revertant viruses, the starting material was 5 µg DNA in total volume 50 µl TE and prepared for fragmentation using Covaris machine. DNA should be sheared in 1x TE. Following fragmentation step, DNAs were electrophoresed on 1% agarose gel on 90V for 30 min to confirm the quality of the fragmentation. DNAs were purified or cleaned up (size selection) from the agarose gel and the conc. has been checked by nanodrop and then undergo the following steps:

5.2.1.4.1. End Prep

In this step the fragmented DNA-ends prepared for the downstream steps as adapter ligations and so on. End Prep protocol that used as follow:

1. To a sterile nuclease-free tube add the following reaction:

Substance	Amount
NEBNext Ultra II End Prep Enzyme Mix	3 µl
NEBNext Ultra II End Prep Reaction buffer	7 µl
Fragmented DNA	50 µl
Total volume	2 µl

2. Using a 100 µl pipette set on 50 µl and pipette the entire reaction up and down at least 10 times to mix thoroughly and then quick spin. It is very important in this step to avoid the presence of bubbles that could have a negative effect on the performance.
3. The thermocycler was placed on and run the following program:

Temperature (°C)	Time
20°C	30 min
65°C	30 min
4°C	hold

Then the samples are ready for the next step.

5.2.1.4.2. Adaptor ligation.

1. The following components were added directly to the End Prep Reaction Mixture:

Amount	Substance
End Prep Reaction Mixture	60 µl
NEBNext Ultra II Ligation Master Mix	30 µl
NEBNext Ultra II Ligation Enhancer	1 µl
NEBNext Adapter for Illumina	2.5 µl
Total volume	93.5 µl

2. Using a 100 µl pipette setted on 80 µl and pipette the entire reaction up and down at least 10 times to mix thoroughly and then quick spin.
3. Incubate at 20°C for 15 min in a thermocyclar with the heated lid off.
4. 3 ul of USER Enzyme were added to the ligation mixture.
5. Mixed well and then incubated at 37°C for 15 min with the heated lid set to > 47 °C.

Table21. Adapter ligation condition

PCR step	Temperature (0 C)	Time	Cycles
Initial denaturation	98°C	30 s	1
Denaturation	98°C	10 s	1
Annealing	65°C	5 min	3-15
Extension	4°C		

5.2.1.4.3. Cleanup of Adaptor-ligated DNA without size selection

1. SPRIselect Beads were re-suspended by vortex.
2. 87 µl from the re-suspended beads were added to the ligation mixture and mixed well by pipetting up and down at least 10 times.
3. This reaction incubated at RT for 5 min.
4. The tubes were placed on a magnetic stand to separate the beads form the supernatant. The solution became clear and the supernatant was carefully discarded. It's very important to not disturb the beads as they contain the target DNA.
5. Then 200 µl of 80% ethanol were added to the tube while in the magnetic stand. Incubated at RT for 30 s followed by removal of the supernatant. This step was repeated for a total of two washes.
6. The tubes were kept in the magnetic stand with the lid opened to let the beads to dry for 5 min.
7. The tubes were removed from the magnetic stand and the DNAs were eluted from the beads by adding 17 µl of 10 mM Tris-HCL.
8. The samples were mixed by pipetting up and down and incubated for 2 min at RT, then spin down briefly before placed again on the magnetic stand.
9. Once the solution became clear approximately after 5 min, 15 µl were transferred to a new PCR tube for amplification.

5.2.1.4.4. PCR Enrichment of Adaptor Ligated DNA

1. To a sterile strip tube the following components were added:

Amount	Substance
Adaptor Ligated DNA fragments	15 µl
NEBNext Ultra II Q5 Master Mix	25 µl
Index Primer/i7 Primer	5 µl
Universal PCR Primer/i5 Primer	5 µl
Total volume	50 µl

The samples had the same i5 Primer and different i7 Primer (index), the wild-type virus has i7 Primer index termed i707 while the revertant virus had i708 Primer index.

2. The mixture was thoroughly mixed by pipetting up and down at least 10 times.
3. The tubes were placed on a thermocycler and PCR amplification was performed using the following PCR cycling conditions:

5.2.1.4.5. Cleanup of PCR Amplification

1. SPRIselect Beads were re-suspended by vortex.
2. 45 µl of the re-suspended beads were added to the PCR reactions and mixed well by pipetting up and down.
3. The tubes were incubated at RT for 5 min.
4. The tubes were placed on the magnetic stand to separate the beads form the supernatant, after incubation about 5 min the solution became clear and supernatant was carefully removed.
5. 200 µl of 80 % ethanol were added to the tubes while in the magnetic stand, incubated at RT for 30 sec, and the supernatant was carefully discarded. This step was repeated for a total two washes.
6. Air-dry the beads for 5 min with the tube lid opened while kept on the magnetic stand.
7. The tubes were removed from the magnetic stand and DNAs were eluted from the beads into 33 µl 0.1x TE and mixed well, incubated 2 min at RT.
8. The tubes were placed again on the magnetic stand and let the beads to settle down and then the solution became clear after 5 min incubation. Libraries could be stored at - 20°C.
9. 1µl of the library was diluted 5 fold with 10 mM Tris-HCl and the size distribution was checked using Bioanalyzer. Then the samples were ready for analysis by NGS.

5.2.1.4.6. NGS for the samples followed by data analysis

The samples were sequenced and then the data analyzed and compared to reference sequence.

5.2.1.5. DNA mini- and midi-preparation

Viral and plasmid DNAs were isolated from bacteria using standard alkaline lysis protocol. In general, bacterial culture was grown overnight (o/n) at 32°C in 2 ml LB medium supplemented with the corresponding antibiotics. The next day, the cells were harvested by centrifugation for 10 min at 5000 rpm and the supernatant was discarded. The bacterial pellets were re-suspended in 300 µl of P1 buffer and cells were lysed by the addition of 300 µl P2 buffer and incubated for 5 min at RT. To neutralize the reaction and to precipitate

proteins, 300 µl of buffer P3 were subsequently added to the mixture. After incubation on ice for 10 min, proteins and cell debris were removed by centrifugation (10 min, 10,000 rpm). The supernatant was transferred into a 2 ml Eppendorf tube new tube, and 900 µl of a phenol: chloroform solution were added to ensure the elimination of proteins and the bacterial genomic DNA. The phenol was mixed with the samples by vortexing and followed by centrifugation for 10 min at 10,000 rpm. The aqueous phase was transferred to a new 1.5 ml Eppendorf tube, mixed with 700 µl of isopropanol and incubated for 10 min at -20 °C. DNA precipitation was carried out by centrifugation of the samples for 15 min at 10,000 rpm and 4 °C. After two washing steps with 70 % fresh prepared ethanol, the residual ethanol was completely removed by incubating the samples for 5 min at 37 °C. Therefore, DNA was dissolved in 1x TE-buffer containing RNase A (final concentration 100 µg/ml) and incubated at 37 °C for 30 min. Subsequently, digestion with appropriate enzymes was performed with the extracted DNA and obtained fragments separated by a 0.8 % agarose gel electrophoresis o/n at 65 V (RFLP). Midi DNA preparations were performed using the Qiagne Midi Prep Kit following the manufacturer's instructions for BAC DNA.

5.2.1.6. Preparation of electrocompetent bacterial cells

GS1783 Red-recombination bacteria harboring the BAC clone of the RB-1B, a very virulent MDV strain, was grown o/n at 32°C in 1 ml LB medium with chloramphenicol (Cam). The following day, 100 ml were inoculated with the o/n culture and incubated at 32°C under vigorous shaking (220 rpm). When the bacteria reached the maximum replication state in culture, the logarithmic growth phase (OD600) was measured after 2-4 hrs. (OD600 0.5 - 0.7), a heat shock was performed to activate the Red-recombination system. For this, bacteria were heated for 15 min to 42 °C at 220 rpm and afterwards cooled down on water-ice bath for 20 min and kept on a shaker at RT. The culture was pelleted by centrifugation (5,000 rpm, 5 min at 4 °C), followed by three washes with 10 ml of an ice-cold 10 % glycerol solution prepared with Millipore water. After the final wash (5,000 rpm, 5 min, 4 °C), bacteria were re-suspended in 1 ml of 10 % glycerol, kept in aliquots in 1.5 ml Eppendorf tubes and snap-frozen for storage at -80 °C.

5.2.1.7. Inoue method for preparation of Ultra-competent cells [152]

For plasmid DNA transformation, chemical competent E.coli was prepared using Inoue method. In general, in day 1; a single colony form TOP 10 or DH10B E.coli strains was inoculated at 250 ml flask containing 25 ml LB broth without antibiotics and incubated 6-8 hrs. at 37°C with continuous shaking at 250-300 rpm. Prepare three 1L-flasks with 250 ml SOB medium, in the first flask add 1ml of the culture, in the second add 50 µl, and 25 µl to

the third flask. The three flasks were incubated overnight at 18-22°C with moderate shacking. In day 2; the logarithmic growth of the bacteria was checked till reached to (O.D600. 0.55). Then the culture flasks were transferred into ice water bath for 10 min. The cells were harvested by centrifugation (3900 rpm, for 10 min at RT). The supernatants were discarded form the tubes and the pellets were dried by inverting the tubes on a paper towel for 2 min. Following that, the cells were re-suspended gently by swirling in 80 ml ice-cold (0°C) Inoue transformation buffer. The previous step was repeated then the cells were re-suspended gently in 20 ml Inoue buffer followed by adding of 1.5 ml DMSO and the cells incubated on ice for 10 min. The cells were kept in aliquotes and snap-freezed for storage in – 80°C for further use. When needed they removed for the freezer, thawed in hand and immediately used. The efficiency of the cells was tested by using PUC18 plasmid DNA.

5.2.1.8. Plasmid DNA transformation into chemically competent cells

Cloned plasmids carrying recombinant DNA (SOI) were transformed into the chemically competent cells. For that purpose, 50 µl frozen aliquots of the bacterial cells were kept on ice until defrosted and then 10 pg-100 ng of plasmid DNA or ligation mixture (usually 1-5µl) were gently swirled with the cells. Following that the mixture was incubated on ice for 30 min. Dry heat shock was performed at 42°C for 90 sec, followed by 1 min incubation on ice. 900 µl SOC medium were added to the mixture and then the tubes were incubated for 1 h at 37°C in shaking incubator. After the incubation, the culture were pelleted by centrifugation (6000 rpm for 2 min at RT). The supernatant (800 µl) were discarded and the pellet was gently re-suspended in the remaining 100 µl and plated by using glass beads on LB agar plates containing the appropriate antibiotics and incubated overnight at 37°C. Individual colonies were replica-plated onto a master plate and inoculated in LB broth culture with the corresponding antibiotic for screening. Colony PCR and DNA restriction endonuclease digestion with several restriction enzymes were used to check the correct clones. Clones that were positive by colony PCR, and presented the expected restriction digest pattern, were sequenced to confirm that the correct sequences were inserted.

5.2.1.9. Preparation of bacterial glycerol stocks

Bacteria harbors the plasmids or BACs were stored in glycerol at - 80°C for long-term use. A single bacterial colony was used to inoculate 3 ml of LB medium containing the appropriate antibiotic. Cultures were incubated overnight at 32°C or 37°C with shaking at 220 rpm in the bacterial incubators, 500 µl of culture were mixed with 500 µl sterile SOB 50% glycerol in a 1.6 ml cryovial and then stored at - 80°C.

5.2.1.10. DNA digestion and de-phosphorylation

For screening of plasmids, restriction enzyme digestion was carried out using multiple restriction endonucleases. DNAs were digested according to the manufacturers' recommendations. Antarctic Phosphatase (AP) (New England Biolabs, UK) was used to remove the 5' phosphate groups prior to ligation which prohibits the plasmid re-ligation. In brief, the digested plasmid DNA was incubated with AP enzyme at the recommended buffer for 1 hour at 37 °C. The AP was inactivated by incubation at 65°C for 15 min.

5.2.1.11. DNA Ligation

All SOI used in this study were cloned into plasmids via cloning using T4 DNA Ligase (New England Biolabs, UK) according to manufacturer instructions. The molarity ratio of vectors and inserts was calculated using NEBioCalculator (http://nebiocalculator.neb.com). Both digested vectors and inserts were mixed together with a molarity ratio 3:1 and incubated with T4 ligase for overnight on 4°C. Vector only ligation, one more tube that has the digested vector without the insert was run in parallel as a control. The ligated DNA fragments were then transformed into competent TOP 10 cells. The Ligation was confirmed through gel electrophoresis before transformation step.

5.2.1.12. Colony PCR

To verify the presence or absence of the inserts in the generated cloned plasmids or BACs inside the bacterial cells, colony PCR has been performed using specific primer set [153]. Single colony was suspended in 10 µl DDW and then 3 µl used for the PCR reaction. The PCR products were then analyzed for the correct size using gel electrophoresis.

5.2.1.13. DNA extraction or clean up from agarose gel

GF1 DNA extraction kit was used to extract the DNA band from agarose gel. The target band was excised from the gel using a sterile scalpel under a UV light. The kit utilized a proprietary silica-based membrane technology in the form of spin column which high capacity to bind up to 10 µg DNA and to process up to 1 gm of agarose. The target band was excised from TAE agarose according to manufacture instructions (Vivantis, Malaysia).

5.2.1.14. Agarose gel electrophoresis

0.8 to 1% (0.8 to 1 gm agarose gel) was dissolved in 100 ml of TAE buffer. After heated up, the dissolved agarose left up at RT till cool down then 5 µl of ethidium bromide stock solution (10 mg/ml) was added and then the gel poured in a particular gel trays with the combs. The electrophoresis chamber filled up with 1x TAE buffer and then the samples were loaded.

DNA samples from BACs DNA, plasmid DNAs, or PCR products were mixed with 6x DNA loading buffer and analyzed on the gel. The electrophoresis conditions were 100-120 v for 20-30 min in case of small gels and 60 V for overnight gels in case of BAC DNAs. 1 kb-plus DNA ladder (Invitrogen) was loaded in the first lane on the gels. Gels were visualized using UV Trans-illuminator gel documentation system (PeqLab, Erlangen).

5.2.2. Cell culture methods

5.2.2.1. CECs preparation

CECs were prepared from Valo-SPF embryos as described before [154]. In general, 11 days old embryos were used, the embryonated eggs were incubated at 37°C with 50-60% humidity. At day 11, eggs were ready to start the preparation. All steps of the preparation were made in a sterilized laminar flow hood, the eggs were sprayed with biogard disinfectant or alcohol. After that by using sterile technique, the shells were opened and the embryos were removed with blunt ended curved forceps. The embryos placed in Petri dish. The embryos-heads and limbs were cut off and the viscera was removed. The body was transferred into new Petri dish containing PBS to let the blood release then the bodies were shredded by carefully chopping them with sterile scissors. Following that, the shredded embryos were washed with PBS with magnetic stirring bar for 10 min to remove the red blood cells. The tissue fragments poured into a trypsinization flask containing the magnetic stirring bar and 100ml of pre-warmed (37°C in water bath) trypsin solution (0.05%) and put on stir plate at slow speed for 20 min. This step was repeated and fresh trypsin was added with a total trypsinization: 3 times. After each step of the trypsinization, the cell suspension was collected and filtered on a sterile gauze and kept in 10% FBS MEM. The cells were then aliquoted into 50 ml falcon tubes and harvested by centrifugation for 10 min at 1200 rpm. The pellets were re-suspended and pooled together with one more wash prior to re-suspension in 120 ml 10% FBS MEM and incubated in 225 ml falcon capacity plastic tissue culture tube for 20 min for sedimentation. Quality of cells was determined using an inverted microscope and the appropriate number of cells was calculated and plated into different tissue culture plates or dishes. To passage CECs, medium was removed and cells were washed with PBS, prior incubation with 0.05% trypsin at 37°C until proper detachment. MEM with10% FBS was added to inactivate trypsin and cells were re-suspended and then splitted at a 1:5 or 1:10 ratio depend on its confluence state.

5.2.2.2. MDV reconstitution and propagation

The recombinant viruses-reconstitution was performed by transfection of chicken embryo cells (CECs) using calcium phosphate transfection protocol. Briefly, 5 x 10^5 fresh CECs were seeded into one well of a 6-well plate with 2 ml of Minimum essential Medium Eagle (MEM) (Biochrom AG, Berlin) supplemented with 10% FBS-1% P/S and incubated overnight at 37ºC and 5% CO2 in humidified air cell culture incubator. Meanwhile, a 0.5-2 µg BAC DNA was diluted to 50 µl final volume with sterile 10 mM Tris (pH 7.5) in a polyethylene tube and co-transfected with plasmid that encodes Cre-recombinase, 388 µl sterile Millipore water were added and gently mixed to dissolve the DNA. 62 µl of 2M CaCl2 were added slowly in drops while gentle mixing. The transfection mixture was incubated overnight at 4ºC. Next day, 500 µl ice-cold 2x HBS were added in a drop wise to the transfection mixture to form a calcium phosphate-DNA co-precipitate and incubated at RT for 15 min in the dark. Meanwhile, CECs were 80% confluent and ready for transfection, media was removed and the cells were washed with 2ml PBS, 500 µl fresh media were added. After 15 min incubation time, 500 µl of the transfection mixture were added to each well, gently mixed and incubated at 37°C for 3 hrs. Following that, the transfection mixture was removed and the cells were washed with 2 ml PBS. Glycerol shock step was performed using 1.5 ml 1x HBS-15% glycerol for 2 min at RT. The HBS-glycerol was immediately removed after 2 min and cells were gently washed with 2 ml PBS, incubated in 2 ml MEM-10%FBS. The following days FBS was gradually reduced till 0.5%. RB-1B plaques could be observed starting from 5 days post transfection. One well with the wild-type virus and another without any DNA were used as a control for transfection. Viruses were propagated on CECs for 2-3 passages for preparing the virus stocks. Stocks from the viruses were made from highly infected cells in 10 %FBS MEM with 8% DMSO. The aliquots were kept in Mr. Frosty freezing containers in -80 °C prior storage in liquid nitrogen for archiving.

5.2.2.3. Immunofluorescence (IFA)

Indirect IF staining was used to visualize viral plaques in the infected CECs. IFA was used to detect MDV plaques in virus titration, plaque size, and multi-step growth kinetics. The cells were washed three times with 1x PBS and fixed with 90% ice-cold acetone for 10 min and incubated for 20 min at -20 ºC followed by air drying. Subsequently, for reducing non-specific binding, cells were blocked by 1% FBS diluted in PBS buffer for 1hr at RT. After removing the blocking buffer, the cells were stained with anti-US2-MDV chicken serum (1:5000) diluted in PBS 1% FBS and incubated for 1hr with shacking at RT, followed by three washes with PBS. Goat anti-chicken Alexa Fluor 488 (1:1000) was used as secondary antibody and cells incubated for 30 min with shaking at RT, then the cells were washed two times by PBS.

Plaques were then counted and imaged with Zeiss AxioVert S100 fluorescence microscope.

5.2.2.4. Plaque size assay

The viral cell-to-cell spread was assessed by plaque size assays as described previously [155]. Briefly, 1×10^6 fresh CECs were infected with 100 PFU of the corresponding viruses, and incubated at 37°C. After 6 days p.i. viral growth was detected. At least 50 plaques from each virus were imaged and the plaque areas were measured by image J software (NIH) (http://imagej.nih.gov/ij/) using a line tool. Plaque areas was converted into diameters and then normalized to the wild-type. Graphs were illustrated in Graph Pad Prism v7 (Graph Pad software, Inc.). Significant difference in plaque diameters was evaluated by One-way analysis of variance (ANOVA). Three independent experiments were performed.

5.2.2.5. Multi-step growth kinetics

Multi-step growth kinetics were performed in order to assess the replication properties of the recombinant viruses, as described previously [155]. Briefly, 1×10^6 fresh CECs were infected with 100 plaque forming unit (PFU) of the corresponding viruses in 6-well plates. After the incubation of the infected cells at 37°C for 6 days, the cells were harvested and titrated into fresh CECs in a triplicate wise at particular time points 1, 2, 3, 4, 5, and 6 dpi. After 6 days p.i the cells were fixed with 90% ice-cold acetone and IFA was performed. Plaque numbers for each time point were calculated and illustrated with Graph Pad Prism 7 (Graph Pad software, Inc.). Significance was evaluated by One-way analysis of variance (ANOVA).

5.2.2.6. DNA extraction form infected cells

To confirm the stability of the inserted sequences after viral passaging in CECs, viral DNA was extracted using the RTP® DNA/RNA Virus Mini Kit (Invitek). The virus aliquot was used form the liquid Nitrogen stocks and subjected into three rounds of thawing-freezing each for 15 min between 37°C water bath and -80°C freezers. Then the cells were pelleted by centrifugation for 10.000 rpm for 3 min at RT. 200 µl of the cell culture supernatant was mixed with 200 µl of ddH2O and then transferred to the provided extraction tube and shortly vortexed and incubated under continuous shacking for 15 min at 65°C and for 10 min at 95 °C. Then 400 µl binding solution were added and then mixed well by pipetting up and down. The mixture was transferred to spin filter and centrifuged for 2 min at 11.000 rpm followed by two washes; the first wash was done by 500 µl wash buffer R1 and the second with 700 µl wash buffer R2, the ethanol residual was removed by centrifugation for 4 min at max speed. Then the DNA was eluted using 30 µl elution buffer R (pre-warmed to 65°C). The area of mutagenesis was sequenced to confirm the presence of the inserted sequences after several

viral passages.

5.2.2.7. Transient transfection using PEI

HEK 293 cells were transfected with the MDV-ICP0 ORF using polyethyleneimine (PEI). Stock solutions of PEI were prepared using a 25 kDa linear PEI (Polysciences, Warrington, PA, USA) in a concentration of 1 mg/mL. PEI solution was prepared in water, pH was adjusted with HCl, sterilized by filtration (0.22 µm filter), and stored at -80 °C. Generally, the transfection was performed in a 6-well plate, 3 µg DNA of cloned plasmid expressing MDV-ICP0-HA tag- were diluted in 200 µl Opti-MEM® I Reduced Serum media (Invitrogen) followed by vortex and spin down. 9 µl PEI were added and then the mixture were incubated at RT for 20 min. The transfection mixture was added to 80% confluence cells and incubated overnight at 37ºC and 5% CO2 in humidified air cell culture incubator. ICP0 was cloned to a plasmid with GFP to be used as a control for transfection. ICP0 expression was analyzed by Western Blot.

5.2.2.8. Quantification of RNAs (vTR, chTR, and EBERs) expression using qRT-PCR

The vTR, chTR and EBERs-expression was quantified during the lytic MDV replication *in vitro* by using qRT-PCR assay. CECs were seeded in 6-well plates at a density $1x10^6$ and then infected with 1000 plaque-forming unit (PFU) of the wild-type vRB-1B, v∆vTR, vchTR, vEBER-1, vEBER-2 or the revertants. The viral plaques were detected 5 days post infection (dpi), then the total RNAs were extracted using RNeasy Plus Mini Kit (Qiagen), according to the manufacturer's instruction. The genomic DNAs were eliminated using gEeliminator columns (Qiagen). The RNAs then treated with 1uL RNase-free DNase I (Promega) at 37°C for 30 min, followed by incubation with DNase inactivation buffer at 60°C for 10 min. The RNAs form the infected and non-infected CECs were reverse-transcriped into cDNAs using one step reaction with High Capacity cDNA Reverse Transcription Kit (applied biosystems), using gene-specific oligos that anneal upstream vTR-region, primers for ICP4 and GAPDH (Table.3), (25°C for 10 min, 37°C for 120 min and 85°C for 5min). Minus-RT reaction was added to serve as a control for genomic DNA contamination. The cDNAs were diluted 1:10 with DEPC- treated water and stored in – 20°C for further use. Quantitative Real time PCR (qRT-PCR) reactions were set up in 96-well plates using 2x SensiFAST probe LO-ROX- one step master-mix (BIOLINE). Each reaction contained 2 µl cDNA, 25 pmol of each gene-specific primer (vTR, chTR, EBER-1 and EBER-2) and 10 pmol of the gene-specific probe in a 20 µl total volume. One reaction was left as NTC. Thermal cycling conditions were as follows: 95°C for 2 min, followed by 40 cycles at 95°C for 3 s and 60°C for 30s. The cycle threshold value (CT) is the cycle number at which the fluorescence generated within a

reaction crosses the fluorescence threshold, plotted to the total copies of each standard dilution in duplicate. The coefficient of regression (R2) was always near to 0.99 for standard curves. Viral ICP4 was quantified for the different viruses for normalization. Using the standard curve generated for each gene; the numbers of copies for vTR, chTR, EBER-1 and EBER-2 were determined by using CT for each sample and normalized against ICP4. qRT-PCR were performed in an ABI Prism 7700 Sequence Detection System (Applied Biosystems, Inc.) and the results were analyzed using Sequence Detection 7500 System (v2.0.6).

5.2.2.9. Western Blot

CECs cells infected with RB1B, vICP0-Stop, vICP0-rev were harvested and lysed in radio-immunoprecipitation assay buffer (RIPA). samples were mixed with 6x SDS sample loading buffer and denatured by heating at 95ºC for 5 min. Lysates were separated by sodium dodecyl sulfate (SDS) polyacrylamide gel electrophoresis (PAGE) using a 10 % gel for 20 min at 60V and 90 min at 130V, followed by transfer of the proteins onto a polyvinylidene difluoride (PVDF) membrane (Roth, Karlsruhe) using the BioRad wet blot system for 1 h at 100 V. Subsequently, membranes were blocked for 1h at RT with 5 % nonfat dried milk powder in PBS-T and incubated o/n at 4 °C with HA-Tag (6E2) mouse mAB (1:1,000) diluted in blocking buffer. Following 3x washing with PBS containing 0.1 % Tween-20 (PBS-T), membranes were incubated for 1h at RT with horseradish peroxidase-conjugated anti-mouse antibody, diluted 1:10,000. Finally, membranes were stained with western blot detection reagent (enhanced chemiluminescence, ECL-prime)s and the signal was recorded using the Chemi-Smart 5100 detection system (Peqlab, Erlangen).

5.2.3. Animal Experiment

To investigate the tumor-promoting functions of the inserted chTR and EBERs, we performed animal experiment. One-day old specific pathogen free (SPF) chickens (ValoBioMedia) were randomly assigned to five groups and infected subcutaneously with 2000 PFU of the wild-type virus vRB-1B (n=10), v∆vTR (n=25), vchTR(n=25), vEBER-1(n=25), or vEBER-2(n=25), and the revertant virus. Both the wild-type and revertant viruses were grouped together (n=35). In order to determine that the recombinant viruses can transmit via natural routes of infection, non-infected birds (n=11) were housed together with the infected animals, hence each group has infected animals and 11 contacts. Peripheral blood samples were collected on certain time points from infected animals; 4, 7, 10, 14, 21 and 28 dpi and from contact animals at 21, 28, 35, and 42 dpi to determine if the viral replication is affected in the absence of vTR and insertion of chTR and EBERs in vivo. DNA was extracted and MDV

genome copies were quantified by qPCR using specific primers and probes targeting viral ICP4 and chicken iNOS (Table 4) [156] and [157] as described previously [158]. Briefly, DNA was extracted from the blood samples using the E-Z 96 blood DNA kit (OMEGA biotek, USA) following the manufacturer's instructions. Infected animals were monitored for onset of clinical symptoms and development of tumors. After the onset of clinical disease, infected animals were euthanized and necropsies were performed to determine the presence and dissemination of tumors in visceral organs. After 13 weeks p.i, the animal experiment was terminated and the survived animals were examined for the presence of gross tumors. To address the role of the vTR-deletion and chTR or EBERs-insertion in the tumor dissemination or metastasis, we determined the number of organs containing gross tumors in the infected chickens during necropsies. The animal experiment was approved from the Landesamt Für Gesundheit und Soziales in Berlin, Germany (LAGESO).

5.2.3.1. Quantification of MDV genome copy in chicken whole blood (qPCR)

MDV genome copies in whole blood during the animal experiment were quantified using qPCR to determine the replication properties of the recombinant virus *in vivo.* 40 µl blood were collected from the wing vein and mixed with 20µl 100 mM EDTA in 96-well blood plates. Blood was collected from 8 birds in each group at different time points. Each qPCR reaction contained TaqMan Fast Universal Master Mix (Applied Biosystems), 10 µl DNA, 25 pmol of each gene-specific primer and 10 pmol of the gene-specific probe in a 20 µl total volume. One reaction was left as NTC. Thermal cycling conditions were as follows: 95°C for 20 s, followed by 40 cycles at 95°C for 3 s and 60°C for 30 s. Threshold was set to start at the exponential phase of the reaction, the cycle threshold value (CT) is the cycle number at which the fluorescence generated within a reaction crosses the fluorescence threshold, plotted to the total copies of each standard dilution in duplicate The coefficient of regression (R^2) was always near to 0.99 for standard curves. Using the standard curve generated for each gene; the numbers of copies for ICP4 and iNOS were determined by using CT for each sample. CT value of 36 indicated no specific amplification of the target DNA and a value of 0 copies in the sample was used in the analysis. All qPCR assays were performed in an ABI Prism 7700 Sequence Detection System (Applied Biosystems, Inc.) and the results were analyzed using Sequence Detection 7500 System (v2.0.6). MDV genome copies were determined by dividing the number of ICP4 copies by the number of iNOS copies, multiplied by 1,000,000 and the values were expressed as the number of MDV copies per 10^6 cells.

5.2.4. Statistical Analysis

Statistical analysis was performed using the GraphPad Prism7 Software . Data sets were first tested for normal distribution. Plaque size data of MDV recombinant viruses were analyzed as diameter using one-way ANOVA. Log10 of qPCR data on MDV genome copies in whole blood samples and growth kinetics were analyzed using Kruskal-Wallis and MannWhitney U tests. For tumor incidence, groups were compared via logestic regression test and Fisher's exact test with a consultation of Dr. Laura Pieper, Institute of Veterinary Epidemiology and Biostatistics, Freie Universität Berlin.

6. Results

6.1. MDV- ICP0 homologue

6.1.1. ICP0 homologue is dispensable for MDV replication properties *in vitro*

The aim of this project was to determine whether MDV- L-ORF-1 (positional herpesvirus ICP0-orthologue which is overlapped with vTR sequence) plays a role in the viral replication properties which subsequent will provide a clear view for the entire vTR-deletion. To investigate MDV replication in the absence of ICP0, stop codon mutations were inserted using RB-1B, a very virulent MDV strain, as a backbone. The resulted recombinant viruses were propagated on CECs and analyzed by plaque size assays to determine if the abrogation of ICP0 could alter the virus phenotype (Figure 16A). Furthermore, we inserted a HA-tag at the N-terminus of the ICP0-ORF in RB-1B and the recombinant viruses were analyzed by Western Blot to detect the viral tagged-protein (Figure 16B).

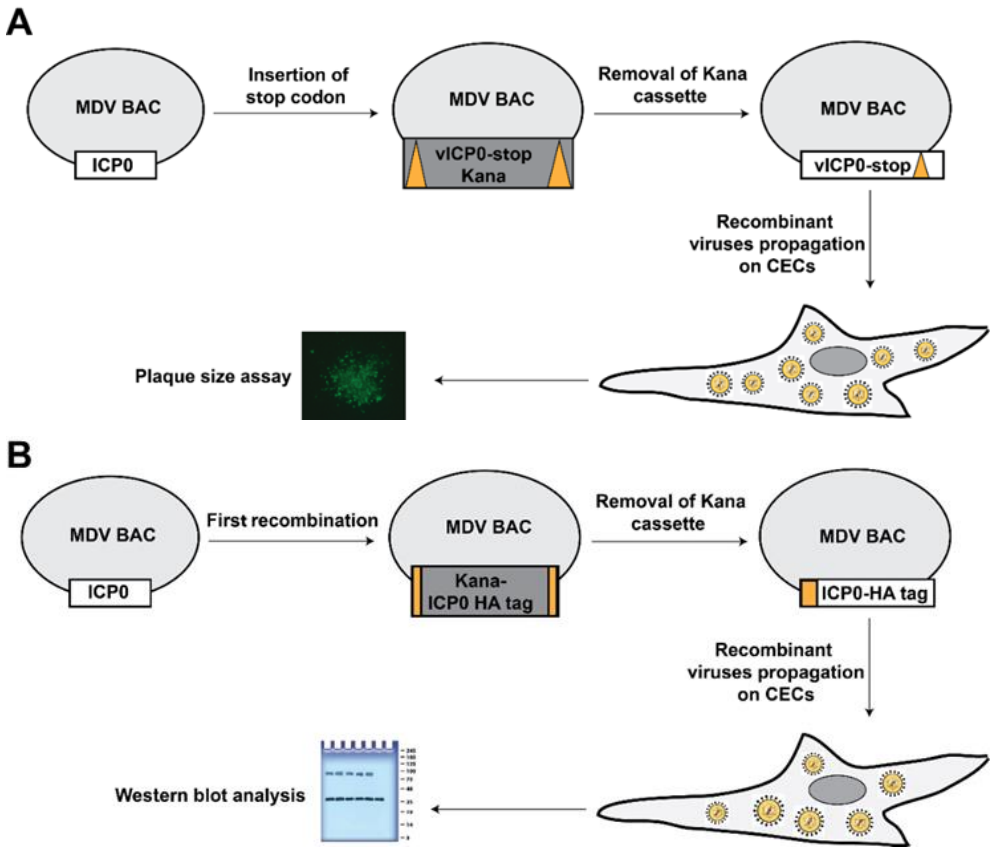

Figure 16. Schematic representation illustrate the *in vitro* analysis of ICP0 in MDV-replication. A. Insertion of stop codon mutations into ICP0-ORF. Recombinant viruses cell-to-cell-spread were assessed by plaque size assays. B. Tagging of the ICP0-ORF with an HA-tag which was inserted in the C-terminus of ICP0 and then the protein expression was checked by Western Blot.

6.1.1.1. Generation and characterization of recombinant MDV-lacking ICP0

Based on the in silico analysis, MDV-ICP0 is 597 bp with three start codons (ATGs) distributed along the entire ORF, 63 bp are separating the first and the second start codon while 456 bp are between the second and the third ATGs, so we decided to insert two stop codon mutations (TAG-TAA) instead of the second ATG (2nd ATG > TGATTA), generating recombinant MDV-lacking ICP0 expression. A revertant virus in which the original start codon restored was generated as well. The recombinant viruses were confirmed by RFLP and the virus cell-to-cell spread in the culture was quantified using plaque size assays. The generated mutants were confirmed by RFLP using three restriction enzymes *HindIII*, *EcoRI*, and *KpnI* compared to expected banding pattern (Figure 17) and finally confirmed by Sanger sequencing (data not shown).

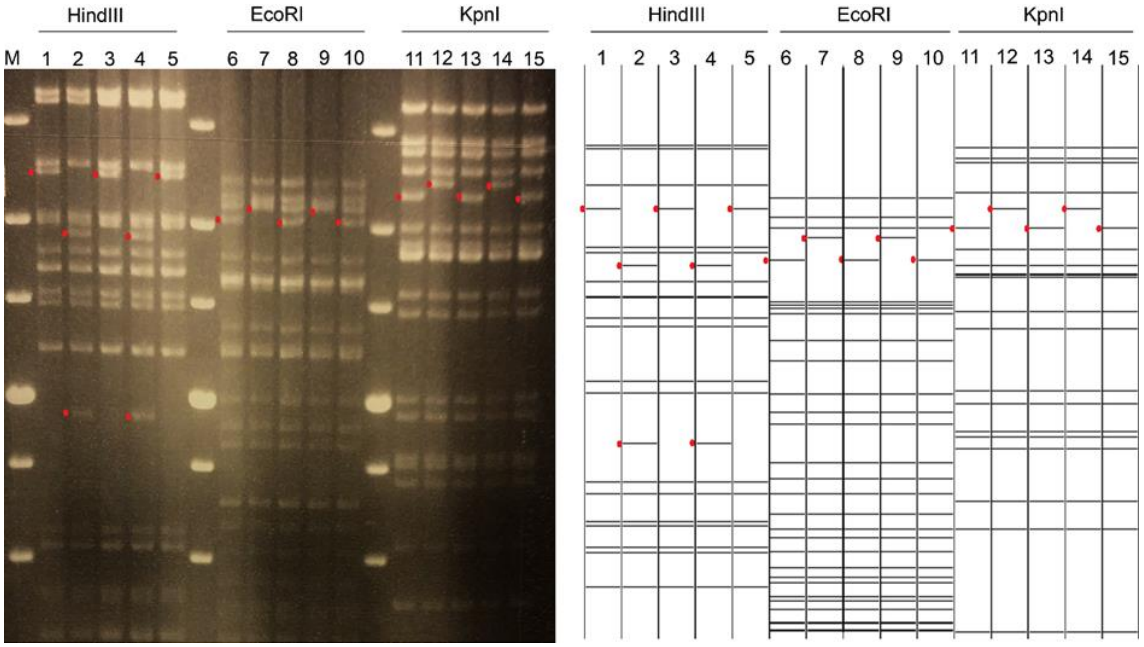

Figure 17. RFLP analysis of ICP0 mutants. Left panel represents the overnight gel using the above-mentioned restriction enzymes, the right panel represents the vector NTI 9.1 RFLP banding pattern prediction for the wild-type and ICP0 mutants. 1,6,11, RB-1B. 2, 7, 12. vICP0-stop-Kana-in. 3,8,13, vICP0-stop-final. 4,9,14, vICP0-stop-Revertant-Kana-in. 5, 10,15, vICP0-stop-final-Revertant.

In order to assess the viral cell-to-cell spread in the culture, CECs were infected with the corresponding recombinant viruses and plaque size assays were performed. Intriguingly, the plaque size assays revealed that recombinant MDV-lacking ICP0 were replicating efficiently in the cell culture similar to the wild-type, suggesting that ICP0 is dispensable for MDV cell-to cell spread *in vitro* (Figure18).

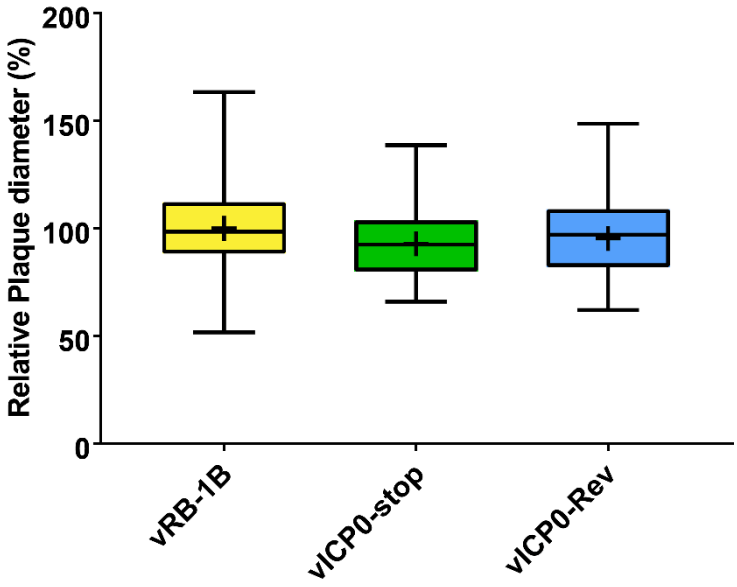

Figure 18. Plaques size assay for ICP0 mutants. vRB1B, vICP0-stop, and revertant. At least 50 plaques for each virus were imaged. The plaque diameters of the wild-type virus was set as 100% and then the relative plaque diameters for other viruses were calculated. Means are shown as`+`. Plaque sizes are shown as box plots with minimums and maximums. P> 0.05; one-way ANOVA. Three independent experiments were performed.

6.1.1.2. Detection of ICP0-protein using Western Blot

The next step was the insertion of an HA-tag with a G-S linker to the C-terminus of the putative ICP0-ORF in RB-1B. I decided not to insert the HA-tag on the N-terminus because this part of the ORF is overlapping with uncharacterized MDV sequences. The generated mutants were confirmed by RFLP and sequencing (data not shown). The ICP0-ORF was cloned into the pVitro-2-MCS-plasmid and was transfected into 293T cells to be used as a positive control in the Western Blot assay. The recombinant viruses were propagated on CECs and viral growth was confirmed through plaque formations and the infected CECs were analyzed by immunoblotting assay. Intriguingly, no ICP0-expression was detected by Western Blot (Figure 19).

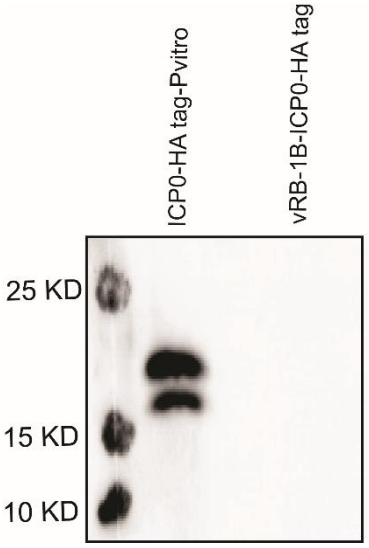

Figure 19. Western Blot analysis of the ICP0-HA tag in the wild-type virus. This western blot represents the ICP0-ORF on plasmid expression as a positive control (1st panel) and (2nd panel) the vRB-1B-ICP0-HA-tag.

6.1.1.3. MDV-ICP0 does not encode secreted protein

To confirm that the putative L-ORF-1 ICP0 does not encode a secreted protein, we performed in silico prediction to check for the signal peptides. Three online signal peptides prediction tools were used:

1. SignalP 4.1 Server (http://www.cbs.dtu.dk/services/SignalP/),
2. Signal3-L2.0: Improved signal peptides predictions (http://www.csbio.sjtu.edu.cn/bioinf/Signal-3L/),
3. Signal-Blast (http://sigpep.services.came.sbg.ac.at/signalblast.html)

All of these programs confirmed that there are no signal peptides.

Based on the previous findings of that there is no phenotype changes with plaque size assays, no expression could be detected by Western Blot and the in silico analysis that confirmed that ICP0 doesn't encode a secreted protein, we decided to delete the entire vTR sequences (CR1-CR8) to generate the platform virus (vΔvTR) in which the chicken telomerase RNA chTR and EBERs will be inserted at the same vTR locus.

6.2. Deletion of the entire vTR and insertion of either chTR or EBERs (EBER-1 or EBER-2).

6.2.1. Engineering of the recombinant viruses

To address the tumor-promoting functions of the overexpression of chTR or EBERs, we initially deleted vTR and subsequently inserted chTR or EBERs (EBER-1 and EBER-2) using Two-step Red recombination system. The sequentially generated viruses were confirmed by RFLP analysis using three restriction enzymes; *HindIII* (figure 20), *EcoRI* (figure 21), *KpnI* (figure 22) and Sanger sequencing over the area of the modifications (data not shown).

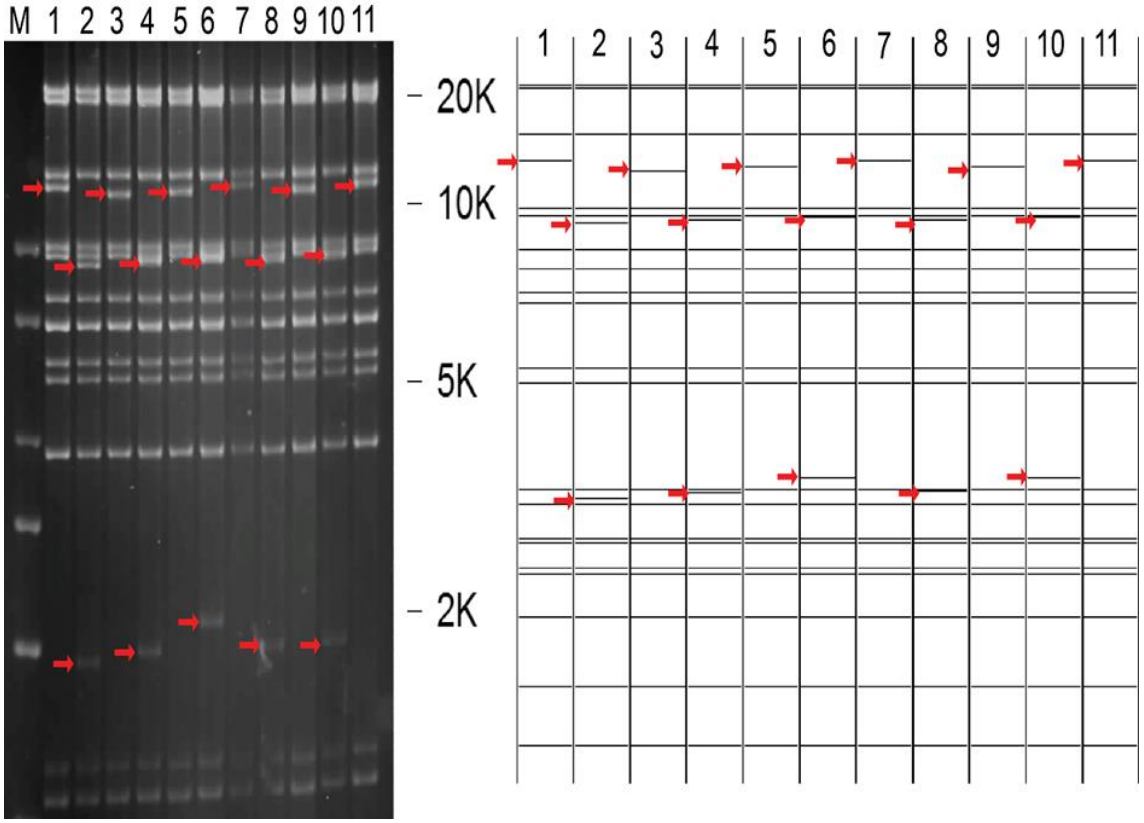

Figure 20. RFLP analysis of Sequential viruses using *HindIII*. Left panel represents the overnight gel using *HindIII*, the right panel is the vector NTI 9.1 prediction RFLP banding pattern for the wild-type and the mutants. 1) vRB-1B, 2) vΔvTR-Kana-Intermediate 3) vΔvTR 4) vEBER-1-Kana-Intermediate 5) vEBER-1 6) vchTR-Kana-Intermediate 7) vchTR 8) vEBER-2-Kana-Intermediate 9) vEBER-2 10) vRevertant-Kana-Intermediate 11) vRevertant.

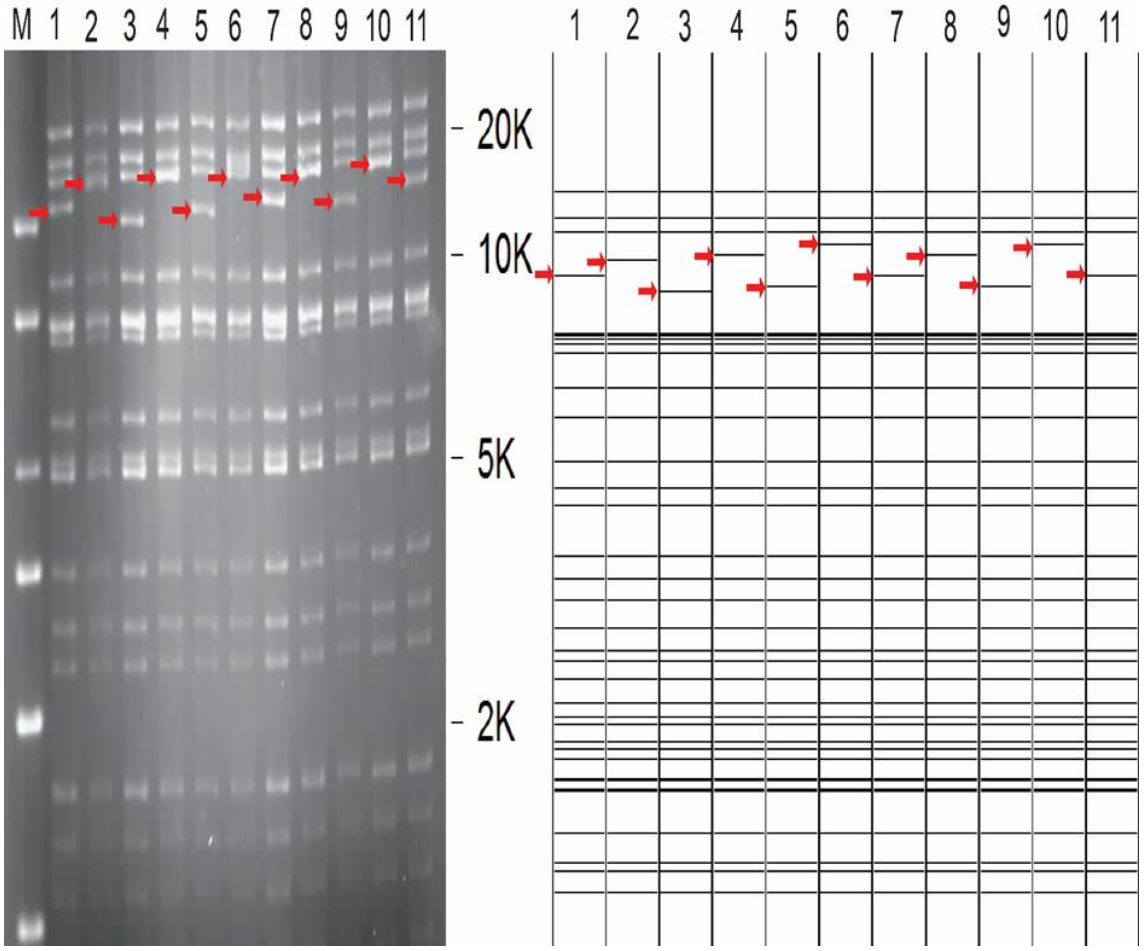

Figure 21. RFLP analysis of Sequential viruses using *EcoRI*. Left panel represents the overnight gel using *EcoRI*, the right panel is the vector NTI 9.1 prediction RFLP banding pattern for the wild-type and the mutants. 1) vRB-1B, 2) vΔvTR-Kana-Intermediate 3) vΔvTR 4) vEBER-1-Kana-Intermediate 5) vEBER-1 6) vchTR-Kana-Intermediate 7) vchTR 8) vEBER-2-Kana-Intermediate 9) vEBER-2 10) vRevertant-Kana-Intermediate 11) vRevertant.

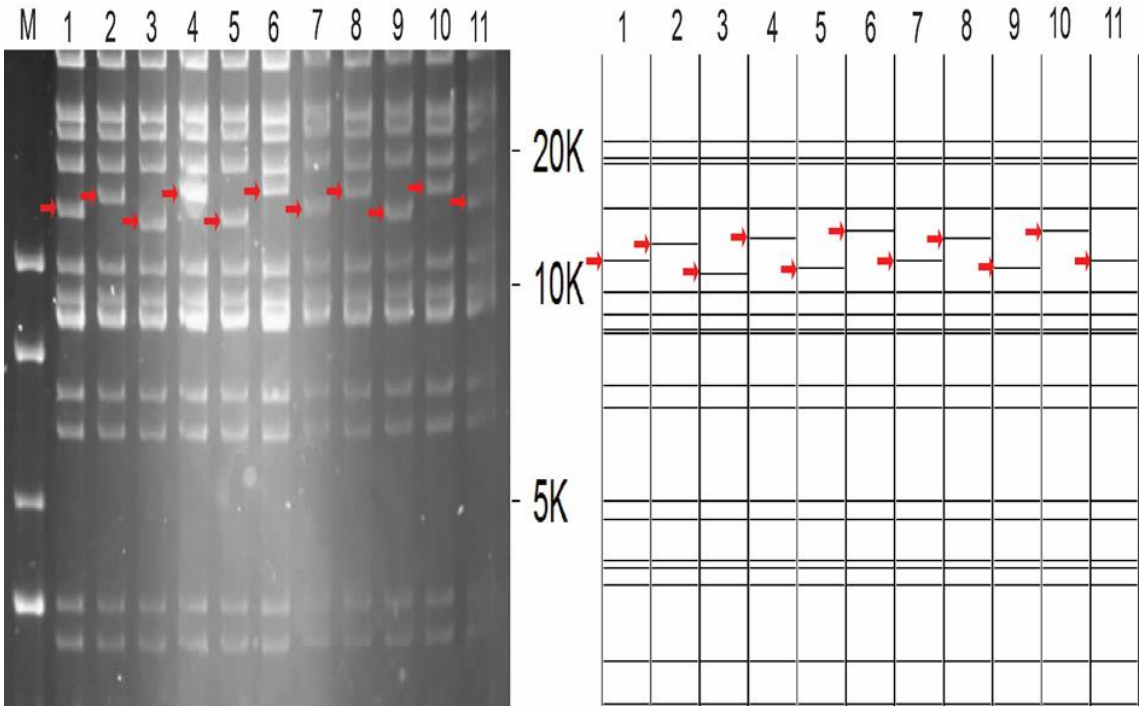

Figure 22. RFLP analysis of Sequential viruses using *KpnI*. Left panel represents the overnight gel using *KpnI*, the right panel is the vector NTI 9.1 prediction RFLP banding pattern for the wild-type and the mutants. 1) vRB-1B, 2) vΔvTR-Kana-Intermediate 3) vΔvTR 4) vEBER-1-Kana-Intermediate 5) vEBER-1 6) vchTR-Kana-Intermediate 7) vchTR 8) vEBER-2-Kana-Intermediate 9) vEBER-2 10) vRevertant-Kana-Intermediate 11) vRevertant.

6.2.2. NGS of wild-type and revertant BACs

To confirm the viral genome integrity after several mutagenesis steps, we analyzed the wild-type and revertant final clones BAC-DNAs with High- throughput illumina MiSeq which revealed that both the wild-type virus and the revertant have the same sequences, the coverage was calculated and it was >1000-fold. The sequence alignment was performed using Burrows-Wheeler transform BWA software. Nine mutations were detected in the wild-type and revertant virus compared the reference strain RB-1B Vector NTI- sequence file, eight mutations were located in the mini-F sequences and one silent point mutation detected in UL32 (table 22):

Position	REF.	ALT	Type	Site
74714	A	G	Silent point mutation	UL32*
152226	C	T		Mini-F
152296	A	T		Mini-F
152299	C	T		Mini-F
152302	A	T		Mini-F
152307	G	A		Mini-F
152355	T	C		Mini-F
152400	A	G		Mini-F
153438	G	A		Mini-F

Table 22. NGS analysis of the wild-type and the revertant viruses of the sequentially-generated vTR mutants. 9 mutations were detected, 8 of them are located in Mini-F plasmid which will be removed prior testing the viruses *in vivo* and one mutation which is located in both wild-type and revertant compared to reference strain. The silent point mutation is located in UL32* ORF (MDV046), which is DNA packaging protein. Position refers to the position of the mutation on MDV BAC sequences. REF. Reference sequence of the wild-type and revertant viruses. ALT. the mutation revealed after sequencing.

6.3. The over-expression of chTR promotes tumor development in MDV-induced tumorigenesis

6.3.1. Deletion of the entire vTR and insertion of chTR are dispensable for MDV-replication in vitro

To determine if the deletion of vTR and insertion of chTR change the viral replication properties *in vitro*, we performed plaque size assays and multi-step growth kinetics for the wild-type vRB-1B, vΔvTR, vchTR, and vchTR-rev. The average plaque diameters of the vΔvTR, vchTR or the revertant virus vchTR-rev, were not significantly different from the wild-type vRB-1B or revertant viruses (Figure 23A) which was confirmed by the multi-step growth kinetics (Figure 23B), indicating that neither the vTR-deletion nor chTR insertion affect the MDV-replication *in vitro*.

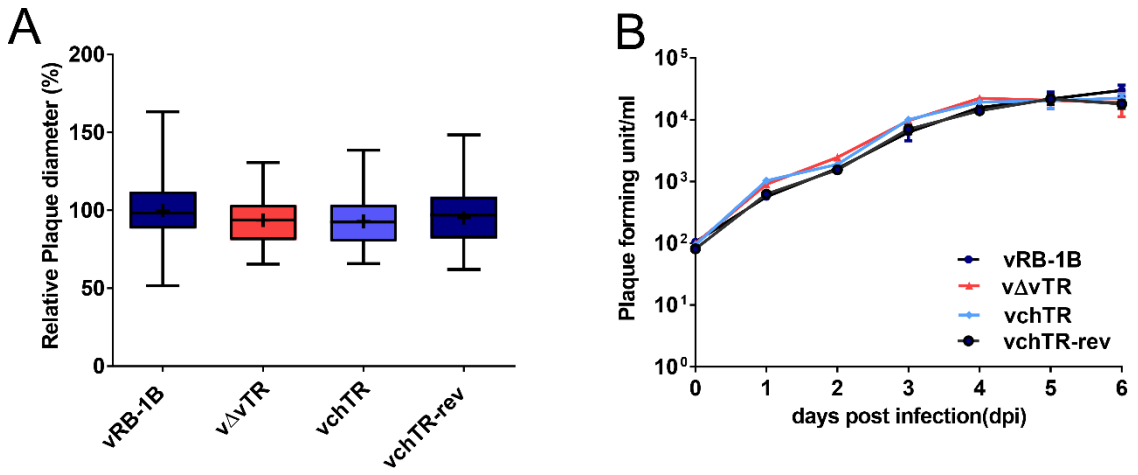

Figure 23. MDV replication properties *in vitro* did not alter in the absence of vTR or insertion of chTR. A. Plaque size assay, 6 d.p.i images of at least 50 plaques for each virus were acquired with a camera. The plaque diameter of the wild-type virus was set as 100% and then the relative sizes for other viruses were calculated. Plaque sizes are shown as box plots with minimums and maximums. (P >0.05; one-way ANOVA). Data represents three independent experiments. B. Multi-step growth kinetics of the corresponding viruses. 6 dpi, the infected CECs were fixed and the plaques were counted. Data are from triplicate measurements and expressed as means ± standard deviations (error bar) (P>0.05; Kruskal-Wallis test).

6.3.2. chTR in vchTR was highly expressed at levels comparable to vTR in wild-type virus *in vitro*

To confirm the overexpression of chTR, we performed qRT-PCR analyses. The CECs were infected with 1000 PFU from the corresponding viruses. Viral ICP4 and cellular GAPDH expression levels were quantified for each virus. No significant difference in ICP4 or GAPDH expression levels among the viruses (Figure 24 A, B). vTR expression levels were almost the same in the wild-type and revertant viruses while, no vTR expression detected in vΔvTR and mock cells (Figure 24 C) confirming the deletions. Our results showed that the chTR in vchTR was highly expressed at a levels comparable to vTR in the wild-type or revertant virus, confirming the overexpression of the cellular TRs due to the strong vTR promoter (Figure 24 D). In order to compare chTR expression in CECs (baseline) and in the recombinant virus expresses chTR (vchTR), we performed another qRT-PCR and we found that the chTR copies in vchTR were up to 100-fold increase than the cellular TR (baseline chTR) (Figure 24 E) confirming the strong over-expression of the chTR in the virus.

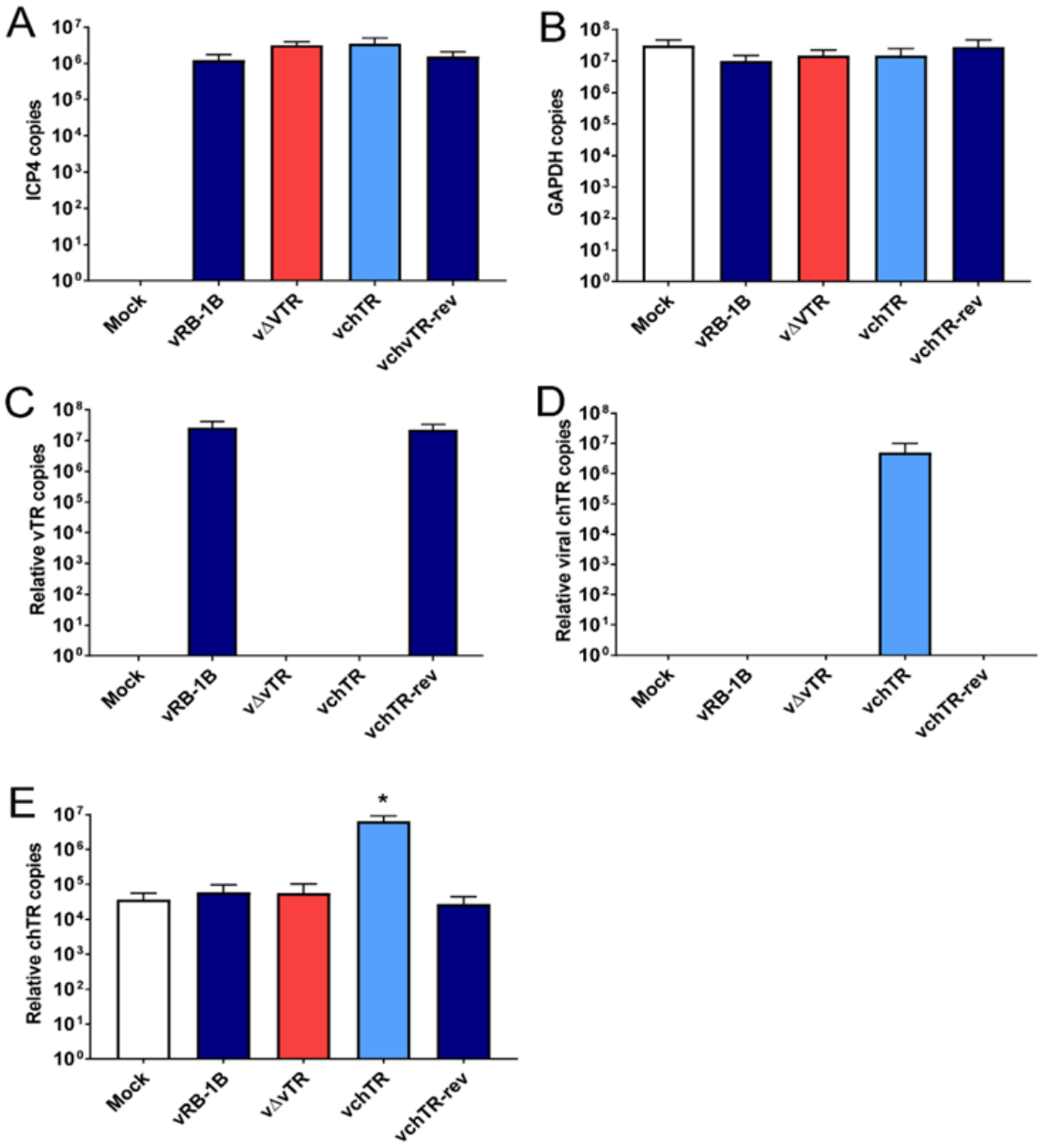

Figure 24. Quantification of vTR and chTR expression during MDV lytic replication *in vitro* using qRT-PCR. Fresh CECs were infected with the corresponding viruses and 6 dpi the total RNAs were isolated, reverse transcriped and the RNAs expression was quantified by qRT-PCR A. Viral ICP4 expression for each virus was quantified. The expression-levels were almost the same indicating the similarity of infection ($P > 0.05$; Kruskal-Wallis). B) Cellular GAPDH expression level was detected too and there was no significant difference detected. C) vTR expression in the cells infected with the corresponding viruses. No significant difference in vTR-expression in the wild-type virus and the revertant ($P > 0.05$; Kruskal-Wallis). vTR expression was not detected in vTR-deletion virus vΔvTR, vchTR, and mock cells. vTR expression was normalized to GAPDH and ICP4 D) vchTR expression in the cells infected with the above-mentioned viruses. Significant difference in chTR expression was detected in between vchTR and cellular chTR baseline ($P < 0.05$; Kruskal-Wallis). chTR expression was normalized to GAPDH and ICP4. E) Cellular and viral chTR expression. chTR in vchTR was up

to 100 fold higher than the cellular chTR. chTR expression was normalized to GAPDH. Figures represent the data of three independent experiments.

6.3.3. Tumor promoting functions of over-expression of chTR *in vivo*

To determine if the over-expression of cellular TRs possess tumor-promoting functions, we performed animal experiment in which we monitored the infected chickens in the different groups for developing clinical symptoms and gross tumors. To investigate whether the deletion of vTR or the insertion of chTR did affect the MDV replication *in vivo*, we quantified the viral genome copy numbers from the infected groups using qPCR (Figure 25A). There was no significant difference in the viral copy number among the different groups, the mutant replication properties was comparable to the wild-type or revertant virus, indicating that the vTR-deletion or chTR insertion were dispensable for the MDV replication *in vivo*. The animals were monitored for the development of MD clinical symptoms. Clinical symptoms for each group were recorded and analyzed as MD incidence. We observed that the MD incidence was severely impaired in the chickens infected with the vΔvTR, while vchTR successfully restored the viral pathogenesis. MD incidence induced by the recombinant viruses was recorded even at later stages of infection compared to the wild-type vRB-1B (Figure 25 B), suggesting that vTR is necessary for the disease onset and the overexpression of chTR restored MD incidence in the infected chickens . Tumor incidence was recorded for the infected animals in each group. Intriguingly, the tumor incidence was severely impaired in the absence of vTR, while chTR restored tumor formation almost to the wild-type levels. At final necropsy, we observed extreme reduction in tumor formation in the chickens infected with vΔvTR, while most of tumors detected in chickens infected with vchTR and revertant virus. No significant difference detected in the tumor incidence between vchTR and wild-type or the revertant (Figure 26 A). To assess the transmission of the viruses via natural routes, we quantified the tumor incidence in the contact animals. Similarly, the tumor incidence was severely impaired the vΔvTR- contacts while the vchTR restored the tumor formation in the contact animals compared to the wild-type or revertant virus. (Figure 26B). Collectively, our data provides the first evidence that the overexpression of cellular TRs complement the function of vTR in MDV-induced tumor formation.

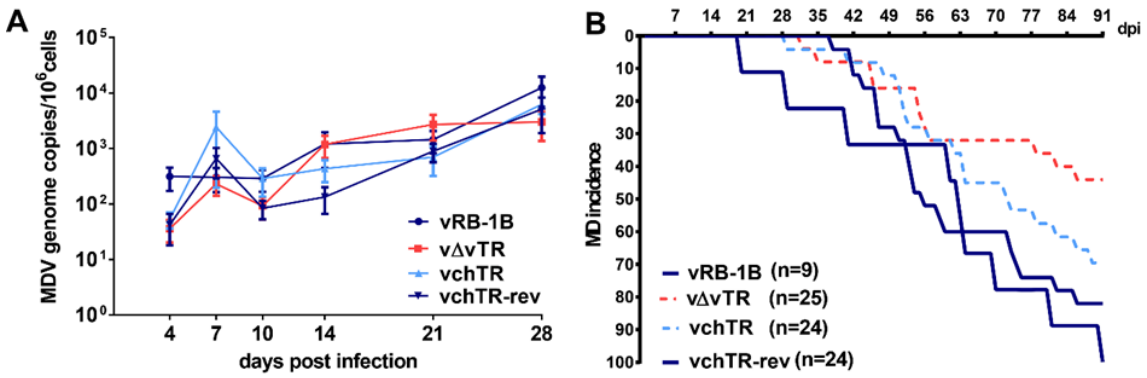

Figure 25. Characterization of recombinant MDV viruses expressing chTR instead of vTR *in vivo*. A. Quantification of MDV genome copy *in vivo* by qPCR. Peripheral blood samples were collected from the chickens infected with the wild-type virus vRB-1B, vΔvTR, vchTR or revertant vchTR-rev. At indicated time points, DNA was extracted. Both viral ICP4 and cellular iNOS genes were analyzed for each virus at the indicated time points. Viral titers shown as mean of the genome copy number per 10^6 cells of eight-infected chickens per group. Each group kept in a separate room. ($P > 0.05$; compared to wild-type virus, Kruskal-Wallis test). **B.** MD incidence referred to the percent of the chickens developing clinical symptoms of MD and /or gross tumors. The MD incidence was severely reduced in the chickens infected with the vTR-deficient virus compared to wild-type. MD incidence induced by the vchTR virus increased up and detected at later stages of infection. Animals infected with vchTR developed prominent tumors on pectoral muscles, heart and gut.

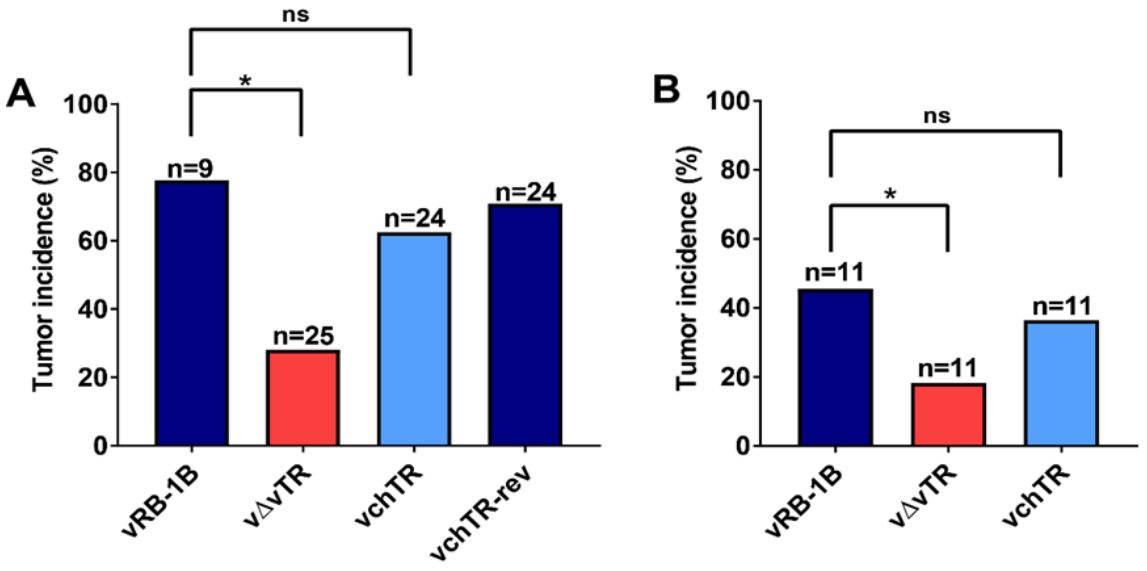

Figure 26.Tumor incidence: chTR restored the tumor formation compared to wild-type. A) Tumor percent means the percent of the birds showing gross tumors. Tumor incidence was significantly reduced in the chickens infected with the vTR-deletion virus compared to wild-type. No significant difference in the tumors induced by vchTR and that induced by wild-type virus vRB-1B. B) Tumors incidence in the contact chickens. Similar to the infected chickens, tumor incidence was significantly reduced in contacts of vTR-deletion virus, while there was no significant difference in

tumors between contacts of vchTR and wild-type vRB-1B. Differences between multiple treatments were evaluated by logistic regression test. Asterisk (*) represent the significant level ($P < 0.05$); ns indicates no significant difference.

Additionally, to address the role of vTR and the overexpression of chTR in tumor dissemination, we determined the number of organs containing gross tumors in the infected chickens during necropsies. Interestingly, the average number of tumors per infected animals was significantly reduced from 2.44 in the wild-type group to 0.88 in the animals infected with vΔvTR, however, no significant difference detected in the average number of tumors in vchTR groups 2.41 compared to the wild-type or revertant 2.00 (Figure 27). Our findings confirmed that, chTR can complement the functions of vTR in MDV-induced tumorigenesis and can promote tumor dissemination.

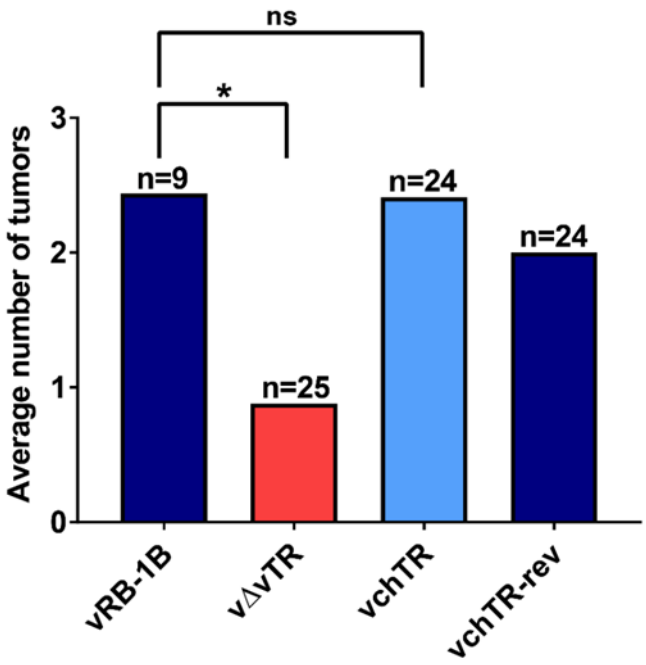

Figure 27. Tumor dissemination pattern: chTR in vhTR displayed an efficient tumor dissemination pattern. The average number of tumors was significantly reduced in the animals infected with vTR-deletion mutant while no significant difference was detected in the average number of tumors between chTR and wild-type or revertant. Differences between multiple treatments were evaluated by logistic regression test. Asterisk (*) represent the significant level ($P < 0.05$); ns indicates no significant difference.

6.4. Tumor promoting functions of the EBV-encoded EBERs in MDV-induced tumorigenesis

EBERs (EBER-1 and EBER-2) were inserted into the vΔvTR at the same vTR locus using the same platform virus. The recombinant viruses were characterized *in vitro* and *in vivo*.

6.4.1. Deletion of vTR and insertion of EBER-1 or EBER-2 did not affect MDV replication *in vitro*

To ensure that the sequentially generated recombinant viruses (vΔvTR, vEBER-1, vEBER-2, and vEBER-2-rev) were efficiently replicating in the cell culture, we performed plaque size assays and multi-step growth kinetics as described previously [155]. No significant difference was detected in the average plaque diameters with the insertion of EBERs compared to wild-type or revertant virus (Figure 28A), indicating that deletion of vTR and the sequential insertion of EBERs did not affect the viral spread from cell-to-cell which was also confirmed by multi-step growth kinetics (Figure 28B). Taken together, vTR-deletion as well as the EBERs insertion were dispensable for MDV-replication *in vitro*.

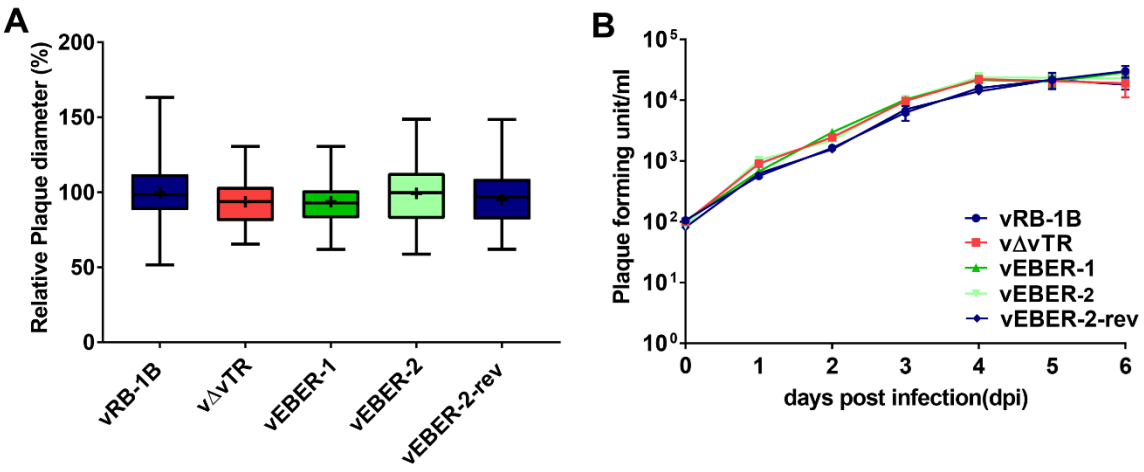

Figure 28. Characterization of recombinant MDV expressing EBER-1 or EBER-2 instead of vTR *in vitro*. A. Plaque size assays. Each virus used to infect CECs at 100 PFU. 6 d.p.i at least 50 plaques for each virus were imaged. The plaque diameters of the wild-type virus were set as 100% and then the relative plaque diameters for each mutant were calculated. Plaque sizes are shown as box plots with minimums and maximums. (P>0.05; one-way ANOVA). **B.** Multi-step growth kinetics. Data are from triplicate measurements and expressed as means ± standard deviations (error bar) (P>0.05; Kruskal-Wallis test).

6.4.2. EBERs are efficiently expressed in MDV infected cells *in vitro*

To confirm the efficient expression of EBERs in culture, we performed qRT-PCR. The CECs were infected with 1000 PFU from the corresponding viruses. The viral ICP4 and cellular GAPDH-expression was quantified for normalization (Figure 29 A and B). No significant difference in ICP4 or GAPDH expression in the infected cells. The qRT-PCR revealed that vTR expression was completely abrogated in the vΔvTR, while wild-type and revertant viruses showed almost the same vTR-expression levels (Figure 29 C). Furthermore, EBER-1 (Figure 29 D) and EBER-2 (Figure 29 E) were expressed at a comparable levels to vTR in the wild-type virus, confirming the efficient expression of EBERs.

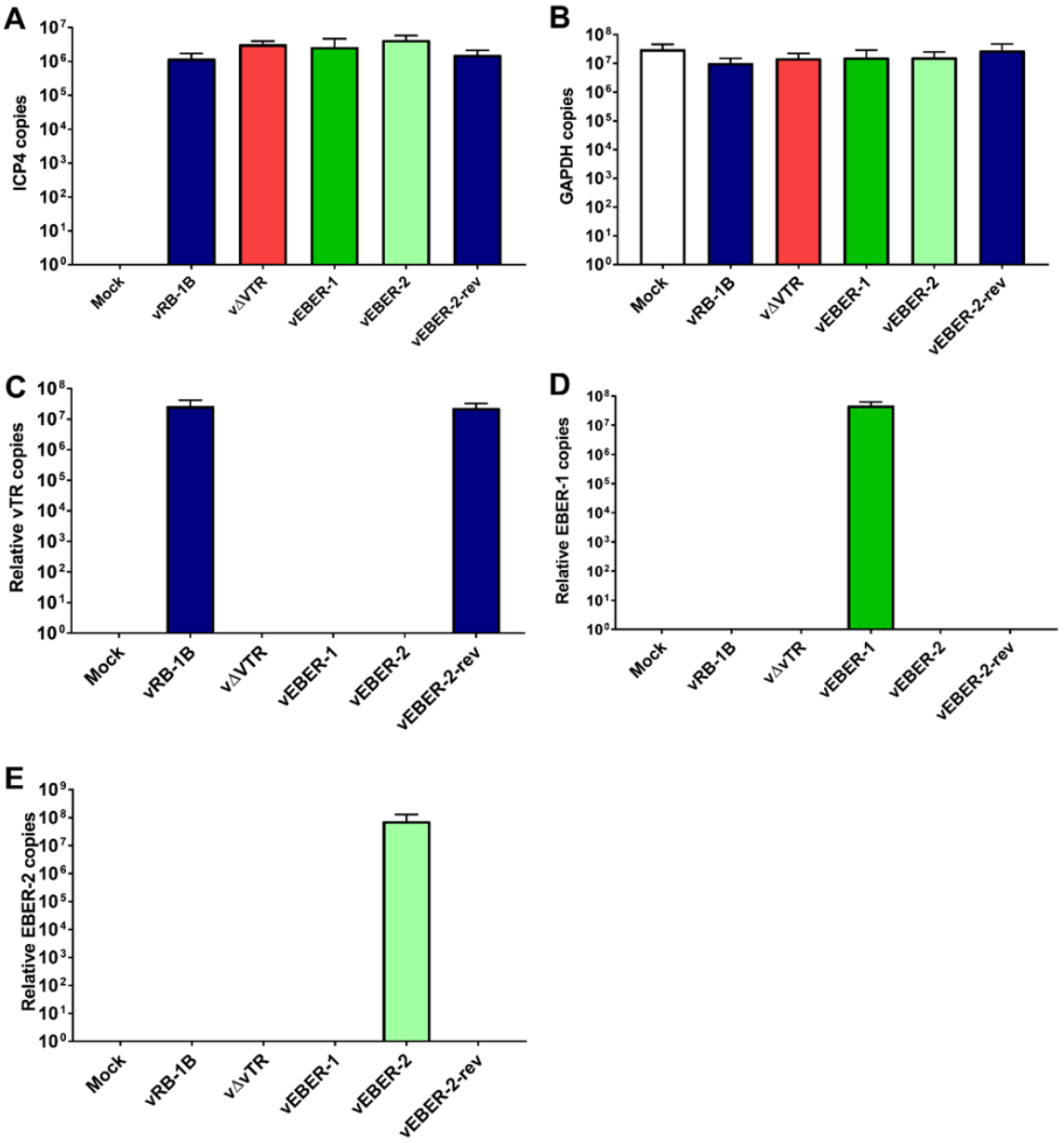

Figure 29. Quantification of EBERs and vTR expression during MDV lytic replication using qRT-PCR. 1×10^6 fresh CECs were infected with 1000 PFU of vRB-1B, vΔvTR, vEBER-1, vEBER-2, and vEBER -2-rev. The virus growth was detected 6 dpi and the genomic RNAs were extracted from corresponding viruses. Following the reverse transcription, the vTR and EBERs- expression levels were quantified using qRT-PCR. **A.** The viral ICP4 expression levels for the corresponding viruses were similar, indicating the similarity of infection ($P > 0.05$; Kruskal-Wallis). **B.** Cellular GAPDH-expression levels were also similar ($P > 0.05$; Kruskal-Wallis). **C.** vTR expression in the cells infected with the indicated viruses, no significant difference in vTR-expression between the cells infected with the wild-type virus vRB-1B and the revertant vEBER -2-rev ($P > 0.05$; Kruskal-Wallis). vTR expression was totally abrogated in either cells infected with the vTR-deletion virus vΔvTR, or mock cells. Relative vTR expression means that vTR expression in the corresponding viruses normalized to GAPDH and ICP4. **D.** EBER-1 expression in the corresponding viruses. EBER-1 expression was only detected in the cells infected with vEBER-1. **E.** EBER-2 expression in the corresponding viruses. EBER-2 expression was only detected in the cells infected with vEBER-2. EBER-2 expression was higher than EBER-1 and their expression levels were almost similar to vTR in the wild-type vRB-1B or revertant virus. vTR and EBERs expression levels were normalized to GAPDH and ICP4. Data represents three independent experiments and expressed as means ± standard deviations (error bar).

6.4.3. *In vivo* study: EBERs complement the loss of vTR in MDV-induced tumorigenesis

To determine if EBERs possess tumor-promoting functions using a small animal model for herpesvirus-induced tumor formation, we performed animal experiment in which the infected chickens were randomized, grouped, and monitored for developing of clinical symptoms and tumors. To determine if the virus replication was altered with the deletion of vTR or insertions of EBERs, we quantified the viral genome copy in the blood using qPCR. As shown in (Figure 30 A), the recombinant viruses were efficiently replicating *in vivo* comparable to the wild-type or the revertant virus vEBER-2-rev, indicating that neither vTR-deletion nor EBERs insertion effect MDV replication properties *in vivo*. During the experiment, the clinical symptoms and tumor incidences were recorded overall the course of infection. The clinical symptoms observed in each group were recorded and analyzed for MD incidence. We observed that the MD incidence was severely reduced in the chickens infected with vΔvTR and vEBER-1 while vEBER-2-induced a higher incidence compared to the wild-type, suggesting that the vTR-deletion or EBER-1 insertion delayed the MD onset, while the insertion of EBER-2 induced clinical symptoms comparable to the wild-type (Figure 30 B). The tumor incidence was significantly reduced ($P<0.125$) in the chickens infected with MDV-deficient vTR (28%) and in chickens infected with vEBER-1 (40%) while there was no significant difference detected between the chickens infected with either vEBER-2 (65.8%) or that infected with the wild type vRB-1B (77.77%) and revertant (70.38%) (Figure 31).

Similarly, at the final necropsy, we observed extreme reduction in gross tumors in the chickens infected with vTR-deletion and vEBER-1 virus while most of the tumors observed in the chickens infected with the vEBER-2 and the revertant. Our results showed that EBERs restored (partially for EBER-1) or (totally for EBER-2) the tumor formation and complement the functions of vTR in MDV-induced tumorigenesis.

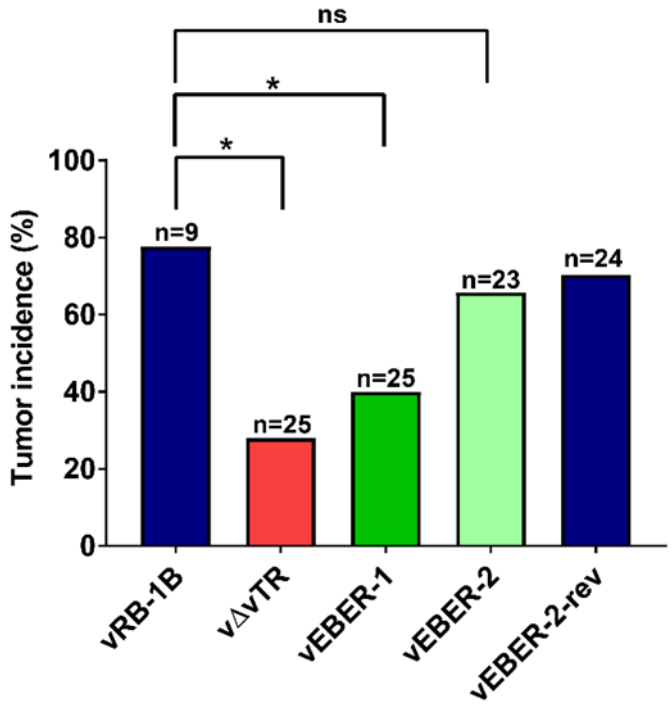

Figure 30. EBERs complement the vTR loss in MDV-induced tumor formation. Tumor percent means the percent of birds showing gross tumors in different body organs following the infection. Tumor percent was significantly reduced in the chickens infected with vTR-deletion virus and vEBER-1 compared to the chickens infected with the wild-type virus vRB-1B ($P<0.125$, Fisher's exact test). There was no significant difference in the tumors induced by vEBER-2 or revertant virus vΔEBER-2-rev compared to the wild-type virus vRB1B ($P>0.125$, Fisher's exact test). Differences between multiple treatments were evaluated by Fisher's exact test. Asterisk (*) represent the significant level ($P<0.125$); ns indicates no significant difference.

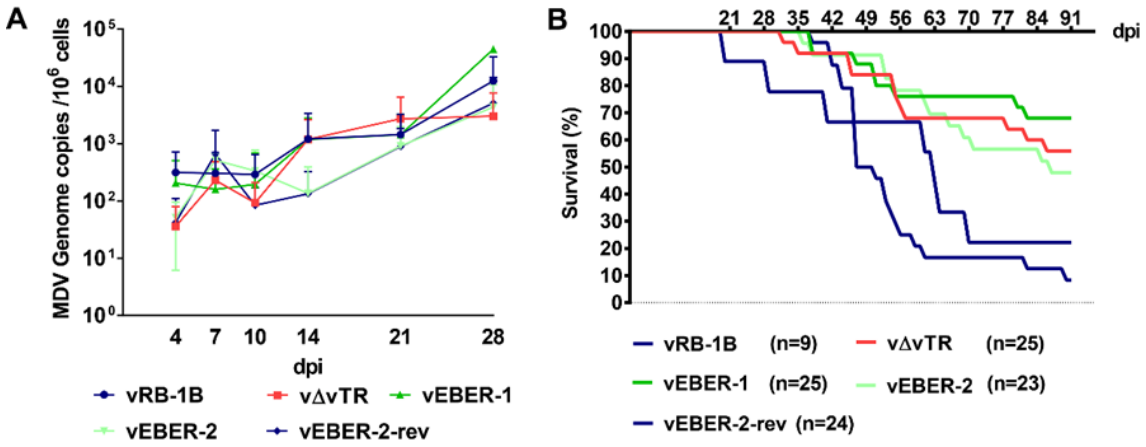

Figure 31. MDV replication *in vivo* did not change with vTR-deletion or EBERs insertion. A. Whole blood samples were collected from the chickens infected with vRB1B, vΔvTR, vEBER-1, vEBER-2 or vEBER-2 -rev at indicated time points, DNA was extracted, the viral ICP4 and host iNOS genes for each virus were quantified using qPCR. Viral titers shown as mean of the genome copy number per 10^6 cells of eight-infected chickens per group. Each group was in a separate room. ($P>0.05$; compared to wild-type virus, Kruskal-Wallis test). **B**. MD incidence was severely reduced in the chickens infected with the vTR-deficient virus compared to the chickens infected with the wild-type virus vRB-1B or revertant virus vEBER-2-rev. MD incidence in the chickens infected with vEBER-2 increased up and was observed at later stages of infection.

6.4.4. EBERs displayed an efficient tumor dissemination pattern

To address the role of EBERs insertion in the tumor dissemination, we determined the number of organs containing gross tumors in the infected chickens during necropsies. We found that the average number of tumors per infected animal was significantly reduced from 2.44 in the wild type group to 0.88 in the group animals infected with vΔvTR, and 1.20 in the vEBER-1 group. There was no significant difference in the average number of tumors between the animals infected with vEBER-2 (2.26) compared to the wild type group or the revertant virus (2.00) (Figure 32). Our findings confirmed that vTR and EBER-2 play an important role in the development and dissemination of tumors and that EBER-2 could complement the vTR-functions in MDV-induced tumor formation and dissemination.

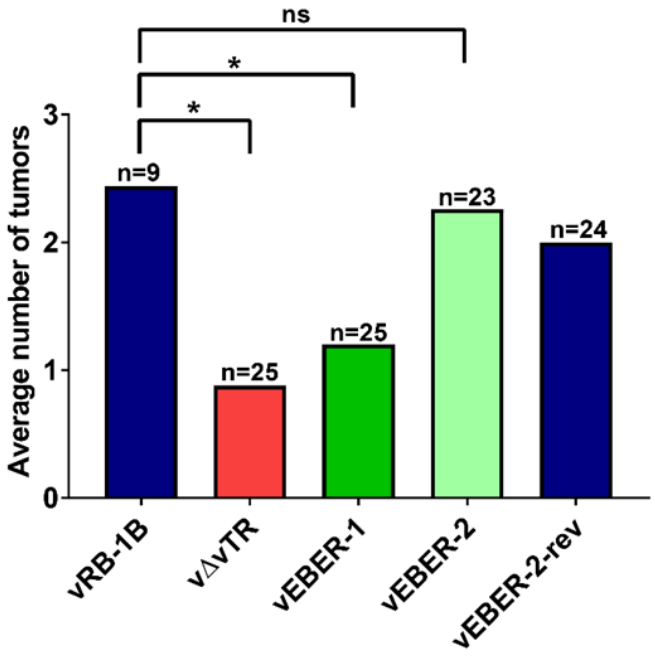

Figure 32. EBERs-induced an efficient tumor dissemination pattern. The average number of tumors per infected animals for each group was significantly reduced in the chickens infected with the vTR-deletion and vEBER-1 compared to the animals infected with the wild-type vRB-1B or revertant virus ($P<0.125$, Fisher's exact test). No significant difference detected in the chickens infected with vEBER-2 compared to the wild-type vRB-1B ($P>0.125$, Fisher's exact test). Differences between multiple treatments were evaluated by Fisher's exact test. Asterisk (*) represents the significant level ($P<0.125$); ns indicates no significant difference.

6.5. Mechanism of vTR in MDV-induced tumor formation

Until now, the mechanism of TRs in tumorigenesis remains elusive. It has been recently demonstrated that TRs have functions in tumorigenesis beyond their role in the telomerase complex. Furthermore, recent work by Kaufer and colleges has proved that vTR interacts and re-localizes the cellular protein RpL22 [113]. However, the role of vTR-RpL22 interaction in MDV-induced tumorigenesis is not fully understood. Additionally, Rao and colleges have shown that RpL22 down-regulation promotes T-cell transformation [116]. Based on these data we hypothesized that vTR can down-regulate RpL22 which plays a crucial role in the virus-induced cellular transformation. We used *in vitro* system to test this hypothesis which was comprising human and chicken cells.

6.5.1. vTR did not down-regulate RpL22 in HeLa cells

vTR, EBER-1 and EBER-2 were cloned to PVitro-2-MCS plasmid and the resulted clones were confirmed by PCR and Sanger sequencing (data not shown). The cloned plasmids were transfected into HeLA cells using lipofectamin 2000 reagents and then RpL22 status

was detected by Western Blot analysis using Anti-RpL22 antibody (Ab77720, Abcam Cambridge, UK). Next day, total RNAs were isolated and transcriped into cDNA. vTR and EBERs expression levels were quantified by qRT-PCR (Figure 33A). Comparable expression levels for EBERs and vTR were detected. RpL22 status was checked by Western Blot analysis (Figure 33B). Our results showed that there was no difference in RpL22 expression levels in the cells transfected with the empty vector (negative control) and cells transfected with EBER-1, EBER-2 or vTR (Figure 34), suggesting that neither EBERs nor vTR can down-regulate RpL22 using HeLa cells.

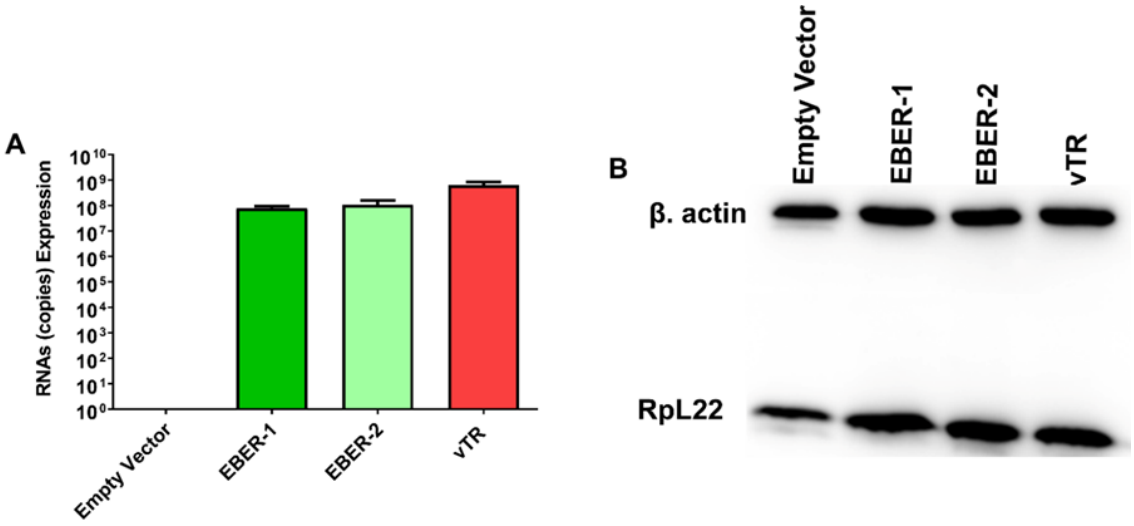

Figure.33. EBERs and vTR were highly expressed after transfection but did not down-regulate RpL22 using HeLa cells. A. The cells were counted and seeded in 6 well plates. After becoming confluent, the cells were transfected with the vTR, EBER-1and EBER-2 (Pvitro-GFP-plasmid). Next day, cells were checked for GFP expression. Genomic RNAs were extracted, reverse transcriped. vTR and EBERs expression was detected using qRT-PCR. Plasmid DNAs from each cloned plasmid were prepared and serially diluted. The copies used to represent the standard curve and calculate the CTs. B. Western Blot analysis to detect RpL22 status upon transfection. Beta-actin was used as a loading control and for normalization.

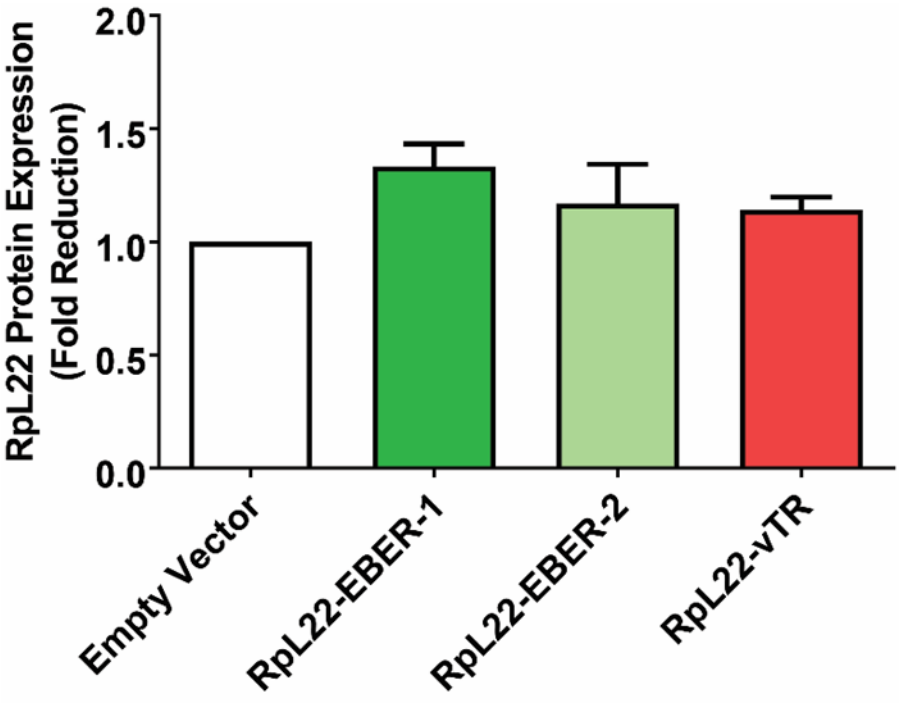

Figure 34. vTR did not down-regulate RpL22 in HeLa cells. RpL22 expression levels were similar in the cells transfected with empty vector or different RNAs (vTR and EBERs) with. Data represents three independent experiments.

6.5.2. vTR did not down-regulate RpL22 using DF-1 cells.

In addition to HeLa cells, RpL22-down-regulation has been tested on DF-1 cells, chicken fibroblast cell line. Similar to HeLa cells, vTR did not down-regulate RpL22 but in this experiment there was RpL22 down-regulation in DF-1 cells transfected with EBER-1 (Figure 35).

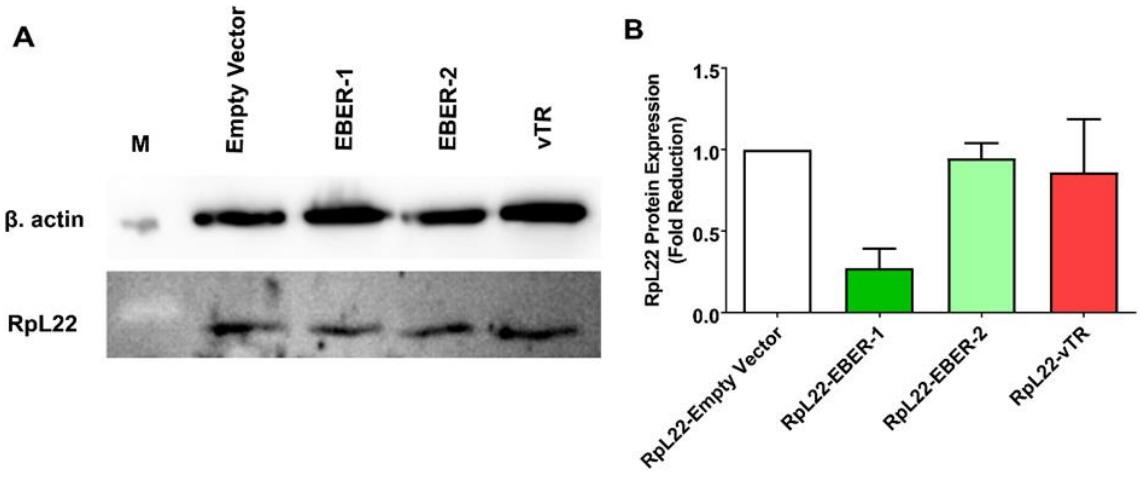

Figure 35. vTR did not down-regulate RpL22 using DF-1 cell lines. A. DF-1 cells were transfected with RNAs-GFP plasmids. 48hrs post transfection the cells were harvested and RNAs were extracted,

the total protein concentration in the cell lysis was measured using Roti Quant. Kit. 20 ug protein from each sample were loaded and RpL22 was detected with Western Blot. Beta-actin was used as a loading control and for data normalization. No fold change was detected in the expression levels of RpL22 in the cells transfected with vTR and empty vector. RpL22 down-regulation was detected in the cells transfected with EBER-1.

6.5.3. The role of vTR-RpL22 interaction in MDV-induced tumor formation

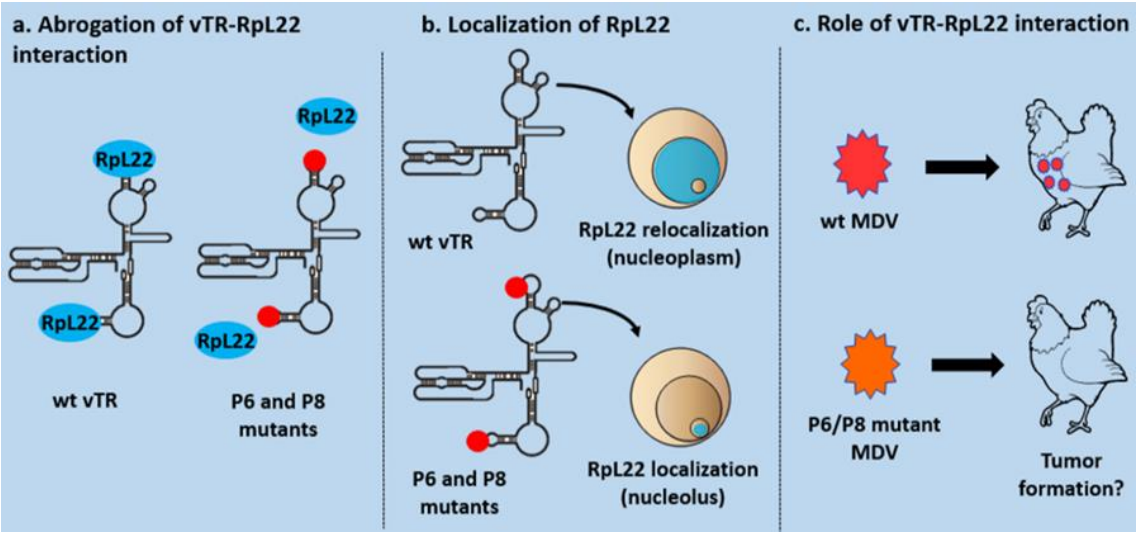

Figure 36. The role of vTR-RpL22 interaction in MDV-induced tumor formation. A. vTR has two stem loops; P6 and P8 that have a high homology to RpL22 binding sites, these sites will be mutated to abrogate vTR-RpL22 interaction *in vitro*. **B.** We will determine RpL22 localization in chicken cells transfected with vTR and the variants P6 and P8. **C.** We will introduce the stem-loop mutations into MDV-BAC then we will characterize the mutants *in vivo* to address the role of this interaction in MDV-mediated transformation.

6.5.3.1. To identify RpL22 binding motifs on vTR

Mutation of vTR stem-loops P6 and P8:

RpL22 consensus motifs on vTR were mutated (stem-loop P6 and P8) using phusion polymerase mutagenesis approach. The mutations were confirmed with sequencing (data not shown).

***In vitro* transcription of EBERs and vTR-variants:**

vTR wild-type and mutant- DNA-plasmids were linearized first and then the target sequences were *in vitro* transcriped (and labelled with Biotin UTP). DNAs contaminating the RNAs were eliminated using RQ1-RNase-free DNase (Promega) and the RNAs were precipitated using ammonium acetate. The RNAs were checked on formaldehyde gel to confirm that the full length sequences were properly transcriped

6.5.3.2. *In vitro* translation of RpL22-His

RpL22-His was obtained by using TNT Quick Coupled Transcription-Translation System (Promega). The translated protein were aliquoted and kept in -80^0 C. The tagged RpL22 was detected by Western Blot (Figure 34).

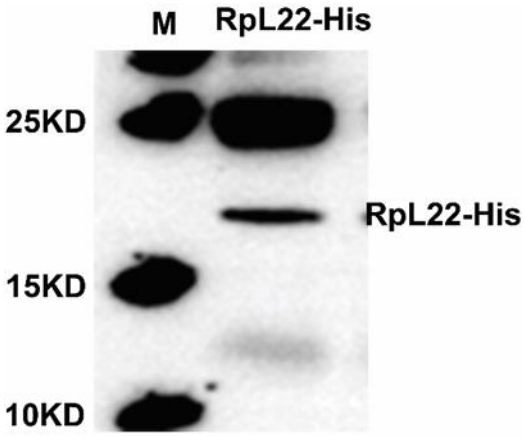

Figure 37. *In vitro* translation system for RpL22 expression. Rabbit Reticulocytes were used for in vitro translation of RpL22-His. The recombinant protein was detected using Western Blot. 2ul of the lysate were denatured and loaded on 12% SDS gel. Rabbit anti-His tag antibody was used. The protein were kept in -80^0 C for further use.

6.5.3.3. Biotin-RNA pull down assay

In order to determine whether vTR stem-loops P6 and P8 represent the binding motifs for RpL22, coIP was performed. *In vitro* translated RpL22 was incubated with the Biotin-UTP labelled-RNAs. Beta-actin RNA was used as negative control. vTR-RpL22 complex was pulled down using streptavidin beads, followed by Western Blot analysis to detect if the protein still bind to mutated RNA or not. Our result for this assay was not so clear. The protocol still has to be optimized. The vTR-double mutants P6 P8 binds to RpL22 similar to wild-type (Figure 35).

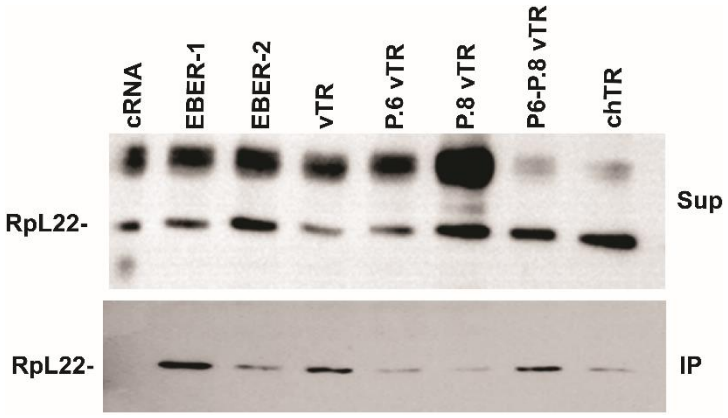

Figure 38. coIP assay. Upper panel represents the supernatant and the lower panel shows IP product. Double mutant plasmid of vTR should not show any IP product. Further investigations will be required to optimize the protocol.

7. Discussion

The aim of this work was to determine if the overexpression of the cellular telomerase RNA (TRs) and herpesviruses RNAs (EBERs) promote tumor development using a natural virus-host infections model for herpesvirus tumorigenesis. To address this aim, we initially deleted vTR from RB-1B, a very virulent MDV strain and subsequentially inserted either chTR or EBERs in the same locus of vTR and their expression was regulated by the same vTR promoter. vTR is overlapping with MDV-L-ORF1, ICP0 orthologue. Therefore, the entire deletion of vTR was performed after we investigated the importance of the putative anti-sense ICP0-OFR for MDV-replication properties.

7.1. MDV-ICP0

Albeit the characterization of some MDV genes and their role in MDV-pathogenesis and tumor formation, some other genes are encoded by MDV and their functions are not fully understood [159]. One of the MDV-ORFs that is not known whether it plays a role in MDV-pathogenesis or not is (R-LORF1, MDV002, ICP0) herpesvirus positional orthologue. The putative ICP0 is located at the junction between IR_L and IR_S. In HSV-1, ICP0 plays a crucial role in the virus infection by inhibiting the host antiviral response [160]. However, its role in MDV-pathogenesis remains concealed. In the current study, due to lack commercial antibodies, an HA-tag sequence was inserted at the C-terminus of the putative ORF. In Western Blot analysis (lysate of infected cells) we could not detect ICP0 protein which means that MDV-ICP0 might not be expressed. Furthermore, the recombinant MDV lacking ICP0 was replicating efficiently and spread from cell-to-cell comparable to the wild-type virus by plaque size assays. Furthermore, a collaborator did RNA seq and ribosomal profiling for vTR region and there was no detectable reads for antisense strand in this region (Personal communication). These findings indicated that ICP0 is not required for MDV lytic replication *in vitro*. Since the cloned ICP0-ORF into Pvitro-2MCS-plasmid downstream CMV promoter was detected by Western Blot, this provides an explanation why ICP0 in MDV genome was not detected. Our results for ICP0 comes in consistent with the finding of Trapp and other colleges who deleted four CRs regions (CR1-CR4) of vTR. These four CRs are already overlapping with 60 bp of ICP0 and they documented that the virus replication *in vivo* and *in vitro* did not change with the deletion [8]. MDV-lacking the entire vTR (CR1-CR8) was replicating efficiently *in vivo* and *in vitro* which was in agreement with Trapp findings and confirmed that either a part of ICP0-ORF (62 bp) or the entire frame is not essential for the virus lytic replication. Taken together, unlike HSV-1, MDV-ICP0 is not expressed and is dispensable for the viral replication *in vitro*. Based on these findings, we decided to delete the entire vTR sequence (CR1-CR8) resulted in a platform virus vΔvTR in which the chTR or

EBERs would be inserted and evaluated for the tumor promoting functions using a small animal model for herpesvirus tumorigenesis.

7.2. Overexpression of cellular TRs (chTR) promotes tumor development in MDV-induced tumor formation

There is a correlation between the telomerase activity and malignancies [161]. It has been shown that TRs-upregulated in several cancers [162]. MDV is currently the only virus that encodes a telomerase RNA (vTR) subunit genes. vTR is essential for MDV-induced transformation; however, the mechanism is not completely understood. vTR is dispensable for MDV replication but it's crucial for the virus oncogenesis. vTR exhibits 88% sequence identity with the chicken telomerase (chTR), this high homology was interpreted to be as evidence for selective pressure [106]. vTR is incorporated into the telomerase complex and was shown to be more efficient than chTR when combined with the recombinant chicken TERT *in vitro* [108]. This model denotes that the chTR levels are limiting in a certain lymphocyte population and TERT level increases while the vTR is efficiently expressed from the virus [163]. It has been recently shown that the transforming properties of vTR is independent on its role in telomerase complex, suggesting new function(s) for the viral telomerase [113]. The promoter of vTR in MDV genome is more efficient than the promoter of the cellular telomerase RNA chTR [112]. The expression levels of vTR are very necessary for the its functions [112]. Recent work, done by Gazzaniga and colleges, has demonstrated that the overexpression of human telomerse RNA (hTR) can inhibit the T-cells apoptosis [139]. We hypothesized that the overexpression of chTR can complement the functions of vTR in MDV-induced tumor formation and contributes to cellular transformation. To test this hypothesis, a recombinant MDV virus that expressing chTR instead of vTR was generated using Two-step-Red-mediated mutagenesis technique and then was characterized *in vitro* and *in vivo* using a natural virus-host model for herpesvirus tumorigenesis. We initially deleted vTR (CR1-CR8) from the virus genome and subsequently inserted chTR into the same vTR locus in RB-1B strain. We also generated a revertant virus in which the vTR sequences were restored. We found that the recombinant viruses replicated efficiently compared to the wild-type and the revertant virus *in vitro*, indicating that vTR-deletion and chTR-insertion were dispensable for the viral replication properties. Our findings regarding the vTR-deletion were in agreement with the previous study performed by Trapp.et al., 2006 [8]. The overexpression of chTR was confirmed by qRT-PCR and the analysis revealed that chTR (in the vchTR) expression levels were comparable to vTR in the wild-type or revertant virus. Furthermore, the chTR expression level in vchTR was up to 100-fold more than the baseline chTR (the cellular telomerase in mock), confirming the strong overexpression.

To investigate the tumor promoting properties of the overexpressed cellular TRs, we infected one day old SPF chicks with the recombinant viruses. Peripheral blood from the infected animals in each group was collected to quantify the MDV genome copy numbers and we found that there was no significance difference in the copy numbers of the vΔvTR or vchTR compared to the wild-type vRB-1B or the revertant vchTR-rev. The MDV genome copy numbers in the peripheral blood corresponds to the number of infected T-cells [164] which explains the variations in the genome copy number among the viruses . Upon infection, MDV establishes a life cycle through different stages defined as lytic, latency and reactivation, we were able to detect the MDV genome copies number for both of vΔvTR and vchTR at later stages of infection meaning that the virus replication has been not affected with the deletion of vTR and insertion of chTR *in vivo*. The animals were monitored on a daily basis for developing of MD clinical symptoms. MD symptoms were recorded and we analyzed the MD incidence for the corresponding viruses. We demonstrated that the MD incidence was reduced in the absence of vTR but restored again in the chickens infected with vchTR comparable to the wild-type and revertant viruses (Fig. 5). The explanation for that that the vTR-incorporated telomerase activity is responsible for the rapid MD-onset. The vTR-deletion mutant lacking the telomerase activity and hence the MD incidence was severely impaired. The insertion of chTR restore the telomerase activity that's why the MD onset was comparable to the wild-type. The chickens were also monitored for tumor development. Our *in vivo* results demonstrated that the tumor development was severely impaired in the chickens infected with the vTR-deletion (28%), while the vchTR restored the tumor formation (63%) compared to the wild-type (77.7%) or the revertant (70.83%). Our findings strongly suggest tumor-promoting functions of the over-expressed cellular TRs and that overexpression of the cellular TRs contributes to cellular transformation. Similarly, the tumor development was severely reduced in the contact animals of vΔvTR compared to the contacts of the wild-type and revertant virus, while the vchTR contacts group restored the tumor formation indicating that the virus transmission and pathogenesis via natural routes was not altered with the insertion of chTR. To investigate the role of vTR and the overexpression of chTR on the tumor dissemination pattern, we counted the number of organs in the infected chickens form the corresponding viruses with visible tumors and we observed that the chickens infected the vTR-deletion developed tumors at least in 4 organs while in the vchTR and wild-type virus the tumors were detected in at least 6 organs. Our findings clearly showed that chTR in vchTR displayed an efficient tumor dissemination pattern. Taken together, the overexpression of the chTR promotes tumor development in MDV-induced tumor formation and enhances the tumor dissemination. (Fig. 7). Furthermore, our small animal model for tumors represents an efficient system to investigate the TRs oncogenic properties and the beyond mechanisms. The molecular mechanism of the TRs in

tumor development still needs further investigations. In a previous study, we proved that vTR and chTR interact with the cellular protein ribosomal L22 (RpL22) [113]. RpL22 is essential for T-cell development and plays an important role in the cellular transformation mediated by herpesvirus EBV-encoded-EBER-1. The viral and cellular TRs-RpL22 interaction might have a role in MDV-induced transformation but we are currently addressing this point. Recent study showed that the genetic or environmental factors that alter hTR levels can directly affect immune cells function to influence health and disease suggesting pro-oncogenic functions [139]. Our findings open a new aspects for the contribution of the cellular TRs in cancer formation. Identifying the molecular basis of the cellular TRs which will provide a better understanding of the role of telomerase RNA in cancers.

7.3. EBERs promote tumor formation in MDV-induced cellular transformation

EBV-encoded RNAs (EBERs) are the most abundant transcripts in EBV-induced tumor and transformed cells [165]. However, the role of these transcripts in tumor formation remains has not addressed. EBER-1 and EBER-2 are highly conserved among EBV strains indicating their functional role in oncogenesis [123]. They are thought to be functional through forming stable complexes with some cellular proteins such as La, RpL22, and PKR. These interactions are necessary for the EBV persistence [126]. The transforming properties of EBERs and their contribution to the viral pathogenesis still unclear. Since the interaction partners of vTR and EBERs are common and highly conserved between human and chickens (RpL22), we hypothesized that EBER-1 and /or EBER-2 possess tumor-promoting functions and could complement the loss of vTR in MDV-induced tumor formation. We generated recombinant MDVs that either encode EBER-1 or EBER-2 instead of vTR. The recombinant viruses were characterized and assessed *in vivo* for their oncogenic potential. The vTR-deletion (vΔvTR) platform virus was used and EBERs were introduced at the same vTR locus resulted in two recombinant viruses that either expressing EBER-1 (vEBER-1) or EBER-2 (vEBER-2) instead of vTR. Our results demonstrated that, the recombinant viruses harbored EBER-1 or EBER-2 were replicating efficiently and similar to the wild-type or the revertant viruses *in vitro* or *in vivo*, suggesting that the insertion of EBERs did not change the MDV-lytic replication. To confirm the overexpression of EBERs, we performed qRT-PCR analysis. The qRT-PCR analysis revealed that both EBER-1 and EBER-2 expression levels were comparable to vTR levels in the wild type and revertant viruses confirming the overexpression. To investigate if EBERs can complement vTR in MDV-induced pathogenesis and tumor formation, we performed an animal experiment in which we monitored the infected chickens for developing lymphomas. The peripheral blood was collected from the infected chickens for each group on a particular time points and the viral genome copy numbers was quantified using qPCR. Our results showed that the *in vivo* replication of the virus did not

change after the insertion of EBERs compared to the wild-type or revertant virus. The ability of the recombinant viruses to transform T-cells *in vivo* is varying among the mutants which biologically explains the difference in the genome copy numbers during the course of infection (Fig. 4). The MDV-lifecycle passes through different lytic, latent and reactivation stages within the host and we could detect the viral genome copies at later stages of infection confirming that the virus lifecycle did not affect with the insertion of EBERs and displayed as a normal lifecycle. We monitored the infected animals for developing clinical symptoms of the disease (MD). The MD incidence was recorded for the corresponding viruses. MD incidence was severely impaired in the chickens infected with the vTR-deletion virus, vEBER-1 and vEBER-2 because vEBER-1 and vEBER-2 are lacking the telomerase activity. Animals infected with MDV harbors EBER-2 developed clinical symptoms similar to the chickens infected with the wild-type virus or revertant virus, while there was no marked difference in the symptoms between the group infected with vEBER-1 and vΔvTR underlying that EBER-1 did not efficiently contribute to cellular transformation compared to EBER-2 . To assess the tumor-promoting functions of vEBER-1 and vEBER-2, we monitored the infected chickens for developing of tumors in different body organs. Our *in vivo* study showed that the lymphoma development was severely impaired in the chickens infected with the vTR-deletion virus and in the chickens infected with vEBER-1 while the vEBER-2 partially restored the tumor formation comparable to the wild-type or revertant virus. These findings are clearly pointing the oncogenic potential of EBER-2 that it can contribute to the transformation of different kinds of cells in different hosts. vEBER-1- induced tumor levels were partially high compared to vTR-deletion (vΔvTR) but not comparable to wild-type or revertant viruses, suggesting the higher potential tumorigenecity of EBER-2 over EBER-1 in this model.

To address the role of EBERs in tumor dissemination, we counted the number of organs containing gross tumors in the infected chickens during necropsies. The average number of tumors per infected animal was significantly reduced in the animals infected with vΔvTR and vEBER-1, while no significant difference detected in the average number of tumors between the animals infected with vEBER-2 and the wild-type or the revertant viruses. Our findings confirmed EBER-2 play an important role in cellular transformation and dissemination. Similarly, the average number of tumors per infected animals in the chickens infected with vEBER-1 was partially high compared to the vΔvTR, indicating the biological role of the common interaction partners in the tumor formation and dissemination, especially the cellular RNA-binding protein RpL22[115]. The vEBER-2 efficiently restored the viral pathogenesis, tumor formation and the dissemination pattern indicating that EBER-2 as a carcinogenic component of EBV has a pro-oncogenic activity in MDV-induced tumor formation.

The molecular mechanisms of the viral and cellular TRs in cancer formation is not yet known but Kaufer and other colleges have shown that vTR could interact RpL22 [113]. The role of vTR-RpL22 interaction in MDV-induced transformation is still unclear. Further investigations are required to define the role of EBER-2- in cellular transformation which may provide novel interaction partners that are conserved between chickens and human. Collectively our data provides the first description of the tumor-promoting functions of EBERs and their contribution in transformation of chicken T-cells. Furthermore, this provides a useful tool for further investigations of the EBERs transforming properties and the underlying mechanisms.

7.4. Role of vTR-RpL22 in MDV-induced tumor formation

Albeit vTR is crucial for the malignant activities induced by the virus, the mechanism remains mystery [113]. Rao and colleges shown that inactivation of human RpL22 promotes T-cell transformation and developing hematologic malignancies [116]. We hypothesized that vTR can down-regulate RpL22 which in turn promotes the cellular transformation. To address that, we established *in vitro* system and determined the RpL22-status using HeLa cells and DF-1 cell lines harbor vTR or EBERs. vTR did not down-regulate RpL22 *in vitro* using the above mentioned-cell lines, suggesting that vTR-RpL22 interaction did not affect the protein expression. The time required for vTR to induce effect on RpL22 may be an important factor, so we have to establish single cell clones that are expressing vTR or EBERs and followed by quantification of RpL22 expression. Furthermore, DNA extracted form MDV-tumors revealed no mutations in RpL22 gene as a kind of selective pressure (data not shown). vTR expression has been previously shown to induce re-localization of RpL22 from nucleolar structures in mammalian cells. To address the importance of this re-localization, we generated a series of vTR mutant-plasmids, using site directed mutagenesis, that are carrying mutation in the P6 and P8 stem-loops that have high homology to RpL22 binding sites with a generalized consensus motif [1]. The interaction of RpL22 with vTR variants (P6 /P8 stem-loops mutants) was evaluated *in vitro*. Biotin-labeled vTR and its variants were generated by *in vitro* transcription and incubated with the *in vitro* translated RpL22 protein (using coupled in vitro transcription and translation system). vTR interacts RpL22 and forming a complex. The resulted complex was pulled down using streptavidin beads and then analyzed on SDS-PAGE. Western Blot was performed using monoclonal anti-HIS antibody to detect IP product. RNA-coIP was optimized several times and the result we got for the last experiment was that RpL22 interacts with EBER-1 and vTR, however, the double mutants plasmid (P6 and P8 stem-loops) interact with the protein too which could mean a cross-contamination from the wild-type. Sequencing are important to determine which RNAs are there. We are currently optimizing the IP protocol. EMSA (Electro-Mobility-Shift Assay) and RNA chip [166] as alternatives. Since the introduced mutations can affect the RNA folding

properties, RNA-folding in silico analysis and TRAP assay as described previously [102] are highly recommended. After confirming the abrogation of vTR-RpL22 interaction, the mutations will be introduced to MDV genome and the recombinant MDVs will be charachterized *in vivo*. This will shed the light on the role of the RNA-binding proteins in MDV-induced cellular transformation.

8. Zusammenfassung

Tumorfördernde Eigenschaften der zellulären Telomerase-RNA und viraler RNAs in Herpesvirus-induzierter Krebsentstehung

Das Virus der Marek'schen Krankheit (MDV) ist ein onkogenes Alphaherpesvirus welches zur Entstehung von tödlichen Lymphomen führt. MDV kodiert für eine virale Telomerase RNA (vTR), die in allen Stufen des MDV-Lebenszyklus stark exprimiert wird. vTR ist für die durch MDV induzierte Tumorentstehung essentiell, wobei der zugrundeliegende Mechanismus nicht komplett verstanden ist. Trotz der hohen Sequenzhomologie zwischen vTR und der Wirtszell-Telomerase RNA (chTR) von 88% ist nicht untersucht ob die Überexpression von chTR zur Zellentartung beiträgt. Interessanterweise haben TRs und Ebstein-Barr-Virus (EBV)-kodierte RNAs (EBER-1 und EBER-2) gemeinsame Wechselwirkungspartner, welche in Menschen und Hühnern hochkonserviert sind. EBERs sind die am stärksten auftretenden viralen Transkripte in EBV Tumorzellen. Die Rolle dieser EBERs in der Tumorentstehung ist jedoch strittig.

Ziel des ersten Teils der Dissertation war die Untersuchung, ob eine Überexpression der zellulären TRs (chTRs) tumorbegünstigende Funktionen im Tiermodell für herpesvirusinduzierte Tumorentstehung haben. In einer vTR Deletionsmutante (vΔvTR) des hochvirulenten MDV Feldstammes RB-1B wurde durch Two-step Red-mediierte Mutagenese chTR in den vTR Locus eingesetzt (vchTR). Per qRT-PCR wurden die vTR und chTR (in vchTR) Expressionsniveaus der Virusmutanten bestimmt. chTR Expressionsniveaus in vchTR war mit vTR im Wildtyp-Virus vergleichbar. Weder die vTR-Deletion noch die chTR Insertion hatte Einfluss auf die Virusreplikation in vitro und in vivo. Die Tumorentstehung war in Abwesenheit von vTR erheblich reduziert wohingegen die Tumorinzidenz in den vchTR infizierten Hühnern vergleichbar mit der Wildtyp- und der Revertantengruppe war. Diese Daten liefern die ersten Hinweise darauf, dass die Überexpression von zellulären TRs die Funktionen von vTR in der MDV induzierten Tumorentstehung komplementieren kann.

Im zweiten Teil der Dissertation haben wurde Rolle der EBERs (EBER-1 und EBER-2) adressiert. Dabei war das Ziel herauszufinden ob die EBERs tumorbegünstigende Funktionen besitzen und Hühner-T-Zellen im Tiermodell für MDV-Tumorgenese transformieren können. Hierzu wurden rekombinante MDV Mutanten generiert die entweder EBER-1 oder EBER-2 an Stelle von vTR exprimieren: vEBER-1 bzw. vEBER-2. Die Expressionsniveaus beider EBERs wurde in lytisch infizierten Zellen in vitro getestet. Beide EBERs wurden stark exprimiert und waren mit der vTR Expression vom Wildtyp und der Revertante vergleichbar. Zusätzlich wurde eine effiziente Virusreplikation in Zellkultur und im

Tiermodell beobachtet. Um die tumorfördernden Eigenschaften der EBERs zu untersuchen wurde ein Tierversuch durchgeführt, wobei die Tiere auf Tumorentstehung kontrolliert wurden. Die EBERs konnten, im Vergleich zur vTR Deletionsmutante, die Tumorentstehung teilweise wiederherstellen. Die Tumorinzidenz von vEBER-2 war höher als die von vEBER-1 verglichen mit dem Wildtyp. Diese Ergebnisse zeigen erstens mögliche tumorfördernde Eigenschaften der EBERs – auch, dass diese unterschiedliche Wirts-Immunzellen transformieren können. Zweitens bieten sie ein nützliches Tiermodell für virusinduzierte Krebsentstehung um die EBER-Aktivitäten in Zelltransformationen und die hier zugrundeliegenden Mechanismen zu untersuchen.

9. Summary

Marek's disease virus (MDV) is a highly oncogenic alphaherpesvirus that causes deadly lymphomas in chickens. MDV encodes a viral telomerase RNA (vTR) that is highly expressed during all stages of the virus life cycle. vTR is crucial for efficient MDV-induced lymphoma formation, however, the mechanism is not completely understood. Despite the high sequence identity between vTR and the cellular telomerase RNA (chTR) of 88%, it remains elusive if the overexpression of the chTR can contribute to cellular transformation. Intriguingly, TRs and Epstein- Barr virus (EBV) encoded RNAs (EBER-1 and EBER-2) have interaction partners in common that are highly conserved in humans and chickens. EBERs are the most abundant viral transcripts in EBV-induced tumor cell. However, their role in tumor development is still controversial.

In the first part of the study, we wanted to investigate if the overexpression of cellular TRs (chTR) have tumor-promoting functions using a natural virus-host animal model of herpesvirus tumorigenesis. We initially deleted vTR (vΔvTR) in the RB-1B genome, a very virulent MDV strain, and subsequently inserted chTR at the vTR locus resulting in vchTR, using the Two-step Red-mediated mutagenesis system. The expression levels of vTR and chTR (in vchTR) were confirmed using qRT-PCR. chTR expression levels in vchTR were comparable to vTR in the wild-type. Neither the vTR-deletion nor the chTR insertion effected the MDV replication properties *in vitro* and *in vivo.* Intriguingly, the tumor formation was severely impaired in the absence of vTR while, the tumor formation in the chickens infected with vchTR was similar to those infected with the wild-type or revertant virus. Our results provided the first evidence that the overexpression of the cellular TRs can complement the functions of vTR in MDV-induced tumorigenesis.

In the second part of this study, we wanted to address if EBERs (EBER-1 and EBER-2) possess tumor promoting functions and can transform chicken T cells using a small animal model for MDV-tumorigenesis. We generated recombinant MDVs expressing either EBER-1 or EBER-2 instead of vTR, termed vEBER-1 and vEBER-2. Expression levels of EBERs were detected during the viral lytic replication in vitro. EBERs were highly expressed and comparable to vTR expression in the wild-type or revertant. Furthermore, the recombinant mutants were replicating efficiently in cell culture and in infected animals. To assess the tumor promoting properties of EBERs, we performed an animal experiment where the infected animals were monitored for tumor development. EBERs partially restored the tumor formation if compared to the vTR-deletion. Tumor incidence with vEBER-2 was higher than with vEBER-1 compared to the wild-type. Our results for this aim displayed the potential tumorigenicity of EBERs their ability to transform different host immune cells. Furthermore, it

provided a useful model to investigate the activities of EBERs in the cellular transformation and the underlying mechanism using a small animal model for virus-induced cancer formation.

10. References

1. **McEachern, M.J., A. Krauskopf, and E.H. Blackburn,** *Telomeres and Their Control.* Annual Review of Genetics, 2000. **34**(1): p. 331-358.

2. **Blackburn, E.H.**, *Telomere states and cell fates.* Nature, 2000. **408**(6808): p. 53-6.

3. **Cong, Y.S., W.E. Wright, and J.W. Shay**, *Human telomerase and its regulation.* Microbiol Mol Biol Rev, 2002. **66**(3): p. 407-25, table of contents.

4. **Butel, J.S.**, *Viral carcinogenesis: revelation of molecular mechanisms and etiology of human disease.* Carcinogenesis, 2000. **21**(3): p. 405-26.

5. **Mark S. Parcells, J.B., Robin w. Morgan,** *Cancer associtaed viruses.* Springer chapter 13 2011: p. 307-337.

6. **Osterrieder, N., et al.**, *Marek's disease virus: from miasma to model.* Nat Rev Microbiol, 2006. **4**(4): p. 283-94.

7. **Fragnet, L., et al.,** *The RNA subunit of telomerase is encoded by Marek's disease virus.* J Virol, 2003. **77**(10): p. 5985-96.

8. **Trapp, S., et al.**, *A virus-encoded telomerase RNA promotes malignant T cell lymphomagenesis.* J Exp Med, 2006. **203**(5): p. 1307-17.

9. **Davison, A.J.,** *Herpesvirus systematics.* Vet Microbiol, 2010. **143**(1): p. 52-69.

10. **Stoopler, E.T. and M.S. Greenberg**, *Update on herpesvirus infections.* Dent Clin North Am, 2003. **47**(3): p. 517-32.

11. **Contreras, A. and J. Slots**, *Herpesviruses in human periodontal disease.* J Periodontal Res, 2000. **35**(1): p. 3-16.

12. **King, A.M.Q., et al.**, *Family - Herpesviridae*, in *Virus taxonomy: classification and nomenclature of viruses: Ninth Report of the International Committee on Taxonomy of Viruses*. 2012, Elsevier: San Diego. p. 111-122.

13. **Roziman B, C.L., Deinhardt F, de The G, Nahmias AJ, Plowright W, et al.**, *Herpseviridae. Definition, provisional nomenclature and taxonomy* Intervirology, 1981: p. 16: 201-217.

14. **Kimberlin, D.W.,** *Human herpesviruses 6 and 7: identification of newly recognized viral pathogens and their association with human disease.* Pediatr Infect Dis J, 1998. **17**(1): p. 59-67; quiz 68.

15. **Hoffman, F.J.J.a.L.J.,** *Overview of Herpesviruses.* Infectious Causes of CancerTargets for InterventionHerausgeber: Goedert, James J. (Ed.) 2000. **XXVI**: p. 33-49.

16. **Schat, K.A.,** *Marek's disease: a model for protection against herpesvirus-induced tumours.* Cancer Surv, 1987. **6**(1): p. 1-37.

17. **Richman, L.K., et al.,** *Novel endotheliotropic herpesviruses fatal for Asian and African elephants.* Science, 1999. **283**(5405): p. 1171-6.

18. **Witter, R.L.,** *Increased Virulence of Marek's Disease Virus Field Isolates.* Avian Diseases, 1997. **41**(1): p. 149-163.

19. **Witter, R.L., et al.**, *Classification of Marek's disease viruses according to pathotype: philosophy and methodology.* Avian Pathol, 2005. **34**(2): p. 75-90.

20. **Witter, R.L.**, *Increased virulence of Marek's disease virus field isolates.* Avian Dis, 1997. **41**(1): p. 149-63.

21. **Knipe, H., Griffin, et al. Moss, B.,** ***Poxviridae:*** *the viruses and their replication.* In Fields Virology, 4th edn., ed., 2001. **vol. 2**: p. pp. 2849–2883.

22. **Lindquester, G.J. and P.E. Pellett,** *Properties of the human herpesvirus 6 strain Z29 genome: G + C content, length, and presence of variable-length directly repeated terminal sequence elements.* Virology, 1991. **182**(1): p. 102-10.

23. **Dominguez, G., et al.,** *Physical and genetic maps of the human herpesvirus 7 strain SB genome.* Arch Virol, 1996. **141**(12): p. 2387-408.

24. **Bornkamm, G.W., et al.,** *Structure of Herpesvirus saimiri genomes: arrangement of heavy and light sequences in the M genome.* J Virol, 1976. **19**(1): p. 154-61.

25. **Russo, J.J., et al.**, *Nucleotide sequence of the Kaposi sarcoma-associated herpesvirus (HHV8).* Proc Natl Acad Sci U S A, 1996. **93**(25): p. 14862-7.

26. **Given, D. and E. Kieff**, *DNA of Epstein-Barr virus. VI. Mapping of the internal tandem reiteration.* J Virol, 1979. **31**(2): p. 315-24.

27. **Rixon, F.J. and T. Ben-Porat**, *Structural evolution of the DNA of pseudorabies-defective viral particles.* Virology, 1979. **97**(1): p. 151-63.

28. **Dumas, A.M., et al.,** *XbaI, PstI, and BglII restriction enzyme maps of the two orientations of the varicella-zoster virus genome.* J Virol, 1981. **39**(2): p. 390-400.

29. **Wadsworth, S., R.J. Jacob, and B. Roizman**, *Anatomy of herpes simplex virus DNA. II. Size, composition, and arrangement of inverted terminal repetitions.* J Virol, 1975. **15**(6): p. 1487-97.

30. **Hayward, G.S., et al.**, *Anatomy of herpes simplex virus DNA: evidence for four populations of molecules that differ in the relative orientations of their long and short components.* Proc Natl Acad Sci U S A, 1975. **72**(11): p. 4243-7.

31. **Sheldrick, P. and N. Berthelot**, *Inverted repetitions in the chromosome of herpes simplex virus.* Cold Spring Harb Symp Quant Biol, 1975. **39 Pt 2**: p. 667-78.

32. **Koch, H.G.,** et al., *Molecular cloning and physical mapping of the tupaia herpesvirus genome.* J Virol, 1985. **55**(1): p. 86-95.

33. **Albrecht, M., G. Darai, and R.M. Flugel,** *Analysis of the genomic termini of tupaia herpesvirus DNA by restriction mapping and nucleotide sequencing.* J Virol, 1985. **56**(2): p. 466-74.

34. **Arvin, A., et al.,** *Comparative virion structures of human herpesviruses*, in *Human Herpesviruses Biology, Therapy, and Immunoprophylaxis*, B.D. Davison A.J. , Editor. 2007, Cambridge: Cambridge University Press: Cambridge.

35. **Mettenleiter, T.C.**, *Budding events in herpesvirus morphogenesis.* Virus Res, 2004. **106**(2): p. 167-80.

36. **Spear, P.G., R.J. Eisenberg, and G.H. Cohen**, *Three classes of cell surface receptors for alphaherpesvirus entry.* Virology, 2000. **275**(1): p. 1-8.

37. **Campadelli-Fiume, G., et al**., *The multipartite system that mediates entry of herpes simplex virus into the cell.* Rev Med Virol, 2007. **17**(5): p. 313-26.

38. **Tischer, B.K., et al.,** *High-level expression of Marek's disease virus glycoprotein C is detrimental to virus growth in vitro.* J Virol, 2005. **79**(10): p. 5889-99.

39. **Jarosinski, K.W. and N. Osterrieder**, *Marek's disease virus expresses multiple UL44 (gC) variants through mRNA splicing that are all required for efficient horizontal transmission.* J Virol, 2012. **86**(15): p. 7896-906.

40. **Eisenberg, R.J., et al.**, *Herpes virus fusion and entry: a story with many characters.* Viruses, 2012. **4**(5): p. 800-32.

41. **Strang, B.L. and N.D. Stow,** *Circularization of the herpes simplex virus type 1 genome upon lytic infection.* J Virol, 2005. **79**(19): p. 12487-94.

42. **Jovasevic, V., L. Liang, and B. Roizman**, *Proteolytic cleavage of VP1-2 is required for release of herpes simplex virus 1 DNA into the nucleus.* J Virol, 2008. **82**(7): p. 3311-9.

43. **Kukhanova, M.K., A.N. Korovina, and S.N. Kochetkov**, *Human herpes simplex virus: life cycle and development of inhibitors.* Biochemistry, 2014. **79**(13): p. 1635-52.

44. **Boutell, C. and R.D. Everett,** *Regulation of alphaherpesvirus infections by the ICP0 family of proteins.* J Gen Virol, 2013. **94**(Pt 3): p. 465-81.

45. **Denesvre, C.**, *Marek's disease virus morphogenesis.* Avian Dis, 2013. **57**(2 Suppl): p. 340-50.

46. **Boodhoo, N., et al.,** *Marek's disease in chickens: a review with focus on immunology.* Vet Res, 2016. **47**(1): p. 119.

47. **Grinde, B.,** *Herpesviruses: latency and reactivation - viral strategies and host response.* J Oral Microbiol, 2013. **5**.

48. **Baringer , J.R. and P. Swoveland** *Recovery of Herpes-Simplex Virus from Human Trigeminal Ganglions.* New England Journal of Medicine, 1973. **288**(13): p. 648-650.

49. **Stevens, J.G. and M.L. Cook,** *Latent herpes simplex virus in spinal ganglia of mice.* Science, 1971. **173**(3999): p. 843-5.

50. **Rock, D.L.,** et al., *Detection of latency-related viral RNAs in trigeminal ganglia of rabbits latently infected with herpes simplex virus type 1.* J Virol, 1987. **61**(12): p. 3820-6.

51. **Wechsler, S.L., et al.**, *Fine mapping of the major latency-related RNA of herpes simplex virus type 1 in humans.* J Gen Virol, 1988. **69 (Pt 12)**: p. 3101-6.

52. **Ho, D.Y. and E.S. Mocarski**, *Herpes simplex virus latent RNA (LAT) is not required for latent infection in the mouse.* Proc Natl Acad Sci U S A, 1989. **86**(19): p. 7596-600.

53. **Steiner, I., et al.,** *Herpes simplex virus type 1 latency-associated transcripts are evidently not essential for latent infection.* Embo j, 1989. **8**(2): p. 505-11.

54. **Natarajan, R., et al.,** *A herpes simplex virus type 1 mutant lacking the ICP0 introns reactivates with normal efficiency.* J Virol, 1991. **65**(10): p. 5569-73.

55. **Maggioncalda, J., et al.**, *Analysis of a herpes simplex virus type 1 LAT mutant with a deletion between the putative promoter and the 5' end of the 2.0-kilobase transcript.* J Virol, 1994. **68**(12): p. 7816-24.

56. **Delecluse, H.J., S. Schuller, and W. Hammerschmidt,** *Latent Marek's disease virus can be activated from its chromosomally integrated state in herpesvirus-transformed lymphoma cells.* Embo j, 1993. **12**(8): p. 3277-86.

57. **Slobedman, B. and E.S. Mocarski,** *Quantitative analysis of latent human cytomegalovirus.* J Virol, 1999. **73**(6): p. 4806-12.

58. **Lyons, S.F. and D.N. Liebowitz**, *The roles of human viruses in the pathogenesis of lymphoma.* Semin Oncol, 1998. **25**(4): p. 461-75.

59. **Jarosinski, K.W., et al.**, *Marek's disease virus: lytic replication, oncogenesis and control.* Expert Rev Vaccines, 2006. **5**(6): p. 761-72.

60. **Churchill, A.E. and P.M. Biggs,** *Agent of Marek's disease in tissue culture.* Nature, 1967. **215**(5100): p. 528-30.

61. **J., M.,** *Multiple nervenentzuendung (polyneuritis) bei huehnern*, in *Dtsch Tierarztl Wochenschr*. 1907. p. 417-421.

62. **Hirai, K.,** *Marek's Disease*. 1 ed. 2001: Springer-Verlag Berlin Heidelberg.

63. **Pappenmeimer AM, D.L.**, Cone V *A study of fowl paralysis (neuro-lymphomatosis gallinarum).* Storrs Agric Exp Sta Bull 1926. **143**: p. 186-290.

64. **Pappenheimer AM, D.L.,** Cone V *Studies on fowl paralysis (neurolymphomatosis gallinarum). I. Clinical features and pathology. .* J Exp Med 1926a. **49**: p. 63-86.

65. **Anon,** *Tentative pathologic nomenclature.* Am J Vet Res 1941. **2:**: p. 116.

66. **GE, C.** *The enigma of avian leukosis.* . in *Proc 89th meeting Am vet Med Ass* 1952.

67. **PM, B.,** *A discussion on the classification of the avian leucosis complex and fowl paralysis. .* BritVet J 1961. **117**: p. 326-334.

68. **JG, C.**, *A proposed classification of the leucosis complex and fowl paralysis. .* Brit Vet J1961. **117**: p. 316-325.

69. **Churchill AE, Payne LN, and C. RC**, *Immunization against Marek's disease using a live attenuated virus. .* Nature l969b. **221**: p. 744-747.

70. **Witter RL, Sharma JM, and O. L,** *Turkey herpesvirus infection in chickens: induction of lymphoproliferative lesions and characterization of vaccinal immunity against Marek's disease.* Avian Dis 1976. **20**: p. 676-692.

71. **Ficken, M.D., et al.**, *Marek's disease virus isolates with unusual tropism and virulence for ocular tissues: clinical findings, challenge studies and pathological features.* Avian Pathol, 1991. **20**(3): p. 461-74.

72. **Venugopal K, B.A., Ross UN, Payne LN** *Pathogenicity of an unusual highly virulent Marek's disease virus isolated in the United Kingdom. I*, in *In: Silva RF, Cheng HH, Coussens PM, LeeLF, Velicer LF (eds) Current Research in Marek's disease. Proc 5th International Symp on Marek'sdisease, .* (1996) p. 119-124.

73. **Davison, F. and V. Nair,** *Use of Marek's disease vaccines: could they be driving the virus to increasing virulence?* Expert Rev Vaccines, 2005. **4**(1): p. 77-88.

74. **Basarab, O. and T. Hall**, *Comparisons of cell-free and cell-associated Marek's disease vaccines in maternally immune chicks.* Vet Rec, 1976. **99**(1): p. 4-6.

75. **Schat, R.L.W.a.K.A.**, *Marek's disease*, in *Diseases of Poultry*, Y.M. Saif, Editor. 2008, Blackwell publishing p. 452-514.

76. **Fabricant, C.G.,** *Atherosclerosis: the consequence of infection with a herpesvirus.* Adv Vet Sci Comp Med, 1985. **30**: p. 39-66.

77. **Dunn, K. and K. Nazerian**, *Induction of Marek's Disease Virus Antigens by IdUrd in a Chicken Lymphoblastoid Cell Line.* Journal of General Virology, 1977. **34**(3): p. 413-419.

78. **Sonoda, K., et al.**, *Development of an effective polyvalent vaccine against both Marek's and Newcastle diseases based on recombinant Marek's disease virus type 1 in commercial chickens with maternal antibodies.* J Virol, 2000. **74**(7): p. 3217-26.

79. **Ball, R.F. and J.F. Lyman,** *Revaccination of chicks for Marek's disease at twenty-one days old.* Avian Dis, 1977. **21**(3): p. 440-4.

80. **Lee, L.F., X. Liu, and R.L. Witter,** *Monoclonal antibodies with specificity for three different serotypes of Marek's disease viruses in chickens.* J Immunol, 1983. **130**(2): p. 1003-6.

81. **Kato, S., and K. Hirai.** , *Marek's disease virus. Advances in virus research*. Vol. 30. 1985.

82. **Lee, S.I., et al.,** *Difference in the meq gene between oncogenic and attenuated strains of Marek's disease virus serotype 1.* J Vet Med Sci, 2000. **62**(3): p. 287-92.

83. **Buckmaster, A.E., et al.**, *Gene sequence and mapping data from Marek's disease virus and herpesvirus of turkeys: implications for herpesvirus classification.* J Gen Virol, 1988. **69 (Pt 8)**: p. 2033-42.

84. **Silva, R.F., L.F. Lee, and G.F. Kutish**, *The genomic structure of Marek's disease virus.* Curr Top Microbiol Immunol, 2001. **255**: p. 143-58.

85. **Nair, V.**, *Evolution of Marek's disease -- a paradigm for incessant race between the pathogen and the host.* Vet J, 2005. **170**(2): p. 175-83.

86. **Silva, R.F.a.R.L.W.,** *Correlation of PCR detection of MDV with the appearance of histological lesions." In Current Research on Marek's Disease*. 1996.

87. **Payne, L.N., J.A. Frazier, and P.C. Powell**, *Pathogenesis of Marek's disease.* Int Rev Exp Pathol, 1976. **16**: p. 59-154.

88. **Davidson, I., M. Malkinson, and Y. Weisman,** *Marek's Disease in Turkeys. I. A Seven-Year Survey of Commercial Flocks and Experimental Infection Using Two Field Isolates.* Avian Diseases, 2002. **46**(2): p. 314-321.

89. **Qian, Z., et al.**, *Transactivation activity of Meq, a Marek's disease herpesvirus bZIP protein persistently expressed in latently infected transformed T cells.* J Virol, 1995. **69**(7): p. 4037-44.

90. **Powell, P.C. and J.G. Rowell,** *Dissociation of antiviral and antitumor immunity in resistance to Marek's disease.* J Natl Cancer Inst, 1977. **59**(3): p. 919-24.

91. **Swayne, D.E., J.R. Beck, and N. Kinney,** *Failure of a recombinant fowl poxvirus vaccine containing an avian influenza hemagglutinin gene to provide consistent protection against influenza in chickens preimmunized with a fowl pox vaccine.* Avian Dis, 2000. **44**(1): p. 132-7.

92. **Nazerian, K.W.R., Lee L, Yanagida N.,** *protection and synergism by recombinant fowlpox vaccines expressing genes form mareks disease virus.* Avian Dis, 1996. **40**: p. 368-376.

93. **Calnek, B.W.**, *Marek's disease--a model for herpesvirus oncology.* Crit Rev Microbiol, 1986. **12**(4): p. 293-320.

94. **Baigent SJ, D.F., *Marek's Disease Virus:*** *Biology and Life Cycle. In: Davison F, Nair V (eds) Marek's disease, an evolving problem,* . 2004, Elsevier Academic Press, Compton, UK,. p. 62–76

95. **Morimura, T., Ohashi, K., Kon, Y. et al.,** *Apoptosis and CD8-down-regulation in the thymus of chickens infected with Marek's disease virus.* Archives of Virology (1996) **141**: p. 2243. .

96. **Shek, W.R., et al.,** *Characterization of Marek's disease virus-infected lymphocytes: discrimination between cytolytically and latently infected cells.* J Natl Cancer Inst, 1983. **70**(3): p. 485-91.

97. **Mark S. Parcells , J.B., Robin W. Morgan**, *Marek's Disease Virus-Induced T-Cell Lymphomas*, in *Cancer research*, E.S. Robertson, Editor. 2011, Springer US. p. 307-335.

98. **Lupiani, B., et al.,** *Marek's disease virus-encoded Meq gene is involved in transformation of lymphocytes but is dispensable for replication.* Proceedings of the National Academy of Sciences of the United States of America, 2004. **101**(32): p. 11815-11820.

99. **Baigent, S.J. and F. Davison,** *Marek's disease virus: biology and life cycle*, in *Marek's disease, An Evolving Problem*. 2004. p. 62-77.

100. **Mark S. Parcells , J.B., and Robin W. Morgan** *Marek's Disease Virus-Induced T-Cell Lymphomas* in *Cancer Associated Viruses*, E.S. Robertson, Editor. 2012, Springer US. p. 307-335.

101. **Delecluse, H.J. and W. Hammerschmidt**, *Status of Marek's disease virus in established lymphoma cell lines: herpesvirus integration is common.* J Virol, 1993. **67**(1): p. 82-92.

102. **Blackburn, E.H.**, *Telomere states and cell fates.* Nature, 2000. **408**(6808): p. 53-56.

103. **Ding, Z., et al.**, *Telomerase reactivation following telomere dysfunction yields murine prostate tumors with bone metastases.* Cell, 2012. **148**(5): p. 896-907.

104. **Shay, J.W. and W.E. Wright,** *Role of telomeres and telomerase in cancer.* Semin Cancer Biol, 2011. **21**(6): p. 349-53.

105. **Kim, N.W., et al.,** *Specific association of human telomerase activity with immortal cells and cancer.* Science, 1994. **266**(5193): p. 2011-5.

106. **Delany, M.E. and L.M. Daniels,** *The chicken telomerase RNA gene: conservation of sequence, regulatory elements and synteny among viral, avian and mammalian genomes.* Cytogenet Genome Res, 2003. **102**(1-4): p. 309-17.

107. **Fragnet, L., et al.,** *The RNA subunit of telomerase is encoded by Marek's disease virus.* J Virol, 2003. **77**(10): p. 5985-5996.

108. **Fragnet, L., E. Kut, and D. Rasschaert**, *Comparative functional study of the viral telomerase RNA based on natural mutations.* J Biol Chem, 2005. **280**(25): p. 23502-15.

109. **Kaufer, B.B., et al.,** *Herpesvirus Telomerase RNA (vTR) with a Mutated Template Sequence Abrogates Herpesvirus-Induced Lymphomagenesis.* PLoS Pathogens, 2011. **7**(10): p. e1002333.

110. **Chen, J.L., K.K. Opperman, and C.W. Greider**, *A critical stem-loop structure in the CR4-CR5 domain of mammalian telomerase RNA.* Nucleic Acids Res, 2002. **30**(2): p. 592-7.

111. **Shkreli, M., et al.**, *Involvement of the oncoprotein c-Myc in viral telomerase RNA gene regulation during Marek's disease virus-induced lymphomagenesis.* J Virol, 2007. **81**(9): p. 4848-4857.

112. **Chbab, N., et al.**, *Viral control of vTR expression is critical for efficient formation and dissemination of lymphoma induced by Marek's disease virus (MDV).* Vet Res, 2010. **41**(5): p. 56.

113. **Kaufer, B.B., et al.**, *Herpesvirus telomerase RNA(vTR)-dependent lymphoma formation does not require interaction of vTR with telomerase reverse transcriptase (TERT).* PLoS Pathog, 2010. **6**(8): p. e1001073.

114. **Toczyski, D.P., et al.**, *The Epstein-Barr virus (EBV) small RNA EBER1 binds and relocalizes ribosomal protein RpL22 in EBV-infected human B lymphocytes.* Proc Natl Acad Sci U S A, 1994. **91**(8): p. 3463-7.

115. **Rao, S., et al.**, *Ribosomal Protein RpL22 Controls the Dissemination of T-cell Lymphoma.* Cancer Res, 2016. **76**(11): p. 3387-96.

116. **Rao, S., et al.,** *Inactivation of ribosomal protein L22 promotes transformation by induction of the stemness factor, Lin28B.* Blood, 2012. **120**(18): p. 3764-73.

117. **Toczyski, D.P. and J.A. Steitz**, *The cellular RNA-binding protein EAP recognizes a conserved stem-loop in the Epstein-Barr virus small RNA EBER 1.* Mol Cell Biol, 1993. **13**(1): p. 703-10.

118. **Lavergne, J.P., et al.,** *Role of acidic phosphoproteins in the partial reconstitution of the active 60 S ribosomal subunit.* FEBS Lett, 1987. **216**(1): p. 83-8.

119. **Houmani, J.L., C.I. Davis, and I.K. Ruf,** *Growth-promoting properties of Epstein-Barr virus EBER-1 RNA correlate with ribosomal protein L22 binding.* J Virol, 2009. **83**(19): p. 9844-9853.

120. **Hayward, S.D. and E.D. Kieff,** *Epstein-Barr virus-specific RNA. I. Analysis of viral RNA in cellular extracts and in the polyribosomal fraction of permissive and nonpermissive lymphoblastoid cell lines.* J Virol, 1976. **18**(2): p. 518-25.

121. **Komano, J., et al.**, *Oncogenic role of Epstein-Barr virus-encoded RNAs in Burkitt's lymphoma cell line Akata.* J Virol, 1999. **73**(12): p. 9827-31.

122. **Komano, J. and K. Takada**, *Role of bcl-2 in Epstein-Barr virus-induced malignant conversion of Burkitt's lymphoma cell line Akata.* J Virol, 2001. **75**(3): p. 1561-4.

123. **Glickman, J.N., J.G. Howe, and J.A. Steitz**, *Structural analyses of EBER1 and EBER2 ribonucleoprotein particles present in Epstein-Barr virus-infected cells.* J Virol, 1988. **62**(3): p. 902-11.

124. **Arrand, J.R., L.S. Young, and J.D. Tugwood**, *Two families of sequences in the small RNA-encoding region of Epstein-Barr virus (EBV) correlate with EBV types A and B.* J Virol, 1989. **63**(2): p. 983-6.

125. **Arrand, J.R. and L. Rymo**, *Characterization of the major Epstein-Barr virus-specific RNA in Burkitt lymphoma-derived cells.* J Virol, 1982. **41**(2): p. 376-89.

126. **Clarke, P.A., et al.**, *Binding of Epstein-Barr virus small RNA EBER-1 to the double-stranded RNA-activated protein kinase DAI.* Nucleic Acids Res, 1991. **19**(2): p. 243-8.

127. **Gottlieb, E. and J.A. Steitz**, *The RNA binding protein La influences both the accuracy and the efficiency of RNA polymerase III transcription in vitro.* Embo j, 1989. **8**(3): p. 841-50.

128. **Takada, K.a.N., A.**, *The role of EBERs in oncogenesis* Cancer Biol., 2001. **11**: p. 461-467.

129. **Nanbo, A., et al.**, *Epstein-Barr virus RNA confers resistance to interferon-alpha-induced apoptosis in Burkitt's lymphoma.* Embo j, 2002. **21**(5): p. 954-65.

130. **Nakao, A., M. Yoshihama, and N. Kenmochi**, *RPG: the Ribosomal Protein Gene database.* Nucleic Acids Res, 2004. **32**(Database issue): p. D168-70.

131. **Toczyski, D.P., et al.**, *The Epstein-Barr virus (EBV) small RNA EBER1 binds and relocalizes ribosomal protein L22 in EBV-infected human B lymphocytes.* Proc Natl Acad Sci U S A, 1994. **91**(8): p. 3463-7.

132. **Houmani, J.L., C.I. Davis, and I.K. Ruf**, *Growth-promoting properties of Epstein-Barr virus EBER-1 RNA correlate with ribosomal protein L22 binding.* J Virol, 2009. **83**(19): p. 9844-53.

133. **Laing, K.G., et al.**, *In vivo effects of the Epstein-Barr virus small RNA EBER-1 on protein synthesis and cell growth regulation.* Virology, 2002. **297**(2): p. 253-69.

134. **Yajima, M., T. Kanda, and K. Takada**, *Critical role of Epstein-Barr Virus (EBV)-encoded RNA in efficient EBV-induced B-lymphocyte growth transformation.* J Virol, 2005. **79**(7): p. 4298-307.

135. **Kitagawa, N., et al.**, *Epstein-Barr virus-encoded poly(A)(-) RNA supports Burkitt's lymphoma growth through interleukin-10 induction.* Embo j, 2000. **19**(24): p. 6742-50.

136. **Repellin, C.E., et al.**, *Lymphoid hyperplasia and lymphoma in transgenic mice expressing the small non-coding RNA, EBER1 of Epstein-Barr virus.* PLoS One, 2010. **5**(2): p. e9092.

137. **Yamamoto, N., et al.**, *Malignant transformation of B lymphoma cell line BJAB by Epstein-Barr virus-encoded small RNAs.* FEBS Lett, 2000. **484**(2): p. 153-8.

138. **Rosa, M.D., et al.**, *Striking similarities are exhibited by two small Epstein-Barr virus-encoded ribonucleic acids and the adenovirus-associated ribonucleic acids VAI and VAII.* Mol Cell Biol, 1981. **1**(9): p. 785-96.

139. **Gazzaniga, F.S. and E.H. Blackburn**, *An antiapoptotic role for telomerase RNA in human immune cells independent of telomere integrity or telomerase enzymatic activity.* Blood, 2014. **124**(25): p. 3675-84.

140. **Li, H. and R. Durbin**, *Fast and accurate short read alignment with Burrows-Wheeler transform.* Bioinformatics, 2009. **25**(14): p. 1754-60.

141. **Jarosinski, K.W., Osterrieder, N., Nair, V. K. & Schat, K, . *A*.** *Attenuation of Marek's disease virus by deletion of open reading frame RLORF4 but not RLORF5a.* J. Virol, (2005). . **79**: p. 11647–59.

142. **Tischer, B.K., G.A. Smith, and N. Osterrieder,** , *En passant mutagenesis: a two step markerless red recombination system. .* Methods Mol Biol,, 2010. . **634**: p. 421-30.

143. **Petherbridge, L., et al.**, *Oncogenicity of virulent Marek's disease virus cloned as bacterial artificial chromosomes.* J Virol, 2004. **78**(23): p. 13376-80.

144. **Tischer, B.K., et al.**, *Two-step red-mediated recombination for versatile high-efficiency markerless DNA manipulation in Escherichia coli.* Biotechniques, 2006. **40**(2): p. 191-7.

145. **Tischer, B.K. and B.B. Kaufer,** *Viral Bacterial Artificial Chromosomes: Generation, Mutagenesis, and Removal of Mini-F Sequences.* Journal of Biomedicine and Biotechnology, 2012. **2012**: p. 14.

146. **Zagursky, R.J. and J.B. Hays**, *Expression of the phage lambda recombination genes exo and bet under lacPO control on a multi-copy plasmid.* Gene, 1983. **23**(3): p. 277-92.

147. **Murphy, K.C.,** *Use of bacteriophage lambda recombination functions to promote gene replacement in Escherichia coli.* J Bacteriol, 1998. **180**(8): p. 2063-71.

148. **Sakaki, Y., et al.,** *Purification and properties of the gamma-protein specified by bacteriophage lambda: an inhibitor of the host RecBC recombination enzyme.* Proc Natl Acad Sci U S A, 1973. **70**(8): p. 2215-9.

149. **Wu, Z., et al.,** *Domain structure and DNA binding regions of beta protein from bacteriophage lambda.* J Biol Chem, 2006. **281**(35): p. 25205-14.

150. **Kmiec, E. and W.K. Holloman**, *Beta protein of bacteriophage lambda promotes renaturation of DNA.* J Biol Chem, 1981. **256**(24): p. 12636-9.

151. **Colleaux, L., et al.**, *Universal code equivalent of a yeast mitochondrial intron reading frame is expressed into E. coli as a specific double strand endonuclease.* Cell, 1986. **44**(4): p. 521-33.

152. **Inoue, H., H. Nojima, and H. Okayama**, *High efficiency transformation of Escherichia coli with plasmids.* Gene, 1990. **96**(1): p. 23-8.

153. **Hofmann, M.A. and D.A. Brian**, *Sequencing DNA amplified directly from a bacterial colony.* Methods Mol Biol, 1993. **15**: p. 205-10.

154. **Osterrieder, N.,** *Sequence and initial characterization of the U(L)10 (glycoprotein M) and U(L)11 homologous genes of serotype 1 Marek's Disease Virus.* Arch Virol, 1999. **144**(9): p. 1853-63.

155. **Schumacher, D., et al.**, *The protein encoded by the US3 orthologue of Marek's disease virus is required for efficient de-envelopment of perinuclear virions and involved in actin stress fiber breakdown.* J Virol, 2005. **79**(7): p. 3987-97.

156. **Jarosinski, K.W., et al.**, *Attenuation of Marek's disease virus by deletion of open reading frame RLORF4 but not RLORF5a.* J Virol, 2005. **79**(18): p. 11647-59.

157. **Chang, L.Y., et al.,** *Telomerase activity and in situ telomerase RNA expression in oral carcinogenesis.* J Oral Pathol Med, 1999. **28**(9): p. 389-96.

158. **Kaufer, B.B., K.W. Jarosinski, and N. Osterrieder**, *Herpesvirus telomeric repeats facilitate genomic integration into host telomeres and mobilization of viral DNA during reactivation.* J Exp Med, 2011. **208**(3): p. 605-15.

159. **Schippers, T., K. Jarosinski, and N. Osterrieder**, *The ORF012 gene of Marek's disease virus type 1 produces a spliced transcript and encodes a novel nuclear phosphoprotein essential for virus growth.* J Virol, 2015. **89**(2): p. 1348-63.

160. **Lin, R., et al.,** *The herpes simplex virus ICP0 RING finger domain inhibits IRF3- and IRF7-mediated activation of interferon-stimulated genes.* J Virol, 2004. **78**(4): p. 1675-84.

161. **Chang, L.-Y., et al.**, *Telomerase activity and in situ telomerase RNA expression in oral carcinogenesis.* Journal of Oral Pathology & Medicine, 1999. **28**(9): p. 389-396.

162. **White, L.K., W.E. Wright, and J.W. Shay**, *Telomerase inhibitors.* Trends in Biotechnology, 2001. **19**(3): p. 114-120.

163. **Artandi, S.E.**, *Telomerase flies the coop: the telomerase RNA component as a viral-encoded oncogene.* J Exp Med, 2006. **203**(5): p. 1143-5.

164. **Davison, T.F. and V. Nair**, *Marek's disease : an evolving problem* 2004, London: lsevier Academic Press.

165. **Moss, W.N., et al**., *RNA families in Epstein–Barr virus.* RNA Biology, 2014. **11**(1): p. 10-17.

166. **Keene, J.D., J.M. Komisarow, and M.B. Friedersdorf**, *RIP-Chip: the isolation and identification of mRNAs, microRNAs and protein components of ribonucleoprotein complexes from cell extracts.* Nat Protoc, 2006. **1**(1): p. 302-7.

11. Academic Achievements

A. Scientific Awards and fellowships & grants

07/2017	Novus Biologicals, LLC- symposium **travel grant Award**
03/2017	FU Bright conference **mobility award**
10/2013 – 10/2017	**PhD scholarship** funded by the Egyptian government
03/2011	**SUSC award** offered for young academic researcher for the best research in the clinical sciences, Sohag University, Egypt.
07/2007	**Undergraduate Award of Excellence**, South Valley University, Egypt

B. Conferences attended

29/07/017-2/08/017	**42nd international Herpesvirus workshop**, 2017 Ghent, Belgium. **Talk:** Evaluation of cellular telomerase TRs and viral RNAs in Herpesvirus cancer formation **Poster:** Tumor promoting functions of the overexpression of chicken telomerase RNA in MDV-induced tumor formation
06/06/01-09/06/016	**11th international symposium on Marek's disease and avian herpesviruses,** 2016, Tours, France. **Poster:** Role of vTR in MDV-induced tumor formation
22/03/017- 5/03/017	**27th Annual Meeting of the Society for Virology, 2017. Marburg, Germany.** **Poster:** Tumor promoting function of the overexpression of the cellular telomerase in herpesvirus induced tumorigenesis

C. Teaching practical courses

06/2014	Tutor at the Virology Practical course of the Veterinary Medicine School
06/2015	Tutor at the Virology Practical course of the Veterinary Medicine School
04/2014	Tutor at the Mutagenesis Practical course for ZIBI students

D. Collaborators

08/2015	Prof. Dr. Alex D. Greenwood and Dr. David Alquezar, Leibniz-Institut für zoo-und Wildtierforschung, Freie Universität Berlin
02/2015	Prof. Dr. Mark S. Parcells, University of Delaware, USA
01/2017	Prof. Dr. Axel Karger, Friedrich-Loeffler-Institute, Griesfeld, Germany

12. Publications

Articles

Kheimar A, Previdelli RL, Wight DJ, Kaufer BB (2017). Telomeres and Telomerase: Role in Marek's Disease Virus Pathogenesis, Integration and Tumorigenesis. Viruses 9 (7). pii: E173. doi: 10.3390/v9070173.

Kheimar A, and Kaufer BB. Epstein Barr Virus-encoded RNAs (EBERs) complement the loss of Herpesvirus telomerase RNA in cancer formation. *In preparation.*

Kheimar A, and Kaufer BB. Tumor promoting functions of the overexpression of cellular TRs (chTR) in herpesvirus induced tumorigenesis. *In preparation.*

Talks

Evaluation of the cellular TRs and herpesviruse RNAs using a small animal model for herpesvirus tumorigenesis. Kheimar A. and Kaufer BB. 42nd Annual International Herpesvirus Workshop (IHW 2017).

Posters

Evaluation of the cellular TRs and viral RNAs using a small animal model for herpesvirus tumorigenesis. Kheimar A. and Kaufer BB. 42nd Annual International Herpesvirus Workshop.

Role of viral telomerase RNA (vTR) in MDV tumor development. Kheimar A and Kaufer BB. 11th International Symposium on Marek's disease and avian herpesviruses.

Cellular telomerase RNA (chTR) complement the functions of Herpesvirus telomerase RNA in virus induced cancer formation. Kheimar A and Kaufer BB. 28th Annual Meeting of the German Society for Virology.

13. Acknowledgements

First of all, I would like to express my gratefulness to **ALLAH** for the power, endurance and everything his majesty gave me throughout my life.

I am and forever will be grateful and owed a lot to Prof. Dr. Benedikt B. Kaufer for giving me the chance to join his awesome team and to be a graduate PhD student. I don't know how to express my appreciation for the encouragement, continuous following up, supplying the facilities, and teaching the ethics of the scientific research. This thesis would not have been possible without his help and his constant source of inspiration throughout the research work.

I would like to express my deepest gratitude and appreciation to Prof. Dr. Klaus Osterrieder for hosting me as a PhD student in Institute of Virology, department of Veterinary Medicine, Freie Universität Berlin and for his critical suggestions, advices and scientific acumen perspicacious remarks.

I want to take this opportunity and express my appreciation to Prof. Dr. Alex D. Greenwood and Dr. David Alquezar, Leibniz-Institut für zoo-und Wildtierforschung, Freie Universität Berlin for hosting me to do some collaborative works. They are very kind and helpful all the time.

Great thanks must be expressed for all scientists in the institute: Dr. Walid Azab, Abdelrahman Said, Darren Wight, Dusan Kunec, Michael Veit, Ludwig Krabben, Timo Schippers, Tobias Bergmann, Chris Höfer, Susanne Kaufer, Annachiara Greco, Cosima Zimmermann and Nina Wallaschek. Thanks to all PhD students in the institute, Nicole Groenke, Mohamed Kamel, Renato Previdelli, Anirban Sanyal, Kathrin Eschke, Jakob Trimpert, Luca bertzbach, Tereza Faflikova, LiubaCherkashchenko, Maksat Akhmedzhanov, Fatma Ali and Mohamed Rasheed for their continuous help and facilitating the practical work. I am also especially indebted to our TAs Ann Reum, Annett Neubert and Michaela Zeitlow for their great assist during the work. Thanks to my college Dr. Ibrahim Elzuheir for sharing with me joys and sorrows of a PhD abroad. Thanks to Ahmed Aglan, typical Egyptian friend who is always there for exchanging the lab knowledge and valuable discussions all over the days, Gamal Wareth, the eldest brother studying in FLI- Jena, to my real brother Mohamed abdelwahab who was always with me during the PhD journey supporting and advising.

Thanks from my heart all members, past and present, of Institute Virology for providing a warm environment for scientific research, sharing ideas, valuable discussions, Seminars, and for their support. I will never forget you guys.

I cannot forget my beloved country, Arab Republic of Egypt for the financial support. Also, I would like to expand my sincere gratitude to all members of Faculty of Veterinary Medicine, Sohag University, Sohag, Egypt.

Obviously, I would not be sitting in front of my monitor to type this acknowledgements without feeling to express my deepest gratitude, thanking, and appreciations to my Family for their unflagging love. I am indebted to my father (ALLAH bless him), he was typical father in an Egyptian family, he spares no effort to support the family and provides the best environment for me, my brother and sisters. I hope that I can meet his expectations. Always keep you in my prayers. Thanks to my mother, i cannot describe her everlasting love to us. Last but not least, thanks to my eldest brother Khaled for his patience and supporting for me.

Thank you very much

Ahmed Kheimar

Selbständigkeitserklärung

Hiermit bestätige ich, dass ich die vorliegende Arbeit selbstständig angefertigt habe. Ich versichere, dass ich ausschließlich die angegebenen Quellen und Hilfen in Anspruch genommen habe.

Berlin, den 08.11.2017 Ahmed Kheimar

mbvberlin | mensch und buch verlag

49,90 Euro | ISBN: 978-3-86387-857-3